

**DOTTORATO DI RICERCA IN**

**ONCOLOGIA E PATOLOGIA SPERIMENTALE**  
**Progetto “Oncologia” - Indirizzo Biologia Molecolare**

Ciclo XXII

Settore scientifico-disciplinare di afferenza: BIO/11

**MOLECULAR ANALYSIS OF  
SPECIAL TYPES BREAST  
CARCINOMAS**

**Presentata dal Dott. de Biase Dario**

**Coordinatore Dottorato**  
**Chiar.mo Prof.**  
**Sandro Grilli**

**Relatore**  
**Chiar.ma Prof.ssa**  
**Maria Pia Foschini**

**Esame finale anno 2010**



# INDEX

<b>1. p63 short isoforms in invasive breast carcinoma .....</b>	<b>7</b>
1.1 Introduction .....	9
1.1.1 p63 .....	9
1.1.2 Gene Structure .....	9
1.1.3 p63 functions .....	11
1.1.4 Tissue-specific roles for p63 in normal development .....	12
1.1.5 p63 in normal tissue.....	12
1.1.6 p63 in human cancer.....	13
1.1.7 p63 shorter isoforms .....	14
1.2 Material and Methods.....	17
1.2.1 Case selection .....	17
1.2.2 Immunohistochemistry .....	18
1.2.3 RNA extraction and RT-PCR.....	18
1.2.4 PCR and nested PCR .....	19
1.2.5 Band purification and sequence analysis.....	20
1.3 Results .....	23
1.3.1 Immunohistochemical results.....	25
1.3.2 Nested PCR .....	26
1.3.3 Sequencing .....	27
1.3.4 Relation between nested PCR results and clinical, morphological and immunohistochemical data .....	28
1.4 Discussion and conclusions.....	31
References .....	33
<b>2. Genetic heterogeneity in metaplastic breast carcinomas .....</b>	<b>37</b>
2.1 Introduction .....	39
2.1.1 Metaplastic breast carcinomas.....	39
2.1.2 Intra-tumour heterogeneity .....	42
2.1.3 Micro-Array CGH .....	43
2.1.4 Array-CGH and the identification of new targets in breast carcinoma.....	46

## Index

2.2 Material and methods .....	49
2.2.1 Case selection .....	49
2.2.2 Microdissection and nucleic acid extraction .....	50
2.2.3 Microarray comparative genomic hybridisation .....	51
2.2.4 Hierarchical cluster analysis .....	54
2.2.5 In situ hybridisation .....	54
2.2.6 Immunohistochemistry .....	55
2.2.7 p53 mutation analysis .....	55
2.2.8 HUMARA assay .....	56
2.2.9 Quantitative real-time reverse transcriptase PCR (qRT-PCR) .....	57
2.3 Results .....	59
2.3.1 Cases 1-4 .....	59
2.3.2 Cases 5-6 .....	61
2.3.3 Cluster analysis .....	68
2.4 Discussion and Conclusions .....	71
References .....	75
<b>3. Oncocytic Breast Carcinoma .....</b>	<b>81</b>
3.1 Introduction .....	83
3.1.1 Oncocytic Tumours .....	83
3.1.2 Mitochondria-rich and oncocytic tumours .....	84
3.1.3 Oncocytic in breast .....	85
3.1.4 Mitochondria .....	87
3.1.5 Genetics .....	88
3.1.6 Mitochondria dysfunctions .....	90
3.1.7 Alterations of energy-supplying pathways in tumours .....	91
3.1.8 ROS impairment .....	92
3.1.9 Upregulation of glycolysis in tumour .....	93
3.1.10 Genetic and biochemical alterations in oncocytic tumours .....	94
3.2 Material and methods .....	95
3.2.1 Case selection .....	95
3.2.2 Immunohistochemistry .....	96
3.2.3 Electron microscopy .....	99
3.2.4 Follow-up .....	99

3.2.5 Microdissection and DNA extraction.....	99
3.2.6 Microarray comparative genomic hybridisation analysis (aCGH).....	100
3.2.7 Mitochondrial DNA sequencing.....	101
3.2.8 Nuclear genes codifying for mitochondrial protein.....	103
3.3 Results .....	105
3.3.1 Group 1 (selected OC).....	105
3.3.2 Group 2 (consecutive cases 1997-1998).....	107
3.3.3 Oncocytic carcinomas .....	111
3.3.4 Anatomico-clinical features .....	114
3.3.5 Immunohistochemical features.....	118
3.3.6 Electron microscopy .....	119
3.3.7 Follow-up .....	119
3.3.8 Molecular analysis (aCGH).....	125
3.3.9 Nuclear genes codifying for mitochondrial proteins .....	129
3.3.10 Mitochondrial DNA sequencing.....	133
3.4 Discussion and Conclusions.....	135
References .....	139



# **1. p63 SHORT ISOFORMS IN INVASIVE BREAST CARCINOMAS**



# 1. p63 SHORT ISOFORMS IN INVASIVE BREAST CARCINOMAS

## 1.1 INTRODUCTION

### 1.1.1 p63

p63 is a sequence-specific DNA-binding factor, homologue of the tumour suppressor and transcription factor p53, located on chromosome 3q27-29. Both family members, p53 and p63, have several common protein domains: a N-terminal transactivation (TA) domain, a central DNA-binding domain (DBD) and an oligomerization domain (OD). p63 isoforms exhibit high degrees of sequence and structural similarity to p53, while at the same time revealing considerable functional divergence. All p63 proteins encode a DNA-binding domain, which is approximately 60% identical at the amino acid level to the DNA-binding domain of p53, and an oligomerization domain with about 37% identity to that of p53 (Figs. 1.1A and 1.1B) [1].

### 1.1.2 Gene Structure

While p53 is a simple gene, with unique strong promoter with a single transcript codifying for only one protein of 393 aminoacids, p63 contains two promoters and is characterized by alternative splicing, leading to six different protein [2-4] (Figures 1.1B and 1.1C).

The human p63 gene is composed of 15 exons and transcription can occur from two distinct promoters: the transactivating isoforms (TAp63) are generated by a promoter upstream of exon 1, while the alternative promoter located in intron 3 leads to the expression of N-terminal truncated isoforms ( $\Delta$ Np63) [5, 6]. C-terminal mRNA splicing generates additional structural and functional p63 transcripts. To date three isoforms have

## 1.1 Introduction

been identified for p63 ( $\alpha$ ,  $\beta$ ,  $\gamma$ ), and two for p53 [7, 8]. The different C-termini of  $\alpha$ ,  $\beta$ , and  $\gamma$  isoforms also contribute to the diversity of p63 proteins [9, 10].

Shortest isoforms, p63 $\gamma$ , are the more similar to p53. These variants are characterized by a splicing that cut off from exon 11 to exon 14. The  $\beta$ -isoforms lack exon 13, while isoforms  $\alpha$  are the longest one and comprise all 15 with an  $\alpha$ -steric (SAM) C-terminal (Figure 1.1).

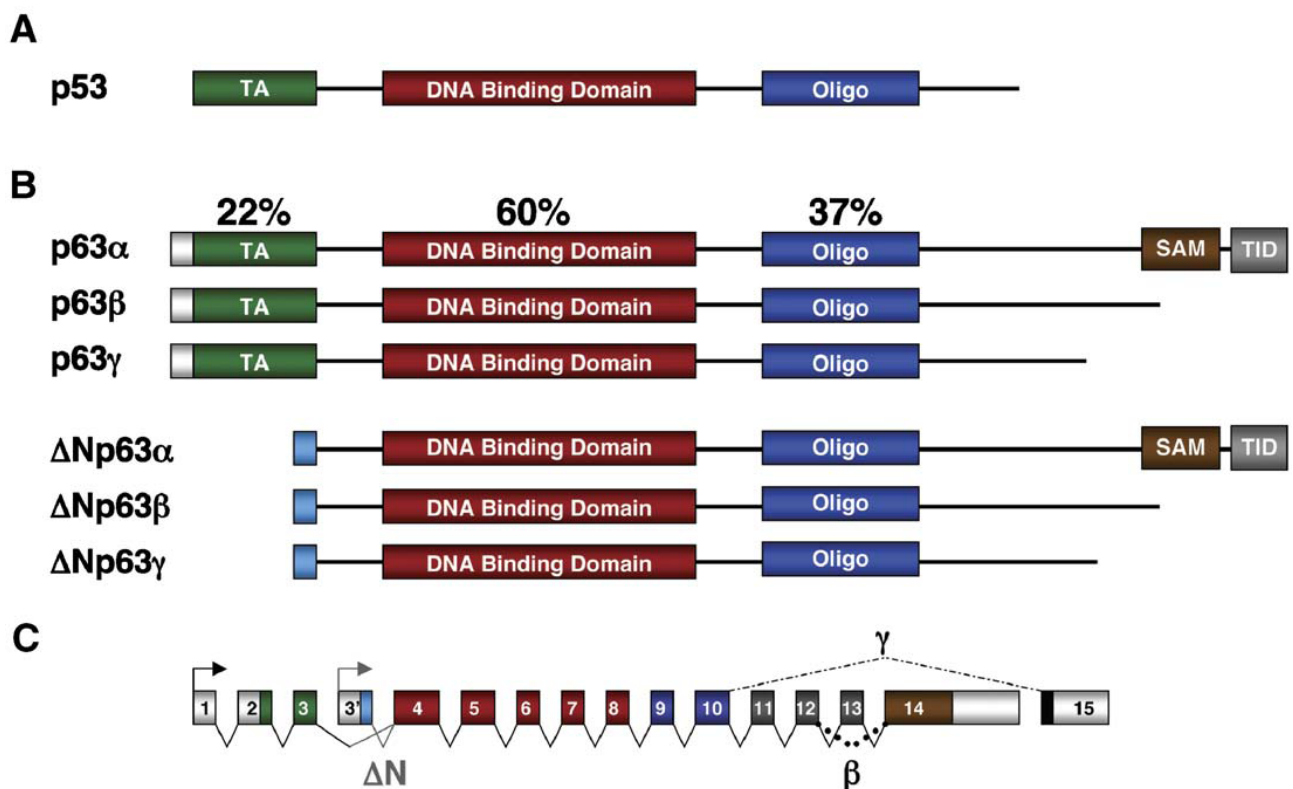


**Figure 1.1: Functional domains of p53 and p63 proteins.** (A) Functional domains of p53. p53 is composed of three primary domains: an N-terminal transactivation domain (TA), a central DNA binding domain, and a C-terminal oligomerization domain (Oligo). (B) Functional domains of p63 proteins. Percentages represent p53-identical residues found in p63. In addition, p63 has additional C-terminal domains called the sterile alpha motif (SAM) domain and transactivation inhibitory domain (TID). (C) Gene structure of p63. Both promoters and the  $\Delta$ N and  $\alpha$ ,  $\beta$ ,  $\gamma$  splicing events are shown.

The TAp63 $\alpha$  isoform is the largest proteins in each family. The TAp63 $\gamma$  isoform most closely resembles full-length p53. In overexpression studies, TAp63 $\gamma$  has been shown to be as potent as p53 in inducing target gene expression and apoptosis. p63 $\alpha$  isoforms also contain a protein–protein interaction domain known as the sterile alpha motif (SAM) [10]. The SAM is a globular domain composed of four  $\alpha$ -helices and a small 310-helix. Although this motif is often found to mediate homodimerization within developmentally regulated proteins, in p53 family members the SAM domain is thought to be monomeric [11]. An additional post-SAM region known as the transactivational inhibitory domain (TID) has been identified in p63 $\alpha$  [12]. This region (about 70 amino acids) has been proposed to inhibit the transcriptional activity of TAp63 $\alpha$  through inter- or intra-molecular association with the TA domain [12]. Indeed, TAp63 $\alpha$  isoforms have decreased potency in transactivation and apoptosis induction compared to other TA isoforms, and deletion of this region restores transactivation potency of TAp63 $\alpha$  [2, 12]. The presence of this domain within  $\Delta$ Np63 $\alpha$  isoform may allow trans-repression of associated TA isoforms, thereby explaining the potent inhibitory effect of  $\Delta$ Np63 $\alpha$  isoform when bound to DNA as hetero-tetramers composed of both  $\Delta$ N $\alpha$  and TA $\gamma$  isoforms [12].

### 1.1.3 p63 Functions

TAp63 isoforms induce cell cycle arrest, play an important role in cell differentiation and also regulate independent sets of genes that are not transcriptional targets of p53 [1]. In contrast  $\Delta$ Np63 proteins act as dominant-negative inhibitors of the p53 family [2, 13], leading to the hypothesis that these isoforms may exhibit proto-oncogenic function. In normal epithelium, balance between these proteins maintains correct cell proliferation and differentiation. Probably an anomalous regulation of the expression of  $\Delta$ N and TA

## 1.1 Introduction

proteins might increase the proliferation rate of epithelia, generating the underground for neoplastic transformation; moreover, in transforming cells, the imbalance between TA and  $\Delta N$  might cause the characteristic aggressive phenotype, inhibiting the cell cycle control by p53. Numerous studies have demonstrated that  $\Delta Np63$  is the predominant isoform expressed in squamous cell carcinomas of oral cavity [14], while loss of p63 expression was associated with progression to metastasis and correlated with poor prognosis in urothelial carcinomas [15].

### 1.1.4 Tissue-specific roles for p63 in normal development

p63 is expressed in a highly restricted pattern during embryonic development. Its expression is first detectable within the primitive ectoderm, which gives rise to the epidermis as well as epithelial appendages including the mammary gland, prostate, teeth and sweat glands. p63 is also expressed in the apical ectodermal ridge, a specialized cluster of ectodermal cells required for inductive events during limb formation [16, 17]. Remarkably, p63 is essential for the development of most tissues in which it is expressed, as p63-null mice exhibit profound developmental abnormalities of the skin, limbs, mammary, prostate and other epithelial tissues [16, 17]. This ectodermal phenotype is recapitulated in humans who inherit a variety of heterozygous mutations in p63 that are thought to function as dominant-negative or potentially dominant gain-of-function alleles [18].

### 1.1.5 p63 in normal tissues

p63 expression follows a restricted pattern in normal tissues. Intense p63 nuclear localization in the basal layer of stratified squamous epithelia, with a gradual diminution of nuclear intensity in the more terminally differentiated cell layers, whereas the most

apical cells had undetectable p63 levels. p63 decorates basal cells of the prostate and of the pseudostratified respiratory epithelium, myoepithelial cells of the bronchial glands, basa/ myoepithelial cells of breast [19-21]. The identification of p63 in basal cell layers of stratified and transitional epithelia is significant because some of these cells act as progenitors of the suprabasal cells, which undergo differentiation and cell death [2].

Data from *TP63* knockout mice point to a pivotal function for p63 in epithelial development and morphogenesis [16, 17]. Hence, they displayed defective epidermal differentiation as well as agenesis of mammary glands, lacrimal glands, and the prostate. It has been reported that p63 overexpression can mimic p53 activities by binding DNA, activating transcription, and inducing apoptosis [2, 4, 22]. Whereas p53 is ubiquitously expressed, although in low to undetectable levels by IHC, p63 is tissue and cell type restricted [2, 23, 24]. It is now evident that p53 has evolved to protect cells from genotoxic insults and unprogrammed proliferation, whereas p63 may have evolved to perform tissue-specific functions distinct from those of p53 [25].

### **1.1.6 p63 in human cancer**

It has been demonstrated that anti-p63 antibodies decorate the majority of squamous cell carcinomas of different organs [19-21, 26], including head and neck [14, 27, 28], cervix [20] and lung [20, 29], as well as basal cell carcinomas of the skin [19, 30], transitional cell carcinomas [20, 31]; moreover tumours with myoepithelial differentiation of the breast [32-34] showed strong nuclear p63 expression. p63 is expressed in a minor proportion of ductal carcinomas of breast (4.6–11%) [32]. Reports have varied as to the frequency of p63 expression in invasive breast carcinomas, with studies ranging from 0 to 30% [34-36]. It now seems clear, however, that p63 is expressed in at least a subset of breast tumours that are known to exhibit a basal epithelial phenotype [37]. Also, some

## 1.1 Introduction

serous and endometrioid carcinomas of the ovary and rare adenocarcinomas of the colon express this marker [21]. p63 also stain rare primary malignant melanomas (10%) and glioblastomas (12%) [21].

It should be noted, that p63 knockout mice are defective in the development of all organs that express p63. Thus, it appears that, in addition to its role in normal development, maintenance of p63 expression is important in the neoplastic transformation of squamous and transitional epithelium. Mesenchymal elements, including fibroblasts and smooth muscle cells, had undetectable p63 [19].

### 1.1.7 p63 shorter isoforms

Two new isoforms have been described with the same sequence as TAp63 and  $\Delta Np63$  but lacking exon 4: d4TAp63 and  $\Delta Np73L$ , respectively (Fig. 1.2).  $\Delta Np73L$  has been found only in squamous cell carcinoma of the oral cavity but not in normal oral mucosa and normal salivary gland tissues [14, 28, 38].

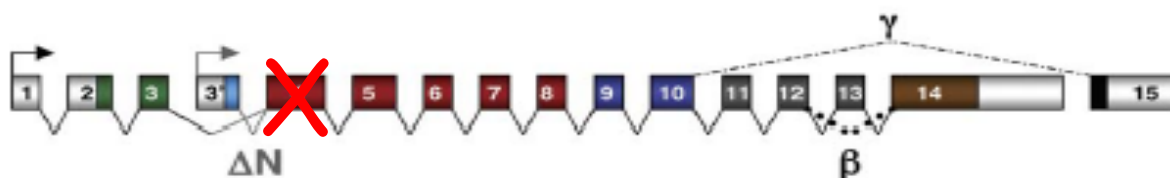


**Figure 1.2: Shorter p63 isoforms.** These proteins are identical to normal isoforms except for the splicing of exon 4.

Immunohistochemical detection of p63 in breast is of practical value as it helps in the differential diagnosis between in situ and invasive carcinomas at light microscopy [39, 40]. Unfortunately the antibodies anti-p63 presently available recognize only  $\Delta Np63$  or TAp63 isoforms but not those lacking exon 4.

Furthermore no data are available on the molecular expression patterns of p63 N-terminal isoforms in normal and neoplastic breast tissues.

Purpose of the study was to investigate the molecular expression of N-terminal p63 isoforms in benign and malignant breast tissues.



## 1.2 MATERIAL AND METHODS

### 1.2.1 Case selection

Forty randomly selected samples of breast tissue, from 32 patients, were collected.

Criteria for inclusion in the study were the following:

- 1) frozen tissue available for molecular study;
- 2) no treatment with any form of adjuvant therapy.

Tissues were received fresh. Each specimen was visualized at frozen section level. Tissue was frozen for molecular analysis, the rest was fixed in 10% buffered formalin and processed as routine for diagnosis. Eighteen cases of invasive breast carcinoma (IBC) and 2 of Ductal In Situ Carcinoma (DIN/DCIS) led to obtain 20 frozen specimens. There were also 12 cases of non neoplastic breast tissues that led to an equal number of specimens. Finally from tissue of quadrantectomies not involved by the tumour, 8 specimens of benign tissue were taken. Therefore in carcinomas each case corresponded to a specimen. In non neoplastic tissue the number of specimens was higher than the number of cases.

Criteria for histological diagnoses were those of WHO [41]. Grading for invasive carcinomas were those of Elston and Ellis [42]. Pleomorphic variety of invasive lobular carcinomas (PILC) were defined according to the criteria described by Eusebi et. al [43]. Rakha et al's criteria [44] were employed to establish the luminal or basaloid phenotypes.

## 1.2 Material and Methods

### 1.2.2 Immunohistochemistry

Immunohistochemistry was performed on 3µm-thick sections cut from selected paraffin blocks. All specimens were stained with monoclonal 4A4 antibody (Labvision/NeoMarkers, Fremont CA, USA, 1:200), that recognizes all p63 isoforms. The additional antibodies reported in Table 1.1 were employed only in cases of IBC. An automatic immunostainer (Ventana-Benchmark, Tucson, Arizona, U.S.A.) was used. Semiquantitative evaluation was performed counting the percentage of positive neoplastic cells in 10 different fields at 40X magnification.

Antibody	Dilution	Antigen Retrieval
Ki67*	1:200	CC1 <sup>^</sup> #
Oestrogen <sup>^</sup>	Prediluted	CC1 <sup>^</sup> #
Progesterone <sup>^</sup>	Prediluted	CC1 <sup>^</sup> #
c-erb-B2 <sup>§</sup>	1:50	CC1 <sup>^</sup> °
CK14 <sup>§</sup>	1:400	CC1 <sup>^</sup> °

**Table 1.1: Antibodies employed in cases of IBC.** \*Dako, Denmark; <sup>^</sup>Ventana-Benchmark, Tucson, Arizona, U.S.A.; <sup>§</sup>Labvision/NeoMarkers, Fremont CA, USA. #Detected by “Universal alkaline phosphatase red detection system” (Ventana-Benchmark); °Detected by “Ultraview universal DAB detection system (Ventana-Benchmark)

### 1.2.3 RNA extraction and RT-PCR

Before proceeding with molecular analyses, a frozen section was obtained to assess the presence of the lesion in the tissue to be processed. Briefly, 5µm frozen sections were cut, collected on glass slide and stained with Haematoxylin and Eosin (H&E). After morphological evaluation the remnant of the sample was collected in RNAlater (Qiagen, Hilden, Germany) and then snap-frozen in liquid nitrogen and stored at -80°C.

For each sample 20-80 µg of frozen tissue was treated according to the RNeasy Protect Mini Kit protocol (QIAGEN, Hilden, Germany). RNA concentration was measured using the Quant-iT™ RNA kit (Invitrogen, Carlsbad, CA). The samples concentration was normalized to obtain a total quantity of RNA of about 500ng of each sample. cDNA synthesis was carried out using 9 µl of total RNA previously denatured at 65°C. Retrotranscription was performed at 37°C for 1 hour in a total volume of 20 µl in the presence of 300 ng of random primers (Invitrogen, Milan), 5U of RNase inhibitor (GE Healthcare, Milan), 0.5mM ΔNTPs (SIGMA, Milan), 10 mM DTT, and 200 U of MMLV (Invitrogen, Milan), followed by a denaturing step at 65 °C for 15 min to inactivate the reverse transcriptase.

#### **1.2.4 PCR and Nested-PCR**

The first PCR was performed using the primers reported in Table 1.2. ΔNp63ex3' and ΔNp63ex7out were used to identify the ΔNp73L, TAp63ex2 and TAp63ex5out for TAp63 isoforms. 200µM ΔNTPs (Sigma-Aldrich S.r.l., Italy), 1X buffer green (Roche, Mannheim, Germany), 0.2µM each primer, 1U FastStart Taq Polymerase (Roche, Mannheim, Germany) and 2µl of cDNA were put in a total reaction volume of 25 µl. After a first denaturation step at 95°C for four minutes, the reaction continued for 38 cycles of 95°C for 30s, 58°C for 1 min. and 72°C for 1 min. The final extension was 72°C for ten minutes. The second PCR was carried out changing the two antisense primers: ΔNp63ex6nst for ΔNp63 and TAp63ex5nst for TAp63. The reaction contained the same reagents of first PCR with the addition of only 1 µl of the first PCR product. The steps of reaction were the same of first PCR but not for number of cycle (33 instead of 38). The PCR products were run in a 3% agarose gel. A PCR for β-Actin analysis was performed

## 1.2 Material and Methods

as a reference control with the same conditions specified for p63 using the primers reported in Table 1.2 (ActBfw and ActBrv).

Name and Exon	Sequence (5'-3')
$\Delta$ Np63ex3' (sense)	ACCTggAAAACAATgCCCAGAC
$\Delta$ Np63ex7out (antisense)	TTCATCCCTCCAACACAACACTgC
TAp63ex2 (sense)	ACCCCAgCTCATTCTCTTggA
TAp63ex5out (antisense)	ggTggggTCATCACCTTgATCT
$\Delta$ Np63ex6nst (antisense)	gCATggCTgTTCCCCTCTACTC
TAp63ex5nst (antisense)	ATggggCATgTCTTTgCAATTT
ActBfw (sense)	TTgCCgACAaggATgCAgAAggA
ActBrv (antisense)	AggTggACA gCGAggCCAggAT

**Table 1.2: Primers used for PCR and nested-PCR analysis.**

### 1.2.5 Band purification and sequence analysis

To be sure that the bands visualized in the agarose gel correspond to isoforms under study we cut them off from the gel and sequenced. The bands were cut off and treated following the protocol of the MinElute Gel Extraction kit (QIAGEN, Hilden, Germany). Preparations of the  $\Delta$ NA sequencing reactions were performed in agreement with the CEQ2000 Dye Terminator Cycle Sequencing with Quick Start Kit (Beckman Coulter, Fullerton, CA, USA). After purification with the Agencourt CleanSEQ kit (Agencourt,

Beverly MA), the products were loaded on the CEQ2000 (Beckman Coulter, Fullerton, CA, USA).



### 1.3 RESULTS

All the patients were female, ranging in age from 37 to 83 years (mean 59.1 years). The samples under study included 15 normal breasts, 1 cystic disease with apocrine cyst, 2 fibroadenomas, 2 specimens containing predominantly epitheliosis (usual duct hyperplasia) and 20 carcinomas: 12 Invasive Ductal Carcinomas (IDC) (6 grade II, 6 grade III), 2 DIN/DCIS, 6 invasive lobular carcinomas (ILC), of which 3 were of the pleomorphic variety. All the carcinomas presented a “luminal” phenotype. Specifically all cases were positive for oestrogen and progesterone receptors and negative for keratin 14 (Tabs. 1.3-1.4).

Tissue	Number of specimens	p63 IHC*	p63 Isoforms (nested PCR)			
			$\Delta Np63$	$\Delta Np73L$	$TAp63$	$d4TAp63$
Normal	15	+	15/15	0/15	12/15	0/15
Apocrine Cyst	1	+	1/1	0/1	0/1	0/1
Fibroadenoma	2	+	2/2	0/2	2/2	0/2
Epitheliosis	2	+	2/2	0/2	1/2	0/2

**Table 1.3: Immunocytochemical and molecular findings in normal tissues and benign breast tissues.** \*positivity is limited to myoepithelial cells located around ducts and lobules.

Case	Sex/ Age	Diagnosis	Grade	pT	pN	IHC						p63 isoforms (nested PCR)			
						ER %	PR%	Ki67 %	HER2/ Neu	CK14	p63%*	ΔNp63	ΔNp73L	TAp63	d4TAp63
1	68	PILC	III	2	2A	80	70	12	2+	-	-	+	+	+	+
2	51	PILC	III	3	1A	70	-	15	-	-	-	+	+	+	-
3	66	PILC	III	1c	3	90	50	15	-	-	rare	+	-	+	-
4	75	ILC	II	2	0	80	-	15	3+	-	-	+	-	+	-
5	73	ILC	III	1c	1A	30	-	20	2+	-	-	+	-	+	+
6	50	ILC	II	1c	0	60	90	5	-	-	-	+	-	+	-
7	72	IDC	III	2	0	90	90	40	-	-	-	+	-	+	+
8	52	IDC	III	2	1A	60	50	25	3+	-	10%	+	+	+	+
9	56	IDC	II	2	2A	90	-	6	3+	-	rare	+	-	+	-
10	67	IDC	II	1c	2A	90	90	5	2+	-	-	+	-	-	-
11	37	IDC	II	1a	0	90	70	30	-	-	-	+	-	+	+
12	80	IDC	II	2	0	90	90	10	-	-	-	+	-	+	-
13	75	IDC	III	2	3A	80	15	20	3+	-	5%	+	-	+	+
14	74	IDC	III	1c	0	90	80	30	2+	-	rare	+	-	+	+
15	58	IDC	II	1b	0	90	50	15	1+	-	rare	+	+	+	+
16	53	IDC	III	2	3A	90	40	25	3+	-	-	+	-	+	+
17	49	IDC	III	2	1A	90	60	25	1+	-	-	+	-	+	+
18	53	IDC	II	1c	0	90	30	5	-	-	-	+	-	+	+
19	66	DCIS	III	/	/	np	np	np	np	np	np	+	-	-	-
20	58	DCIS	II	/	/	np	np	np	np	np	np	+	-	+	-

**Table 1.4: Histological, immunohistochemical and molecular findings in carcinomas.** ILC: Invasive Lobular Carcinoma; IDC: Invasive Ductal Carcinoma; DCIS: Ductal Carcinoma in Situ; PILC: Pleomorphic ILC; T: tumour ; N: lymph nodes ; \*percentage evaluate in neoplastic cells (excluding normal myoepithelial cells present); +: positive; -: negative; rare: up to 1% of positivity; Er: Oestrogen receptors; Pr: Progesterone receptors; CK: Cytokeratin; na: not available; ned: no evidence of disease; Met: distant metastases; Met<sup>o</sup>: distant metastases at presentation; np: not performed.

### 1.3.1 Immunohistochemical results

Normal breast and benign lesions (Table 1.3): the p63 and CK14 antibodies stained the nuclei and cytoplasm respectively of myoepithelial cells that were present in the ducts and acini. No staining was observed in luminal cells (Fig. 1.3).

Carcinomas (Table 1.4): in four cases p63 antibody stained the nuclei of rare (no more than 1%) neoplastic cells scattered through the invasive carcinoma. In two additional cases p63 antibody stained 5% (case 13) and 10% (case 8) of the neoplastic cells (Fig. 1.4). In this latter case p63 positive neoplastic cells were detected also in the related lymph node metastasis. No p63 positive cells were detected in the remaining 14 carcinomas. Myoepithelial cells of residual normal ducts, when present, in the different sections constituted internal positive controls.



**Figure 1.3: Case 1: Pleomorphic invasive lobular carcinoma.** Myoepithelial cells only stain for p63 in one entrapped non neoplastic small duct.

### 1.3 Results

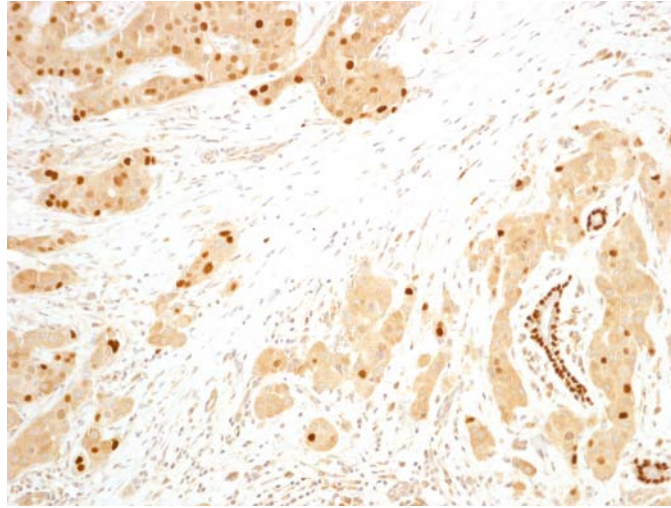


**Figure 1.4: Case 8: IDC grade III.** p63 stains myoepithelial cells of one entrapped non neoplastic small duct as well as 10% of nuclei of neoplastic elements.

#### 1.3.2 Nested PCR

Normal breast and benign lesions (Table 1.3): all samples expressed  $\Delta$ Np63, TAp63 or both isoforms at the same time.  $\Delta$ Np63 was expressed in all samples, while TAp63 was expressed in 15 out of 20 (75%) samples. The short variants,  $\Delta$ Np73L and d4TAp63, were never expressed.

Carcinomas (Table 1.4): all cases of in situ and invasive carcinomas expressed  $\Delta$ Np63, TAp63 or both isoforms at the same time.  $\Delta$ Np63 was expressed in all cases, while TAp63 in 18 out of 20 (90%) cases. The short isoforms appeared only in cases of invasive carcinomas, while were absent in the two DIN/DCIS. Specifically  $\Delta$ Np73L was expressed in 4 out of 18 (22%) cases and d4TAp63 in 11 out of 18 (61%) cases of IBC.

### 1.3.3 Sequencing

In all cases the sequences obtained from “normal band” (normal isoforms,  $\Delta Np63$  and TAp63), revealed the last aminoacid of exon 3 (Tryptophane) linked to the complete sequence of exon 4. Viceversa in IBC the electropherogram obtained from a lower band, revealed the last aminoacid of exon 3 linked to the complete sequence of exon 5, indicating that exon 4 was spliced out (Figs. 1.5 and 1.6).

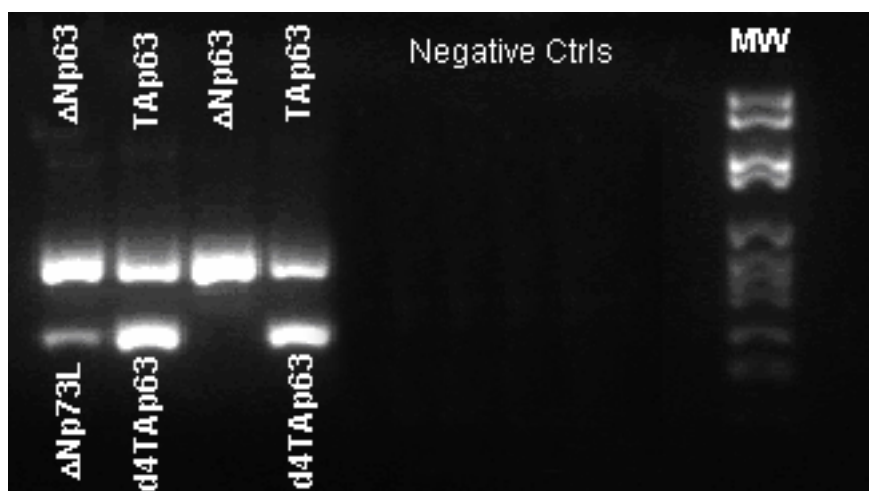


**Figure 1.5. Gel of p63 isoforms.** Lower bands represent the short isoforms (lacking exon 4), while upper bands represent the full-length isoforms. Ctrl: controls; MW: molecular weight marker ( $\Delta$ NA molecular weight marker VI, Roche Diagnostics Corporation, IN, USA).

## 1.3 Results

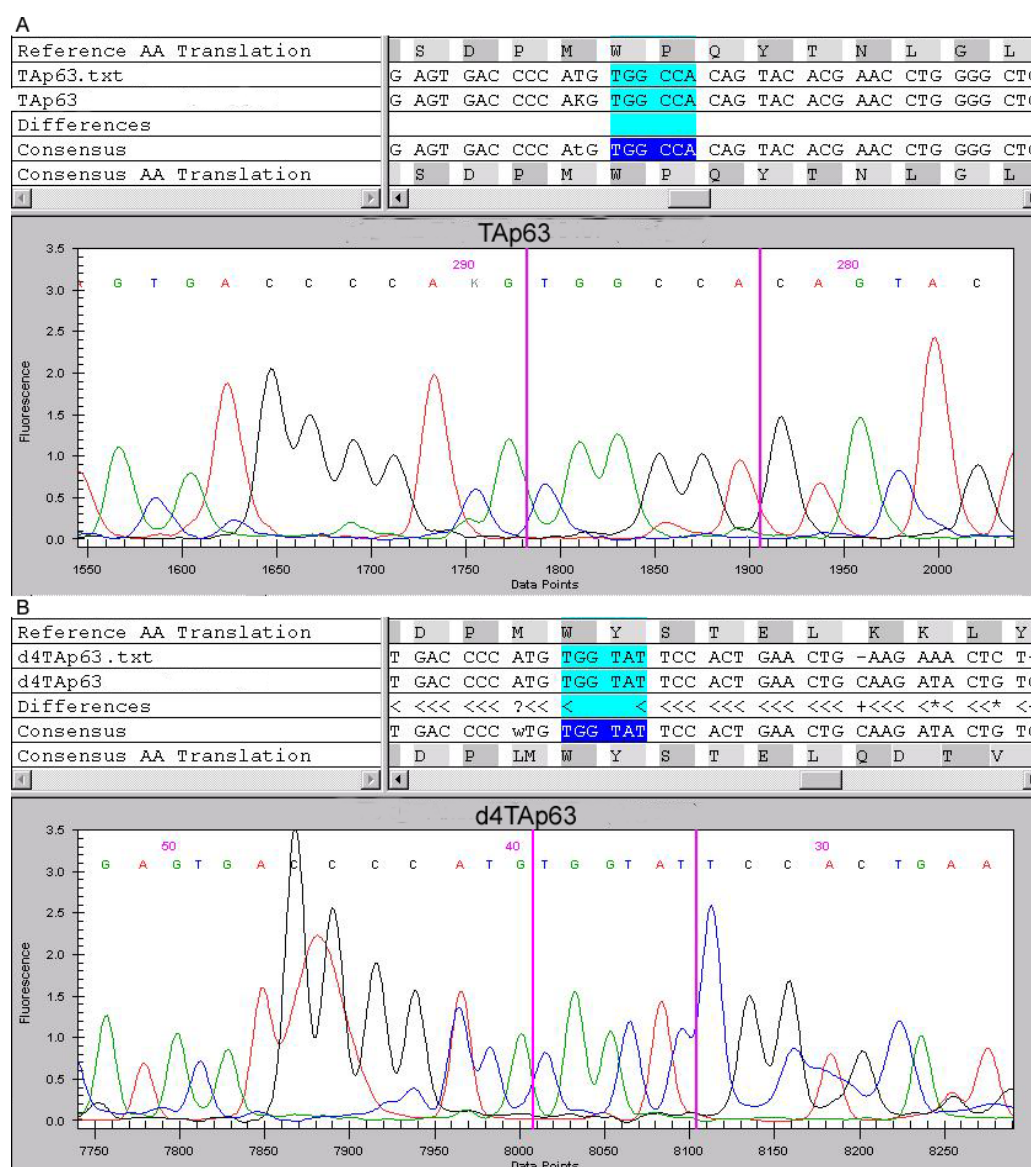


**Figure 1.6: Electropherogram of bands obtained after nested PCR.** (A) Sequences of full-length (TAp63) and (B) shorter isoform (d4TAp63). In shorter isoform sequence, it is possible to observe as Tryptophan (last aminoacid of exon 3) is followed by the sequence of exon 5 (starting with a Tyrosine) and not by a Proline (first aminoacid of exon 4).

### 1.3.4 Relation between nested PCR results and clinical, morphological and immunohistochemical data

The four invasive carcinomas presenting the  $\Delta$ Np73L isoform were histologically diagnosed as IDC in two cases (grade III and grade II respectively) and ILC, pleomorphic type (grade III) in the remaining two. Three out of these 4 (75%) cases that expressed  $\Delta$ Np73L, had lymph node metastases at presentation (Table 1.4).

It is pertinent to emphasize that immunohistochemistry was less sensitive as p63 positivity was detected in the two cases of IDC only (table 4, cases 8 and 15).

d4TAp63 (Table 1.4) isoform was observed in 11 out of 18 (61%) cases of invasive carcinoma which were two ILC (cases 1, 5) and nine IDC (cases 7, 8, 11, 13, 14-18). Six cases (55%) had lymph node metastases. On immunohistochemistry p63 positivity was observed in four cases (cases 8, 13, 14, 15).



## 1.4 DISCUSSION AND CONCLUSIONS

In the present study 40 specimens from normal breast, benign lesions, DIN/DCIS, and invasive carcinomas were analyzed by immunohistochemistry and RT-PCR (Reverse Transcriptase-PCR) in order to disclose the patterns of p63 expression.

Immunopositivity for p63 in invasive carcinomas of the breast has been described in myoepithelial, metaplastic and some salivary-like carcinomas [39, 40, 45, 46]. p63 was found to be positive in 55.5% of basal-like carcinoma of the breast [47], while a much lower positivity that ranged from 0.6% to 19.5% was observed in “ordinary” luminal type invasive carcinomas [21, 45, 47]. The present cases were all luminal type invasive carcinomas [44, 46], negative for CK14. With the exception of four cases that contained rare positive cells and two in which p63 positivity was found in 5% and 10% of the neoplastic cells, the remaining invasive carcinomas were devoid of p63 immunostaining.

In normal breast, in benign lesions and in the 2 cases of DIN/DCIS immunohistochemistry for p63 stained myoepithelial cells only. In addition the full-length isoforms (with exon 4),  $\Delta$ Np63 and TAp63, were detected at molecular level, suggesting that the full length isoforms detected by PCR are most probably expressed by normal myoepithelial cells.

On the contrary, the full length isoforms were consistently found at molecular level in all invasive carcinomas at variance with immunohistochemistry that stained for p63 only occasional cells in 6 cases. These discrepant data between molecular and immunohistochemical techniques are more likely consequent to the fact that PCR is a sensitive technique that reveals isoforms even if expressed in small quantity.

Invasive carcinomas in addition showed in 12 cases one of the two or both short isoforms ( $\Delta$ Np73L and d4TAp63, lacking exon 4). This parallel other malignant lesions

## 1.4 Discussion

from other organs such as salivary gland carcinomas [28] and squamous cell carcinomas of oral cavity [14, 48], where the two short-isoforms appear only in tumoural cells.

Therefore, it seems from the present data that IBC with luminal phenotype can express p63, especially in its altered forms. The fact that short isoforms were not found in DIN/DCIS (admittedly two cases only) might indicate that these same isoforms are sign of tumoural progression.

In conclusion it appears that:

- 1- The full-length isoforms can be detected in non neoplastic and neoplastic lesions at molecular level.
- 2- The short isoforms that lack exon 4 are only present in the neoplastic cells of invasive carcinomas.
- 3- Presence of p63 in invasive carcinomas of luminal type as seen at molecular level suggests caution to include p63 as a specific marker of basal-like carcinomas.

## REFERENCES

1. Barbieri, C.E. and J.A. Pietenpol, *p63 and epithelial biology*. Exp Cell Res, 2006. **312**(6): p. 695-706.
2. Yang, A., et al., *p63, a p53 homolog at 3q27-29, encodes multiple products with transactivating, death-inducing, and dominant-negative activities*. Mol Cell, 1998. **2**(3): p. 305-16.
3. Augustin, M., et al., *Cloning and chromosomal mapping of the human p53-related KET gene to chromosome 3q27 and its murine homolog Ket to mouse chromosome 16*. Mamm Genome, 1998. **9**(11): p. 899-902.
4. Osada, M., et al., *Cloning and functional analysis of human p51, which structurally and functionally resembles p53*. Nat Med, 1998. **4**(7): p. 839-43.
5. Levrero, M., et al., *The p53/p63/p73 family of transcription factors: overlapping and distinct functions*. J Cell Sci, 2000. **113** ( Pt 10): p. 1661-70.
6. Strano, S., et al., *From p63 to p53 across p73*. FEBS Lett, 2001. **490**(3): p. 163-70.
7. Moll, U.M. and N. Slade, *p63 and p73: roles in development and tumor formation*. Mol Cancer Res, 2004. **2**(7): p. 371-86.
8. Bourdon, J.C., et al., *p53 isoforms can regulate p53 transcriptional activity*. Genes Dev, 2005. **19**(18): p. 2122-37.
9. Schultz, J., et al., *SAM as a protein interaction domain involved in developmental regulation*. Protein Sci, 1997. **6**(1): p. 249-53.
10. Thanos, C.D. and J.U. Bowie, *p53 Family members p63 and p73 are SAM domain-containing proteins*. Protein Sci, 1999. **8**(8): p. 1708-10.
11. Chi, S.W., A. Ayed, and C.H. Arrowsmith, *Solution structure of a conserved C-terminal domain of p73 with structural homology to the SAM domain*. EMBO J, 1999. **18**(16): p. 4438-45.
12. Serber, Z., et al., *A C-terminal inhibitory domain controls the activity of p63 by an intramolecular mechanism*. Mol Cell Biol, 2002. **22**(24): p. 8601-11.
13. Lee, H.O., et al., *A dominant negative form of p63 inhibits apoptosis in a p53-independent manner*. Biochem Biophys Res Commun, 2006. **344**(1): p. 166-72.
14. Foschini, M.P., et al., *Pattern of p63 expression in squamous cell carcinoma of the oral cavity*. Virchows Arch, 2004. **444**(4): p. 332-9.
15. Urist, M.J., et al., *Loss of p63 expression is associated with tumor progression in bladder cancer*. Am J Pathol, 2002. **161**(4): p. 1199-206.
16. Mills, A.A., et al., *p63 is a p53 homologue required for limb and epidermal morphogenesis*. Nature, 1999. **398**(6729): p. 708-13.
17. Yang, A., et al., *p63 is essential for regenerative proliferation in limb, craniofacial and epithelial development*. Nature, 1999. **398**(6729): p. 714-8.
18. van Bokhoven, H. and H.G. Brunner, *Splitting p63*. Am J Hum Genet, 2002. **71**(1): p. 1-13.
19. Di Como, C.J., et al., *p63 expression profiles in human normal and tumor tissues*. Clin Cancer Res, 2002. **8**(2): p. 494-501.
20. Kaufmann, O., et al., *Value of p63 and cytokeratin 5/6 as immunohistochemical markers for the differential diagnosis of poorly differentiated and undifferentiated carcinomas*. Am J Clin Pathol, 2001. **116**(6): p. 823-30.
21. Reis-Filho, J.S., et al., *Distribution of p63, cytokeratins 5/6 and cytokeratin 14 in 51 normal and 400 neoplastic human tissue samples using TARP-4 multi-tumor tissue microarray*. Virchows Arch, 2003. **443**(2): p. 122-32.

## References

22. Gaiddon, C., et al., *A subset of tumor-derived mutant forms of p53 down-regulate p63 and p73 through a direct interaction with the p53 core domain*. Mol Cell Biol, 2001. **21**(5): p. 1874-87.
23. Parsa, R., et al., *Association of p63 with proliferative potential in normal and neoplastic human keratinocytes*. J Invest Dermatol, 1999. **113**(6): p. 1099-105.
24. Hall, P.A., et al., *Expression of the p53 homologue p63alpha and deltaNp63alpha in normal and neoplastic cells*. Carcinogenesis, 2000. **21**(2): p. 153-60.
25. Yang, A. and F. McKeon, *P63 and P73: P53 mimics, menaces and more*. Nat Rev Mol Cell Biol, 2000. **1**(3): p. 199-207.
26. Glickman, J.N., et al., *Expression of p53-related protein p63 in the gastrointestinal tract and in esophageal metaplastic and neoplastic disorders*. Hum Pathol, 2001. **32**(11): p. 1157-65.
27. Choi, H.R., et al., *Differential expression of p53 gene family members p63 and p73 in head and neck squamous tumorigenesis*. Hum Pathol, 2002. **33**(2): p. 158-64.
28. Foschini, M.P., et al., *p63 expression in salivary gland tumors: role of DeltaNp73L in neoplastic transformation*. Int J Surg Pathol., 2005. **13**(4): p. 329-35.
29. Pelosi, G., et al., *p63 immunoreactivity in lung cancer: yet another player in the development of squamous cell carcinomas?* J Pathol, 2002. **198**(1): p. 100-9.
30. Reis-Filho, J.S., et al., *p63 expression in normal skin and usual cutaneous carcinomas*. J Cutan Pathol, 2002. **29**(9): p. 517-23.
31. Reis-Filho, J.S. and F.C. Schmitt, *Taking advantage of basic research: p63 is a reliable myoepithelial and stem cell marker*. Adv Anat Pathol, 2002. **9**(5): p. 280-9.
32. Barbareschi, M., et al., *p63, a p53 homologue, is a selective nuclear marker of myoepithelial cells of the human breast*. Am J Surg Pathol, 2001. **25**(8): p. 1054-60.
33. Wang, X., et al., *Metaplastic carcinoma of the breast: p53 analysis identified the same point mutation in the three histologic components*. Mod Pathol, 2001. **14**(11): p. 1183-6.
34. Koker, M.M. and C.G. Kleer, *p63 expression in breast cancer: a highly sensitive and specific marker of metaplastic carcinoma*. Am J Surg Pathol, 2004. **28**(11): p. 1506-12.
35. Wang, X., et al., *p63 expression in normal, hyperplastic and malignant breast tissues*. Breast Cancer, 2002. **9**(3): p. 216-9.
36. Ribeiro-Silva, A., et al., *p63 correlates with both BRCA1 and cytokeratin 5 in invasive breast carcinomas: further evidence for the pathogenesis of the basal phenotype of breast cancer*. Histopathology, 2005. **47**(5): p. 458-66.
37. Perou, C.M., et al., *Molecular portraits of human breast tumours*. Nature, 2000. **406**(6797): p. 747-52.
38. Senoo, M., et al., *Transcriptional dysregulation of the p73L / p63 / p51 / p40 / KET gene in human squamous cell carcinomas: expression of Delta Np73L, a novel dominant-negative isoform, and loss of expression of the potential tumour suppressor p51*. Br J Cancer., 2001. **84**(9): p. 1235-41.
39. Barbareschi, M., et al., *p63, a p53 homologue, is a selective nuclear marker of myoepithelial cells of the human breast*. Am J Surg Pathol., 2001. **25**(8): p. 1054-60.

40. Reis-Filho, J.S., et al., *Distribution of p63, a novel myoepithelial marker, in fine-needle aspiration biopsies of the breast: an analysis of 82 samples*. *Cancer.*, 2003. **99**(3): p. 172-9.
41. Tavassoli, F.A. and P. Devilee, *WHO. Pathology and Genetics of Tumours of the Breast and Female Genital Organs*. 3rd ed. 2003, Lyon: IARC Press.
42. Elston, C.W. and I.O. Ellis, *Pathological prognostic factors in breast cancer. I. The value of histological grade in breast cancer: experience from a large study with long-term follow-up*. *Histopathology.*, 2002. **41**(3A): p. 154-161.
43. Eusebi, V., F. Magalhães, and J.G. Azzopardi, *Pleomorphic lobular carcinoma of the breast: an aggressive tumor showing apocrine differentiation*. *Hum Pathol*, 1992. **23**: p. 655-662.
44. Rakha, E.A., et al., *Morphological and immunophenotypic analysis of breast carcinomas with basal and myoepithelial differentiation*. *J Pathol.*, 2006. **208**(4): p. 495-506.
45. Koker, M.M. and C.G. Kleer, *p63 expression in breast cancer: a highly sensitive and specific marker of metaplastic carcinoma*. *Am J Surg Pathol.*, 2004. **28**(11): p. 1506-12.
46. Tavassoli, F.A. and V. Eusebi, *Tumors of mammary gland*. 2009, Washington, DC: AFIP Atlas of Tumor Pathology. 238-240.
47. Matos, I., et al., *p63, cytokeratin 5, and P-cadherin: three molecular markers to distinguish basal phenotype in breast carcinomas*. *Virchows Arch.*, 2005. **447**(4): p. 688-694.
48. Foschini, M.P., et al., *E-cadherin loss and Delta Np73L expression in oral squamous cell carcinomas showing aggressive behavior*. *Head Neck.*, 2008. **30**(11): p. 1475-1482.



## **2. GENETIC HETEROGENEITY IN METAPLASTIC BREAST CARCINOMAS**



## 2. GENETIC HETEROGENEITY IN METAPLASTIC BREAST CARCINOMAS

### 2.1 INTRODUCTION

#### 2.1.1 Metaplastic Breast carcinoma

Most benign and malignant tumours of the breast arise from glandular epithelium. However, in some cases glandular epithelium differentiates into nonglandular tissue, a process called metaplasia. Although both the basis and true incidence of this process is unknown because it often is not reported when it occurs microscopically, such differentiation may become such a significant component of the tumour as to characterize it as a distinct entity for purposes of diagnosis and treatment. Oberman proposed the term metaplastic carcinoma to account for all mixed carcinomas of the breast. Metaplastic carcinomas of the breast are a heterogeneous group of neoplasms which exhibit varied patterns of metaplasia and differentiation along multiple cell lines [1].

*Histopathological findings.* Metaplastic carcinoma comprises a heterogeneous group of neoplasms generally characterized by an intimate admixture of adenocarcinoma with areas of spindle, squamous, chondroid, and osseous differentiation; the metaplastic spindle and squamous carcinomas may be present in pure form, without any recognizable adenocarcinoma component. Either purely epithelial or with a mesenchymal component, classification according to the apparent phenotype of the tumour is now required and immunohistochemical confirmation is necessary (Table 2.1) [2].

---

**CLASSIFICATION OF METAPLASTIC CARCINOMA**

---

**Purely Epithelial Carcinoma**

Squamous Carcinoma

Large cell type, keratinizing or nonkeratinizing

Squamous carcinoma with spindle cell metaplasia  
(with or without acantholytic changes)

Adenosquamous Carcinoma

High Grade

Low Grade

Adenocarcinoma with Spindle Cell Metaplasia

**Mixed Epithelial and Mesenchymal Carcinoma**

Carcinoma with chondroid differentiation

Carcinoma with osseous differentiation

Carcinoma with rhabdomyosarcomatous component

Carcinosarcoma

---

**Table 2.1: Classification of Metaplastic Carcinomas**

In FNA (Fine Needle Aspiration) smears, only 57% of cases show ductal carcinoma and metaplastic components. Thus, in almost one half of cases, the diagnosis is not possible by FNA [3, 4]. The diagnosis of metaplastic breast carcinoma often requires immunohistochemistry with a cytokeratin panel to distinguish such cases from phyllodes tumours, primary sarcomas, and fibromatoses [5]

*Clinical findings.* Metaplastic carcinoma of the breast occurs in less than 5% of breast carcinoma patients [6] and has an uncertain prognostic significance. Tavassoli [7] reported an incidence of less than 1% and Smith et al. [8] 0.02% for this type of tumour.

First described by Huvos et al. [9], the average age of the patients with metaplastic carcinoma, the clinical presentation, and the overall 5-year survival rate of 55% were similar to such findings in patient with regular infiltrating duct carcinoma. When patients with tumours showing spindle and squamous differentiation were combined in one group, they had a 63 percent 5-year survival rate and 56 percent of the women had axillary node metastases. Only 19 percent of patients with neoplasms showing osseous and chondroid

differentiation had axillary node metastases and their 5-year survival rate was 28 percent [2].

Oberman suggested that all these tumours be categorized as metaplastic carcinoma of the breast, deemphasizing whether the metaplastic component is of mesenchymal or epithelial origin [6].

Metaplastic carcinomas are usually not associated with oestrogen or progesterone receptors. As in other carcinomas, tumour size appears to be important. Axillary lymph node involvement is reported in 6% [10], 26% [11], and 25–30% [12] of cases. As with other breast carcinomas, these tumours have a high metastatic potential despite frequently negative lymph nodes, as observed in several studies [11, 13, 14]. Most published data on metastases of metaplastic carcinoma have shown haematogenous (lung and bone) metastases rather than lymphatic spread [6, 10, 15].

*Prognosis.* The precise histogenesis and prognosis of metaplastic carcinomas is still poorly understood, although some studies have shown a good prognosis in a relatively short follow-up period [16, 17]. Duration of symptoms, TNM stage, tumour size, and axillary nodal status were significant prognostic factors of survival [2]. However, a Mayo Clinic study showed that only age and prior oestrogen use were found to be significantly associated with either free or overall survival [14]. Clinic were more commonly (87%) node negative at presentation, and had a 3-year overall survival rate of 71%. Women older than 60 years at diagnosis were found to have an increased disease-free survival time compared to those less than 60 years old, but no difference in overall survival was found. About 50% of the women developed metastases.

*Therapy.* There is little information available on the efficacy of current therapies in the management of metaplastic carcinoma. Most studies that have addressed treatment of these lesions have not separated the subtypes, unfortunately. Anyway it appears that

## 2.1 Introduction

metaplastic breast carcinomas are less responsive to therapy with the conventional regimens used for typical adenocarcinoma of the breast [2]. This is particularly true in case of metastatic disease. Rayson et al. reported the median survival from detection of metastatic disease as 8 months, using systemic treatment [14]. Wargotz et al. [10], also found no survival advantage for patients treated either by chemotherapy or radiation for distant metastases. These data suggest that patients with metastatic metaplastic breast carcinoma may be candidates for innovative chemotherapeutic regimens as first-line therapy for metastatic disease [2]. Based on a smaller number of cases, others have advocated that surgical and adjuvant therapy should follow the guidelines used for common breast cancers.

### 2.1.2 Intra-tumour heterogeneity

Several lines of evidence indicate that cancers may be composed of multiple sub-modal clones harbouring the same initiating genetic changes followed by the acquisition of additional divergent genetic hits [18]. The existence of such non-modal populations harbouring distinct genetic aberrations may explain the phenotypic diversity observed within a given tumour [19]. Furthermore, disease progression and resistance to chemo- and targeted therapies may occur due to the selection of sub-clones harbouring specific genetic aberrations that render them more aggressive and insensitive to treatment [19-21].

Apart from the existence of genetically distinctive non-modal populations, intra-tumour phenotypic diversity can be explained by non-genetic mechanisms, including epigenetic regulation of genes and molecular networks, epithelial-to-mesenchymal transition, interaction with specific niches and tumour microenvironment [19, 22-25], and by the ‘cancer stem cell’ hypothesis [26-30]. This hypothesis proposes that the intra-tumour heterogeneity stems from and is maintained by a small population of cells (the so-

called ‘cancer stem cells’), which give rise to more differentiated cells and thus create the phenotypic diversity of tumours [19, 26-28].

Intra-tumour morphological heterogeneity is not uncommon in breast cancer. It can often be appreciated in mixed carcinomas, which are characterised by distinct histological growth patterns admixed together, and in metaplastic breast carcinomas, which are defined by the presence of areas composed of cells with divergent morphological differentiation, towards squamous epithelium or mesenchymal elements [31]. The vast majority of metaplastic breast carcinomas are of basal-like molecular subtype (>90%) [31, 32] and harbour *TP53* mutations in >70% of the cases [33].

### 2.1.3 Micro-Array CGH

Microarray-based comparative genomic hybridization (aCGH) was developed in the late 1990s and brought with it the advantages of rapid, high-resolution screening of entire genomes.

Microarray-based CGH (array-CGH, aCGH) is a technique that provides detailed characterisation of numerical DNA aberrations in a genome-wide fashion [34], such as aneuploidy, unbalanced translocations, amplifications and deletions [35]

From a technical point of view, a test (tumour) and reference (normal genomic) DNA are differentially labelled with green and red fluorescent dyes, mixed in a 1:1 ratio in the presence of human cot-1 DNA in order to block repetitive sequences, and co-hybridized to a representation of the genome, i.e. a platform composed of DNA inserts spaced throughout the whole genome in predefined intervals. Specialized image analysis softwares coupled with a dedicated scanner are then used to capture the images and convert hybridization intensity data to a red–green ratio profile [34].

## MICROARRAY-CGH, THE TECHNIQUE

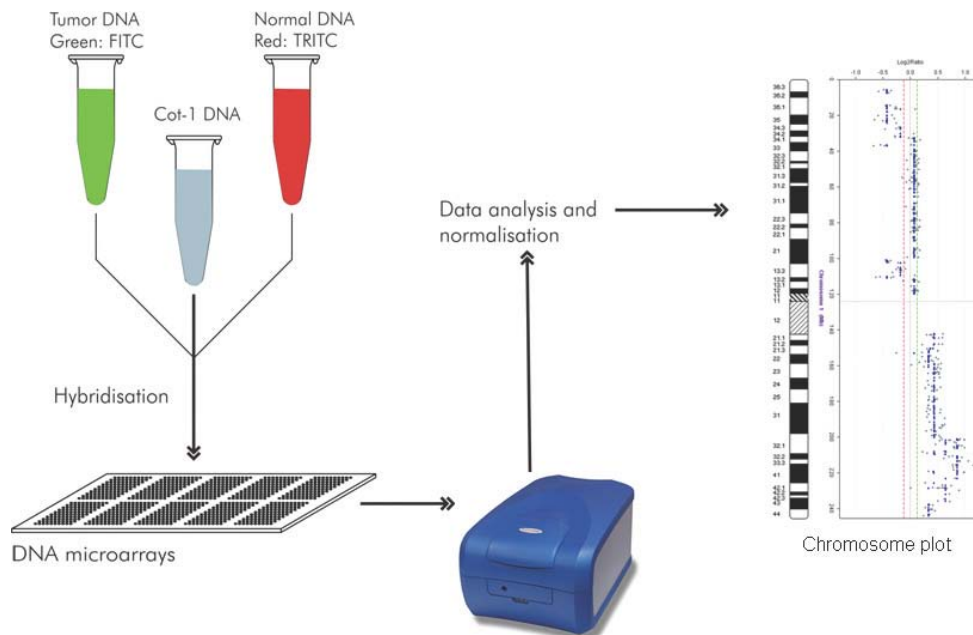


**Figure 2.1:** Schematic representation of the microarray-CGH technique. The test (tumour) and the reference (normal genomic) DNA are differentially labelled with green and red fluorescent dyes, mixed in a 1:1 ratio in the presence of human cot-1 DNA (to block repetitive sequences), and finally co-hybridized to a chip of a given platform. Specialized image analysis softwares coupled with a dedicated scanner are then used to capture the images and convert hybridization intensity data to a red–green ratio profile. Representation of the genomic changes of a given sample can be visualised either throughout the genome (genome plot) or chromosome by chromosome (see chromosome plot on the right hand side).

Deviations from a 1:1 ratio are counted as a significant change in DNA copy number when defined thresholds are crossed and statistical verification applied.

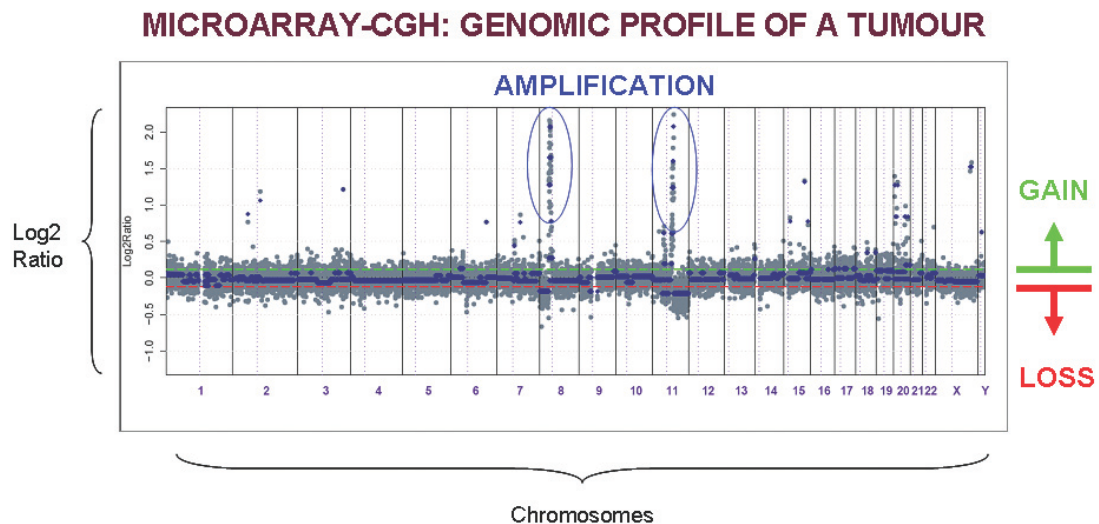


**Figure 2.2:** Example of a genome plot illustrating the genomic profile of a breast cancer using a BAC array platform. Log<sub>2</sub> ratios are plotted on the Y axis against each clone according to genomic location on the X axis.

A plethora of different aCGH platforms are currently available, most of them can be obtained commercially and each of them displays both advantages and drawbacks (for a comprehensive discussion of these technologies see [36]). The platform used in the present study is a BAC array platform, ie a platform composed of bacterial artificial chromosomes (BACs) containing sequence-verified, fluorescent *in situ* hybridization (FISH)-mapped DNA inserts spaced throughout the whole genome in predefined intervals. Bacterial artificial chromosomes are large-insert genomic clones which have been widely used in aCGH studies [37-39]. BAC probes vary in length from 100 to 200 kb and the resolution of each BAC array is defined by the number of unique probes it contains. The probe content of genome-wide BAC arrays range from a few hundreds to approximately 32,000 unique elements (tiling path array, as the one used in this study). Tiling path arrays (that is, arrays where each BAC overlaps with its contiguous BACs) provide a resolution of up to approximately 50 kb, given that a genomic change can only be detected if it is sufficiently big to significantly change the hybridisation intensity in one of the channels (that is, change the red:green ratios). These platforms provide

## 2.1 Introduction

sufficiently intense signals for the detection of single-copy number changes, are able to accurately define the boundaries of genomic aberrations and, importantly, can be readily applied to DNA extracted from archival formalin-fixed paraffin-embedded (FFPE) tissue as well [40, 41]. One of the main drawbacks with BAC arrays is their limited availability from commercial sources and the expensive and highly labour-intensive in-house production.

### 2.1.4 Array - CGH and the identification of new targets in breast cancer

In the past years conventional and array-based CGH has helped characterise the relationship between putative breast cancer precursors and invasive carcinoma, define the molecular genetic pathways of breast cancer, as well as the typical genetic changes of different types of breast cancers, but most importantly has contributed to the identification of genomic regions harbouring oncogenes that might be activated in specific breast cancer histological subtypes [34, 42]. Putative therapeutic targets for specific subgroups of breast cancer have been recently found. As an example, a recurrent amplification of 8p11.2-p12 has been identified in classic lobular breast carcinomas [43]. By applying array CGH and expression analysis to breast cancer cell lines, the cell line MDA-MB-134 that harbours a simple karyotype, deletion of 16q and E-cadherin inactivation (hallmark features of lobular breast carcinomas) was identified. In addition, this cell line displayed an amplification on 8p11.2-p12 remarkably similar to that found in lobular carcinomas. By subjecting the MDA-MB-134 cell line and control cell lines to gene expression profiling, *FGFR1* was identified as a putative amplicon driver of the region. Most importantly, functional analysis with RNA interference and with chemical compounds against FGFR1 revealed that MDA-MB-134 cells are dependent on signalling by the tyrosine kinase receptor. These findings suggest FGFR1 may be a therapeutic

target in lobular carcinomas. Subsequent analysis of a large series of ER-positive cancers demonstrated that *FGFR1* amplification is also an independent predictor of outcome in this group of cancers [44].

A putative therapeutic target has recently identified also in metaplastic carcinomas, a specific subtype of basal-like carcinomas, known not to express hormone receptors or HER2, to have a poor prognosis and not to respond to conventional chemotherapy regimens. Hence, the identification of novel therapeutic targets for these tumours would be invaluable. Approximately 2/3 of metaplastic breast cancers show EGFR overexpression, however, EGFR overexpression *per se* has been reported to be a poor predictor of response to specific therapy such as EGFR tyrosine kinase inhibitors; on the other hand, *EGFR* activating mutations and/ or gene amplification have been shown to be associated with increased response to these agents [45-49]. The presence of *EGFR* gene mutations and amplification has been recently investigated and *EGFR* gene amplification was found in approximately 25% of EGFR overexpressing cases, whereas no activating mutations could be detected. Although overexpression was much more pervasive than gene amplification, a significant correlation between *EGFR* amplification and overexpression was observed [50]. Currently, studies testing whether EGFR tyrosine kinase inhibitors are effective in *EGFR* amplified breast cancer models are currently being carried on. If addition to EGFR signalling will be proven in this subgroup of breast cancers, EGFR inhibitors or antibodies against EGFR may emerge as a novel targeted therapy for these patients.

The above markers identified first by aCGH are not ready for prime time as yet, however, these studies provide an algorithm for the identification of putative oncogenes that can be targeted based on the principle of oncogene addiction (which proposes that

## 2.1 Introduction

although cancers are affected by multiple genetic and epigenetic abnormalities, they are dependent on one or few genes for maintenance of the malignant phenotype [51]) and they exemplify the way molecular genetics may contribute to individualised therapy for breast cancer patients. Furthermore, given that the expression of the above genes seems to be driven by an increase in copy number, the identification of patients who may benefit from drugs targeting FGFR1 or EGFR can be performed by methods that are more palatable for diagnostic pathologists, such as a combination of *in situ* hybridisation, either chromogenic or fluorescent, and immunohistochemical analysis.

To determine the existence of intra-tumour genetic heterogeneity in breast cancers and whether areas with distinct morphological features in a given tumour might be underpinned by distinct patterns of genetic aberrations, we analysed six metaplastic breast carcinomas with at least two morphologically distinct components. In this proof of principle study, the components of each case were microdissected separately and subjected to high-resolution microarray-based comparative genomic hybridisation (aCGH) analysis, using a validated 32K bacterial artificial chromosome (BAC) array platform [52], followed by immunohistochemistry. Although in the majority of the cases, the distinct components displayed similar genomic and immunophenotypic profiles, in two cases our analysis revealed significant differences, with specific genetic alterations in the distinct components, providing direct evidence of intra-tumour genetic heterogeneity.

## 2.2 MATERIAL AND METHODS

### 2.2.1 Case selection

47 cases of metaplastic breast carcinomas from the pathology files of the Royal Marsden Hospital, London, UK were retrieved. All cases were reviewed by two pathologists and only cases with  $\geq 2$  morphologically distinct components, which were of sufficient dimensions to be microdissected independently, were retrieved. Out of the 47 cases, 9 had areas that were of sufficient dimensions to be independently microdissected without any contamination by cells of the other component(s); however 3 of these cases were excluded due to DNA of insufficient yield or quality for downstream analysis. The final series included in this study comprised six metaplastic breast carcinomas with at least two morphologically distinct components, of which one also had a matched axillary lymph node metastasis present at time of diagnosis.

All morphologically distinct components but the chondroid component of case 4 and the lobular component of case 5 were of histological grade 3 as defined by the Nottingham grading system [53] (Table 2.2). None of the patients received chemotherapy prior to the excision of the primary tumours and lymph node metastasis.

## 2.2 Material and Methods

Case	Component	Histological Grade <sup>o</sup>
1	chondroid spindle	3
		3
2	chondroid spindle rhabdoid	3
		3
3	epithelial chondroid	3
		3
4	chondroid spindle	2
		3
5	squamous lobular	3
		2
6	ductal	3
	squamous	3
	spindle	3
	metastasis	3

**Table 2.2: Morphologically distinct components of six metaplastic breast carcinomas.** <sup>o</sup> Nottingham grading system.

### 2.2.2 Microdissection and Nucleic Acids Extraction

The distinct components from each case were separately microdissected to ensure >90% of purity of neoplastic cells. Microdissection was performed with a sterile needle under a stereomicroscope (Olympus SZ61, Tokyo, Japan) from ten consecutive 8 µm thick representative sections of the tumours stained with nuclear fast red as previously described [54]. In addition, we extracted DNA from ten consecutive sections of morphologically confirmed adjacent normal breast from each case. DNA was extracted using the DNeasy Kit (Qiagen Ltd, Crawley, UK) according to the manufacturer's recommendations. DNA concentration was measured with the PicoGreen<sup>®</sup> assay as per the manufacturer's instructions (Invitrogen, Paisley, UK) [54]. RNA from case 6 was extracted from whole tissue sections characterised by only one of the distinct morphological components with RNeasy FFPE Kit (Qiagen Ltd, Crawley, UK) according to the manufacturer's recommendations.

### 2.2.3 Microarray Comparative Genomic Hybridisation

The 32K BAC re-array collection (CHORI) tiling path aCGH platform used for this study was constructed at the Breakthrough Breast Cancer Research Centre (Institute of Cancer Research, London - UK). This platform comprises >32,000 clones, spotted onto Corning GAPSII coated glass slides (Corning, NY, USA) (Fig. 2.3). This type of BAC array platform has been shown to be as robust as and to have comparable resolution with high density oligonucleotide arrays [55].

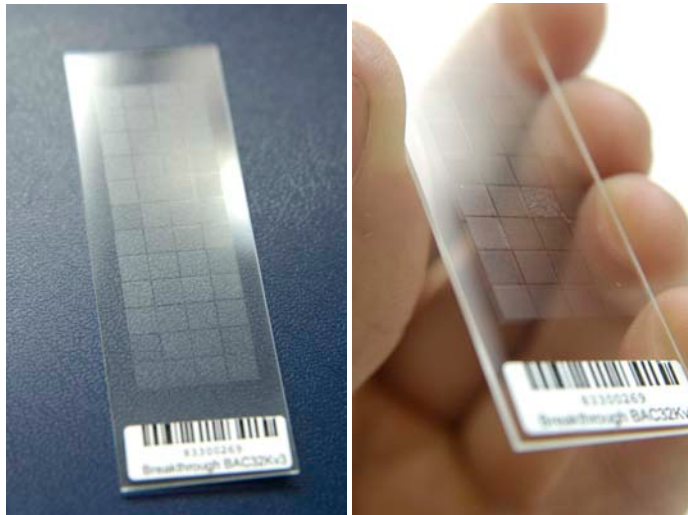


**Figure 2.3: Microarray chip** pertaining to the 32K BAC re-array collection (CHORI) tiling path aCGH platform constructed in the Breakthrough Breast Cancer Research Centre. The chip contains >32,000 clones, spotted onto Corning GAPSII coated glass slides (Corning, NY, USA). The images are courtesy of the Breakthrough Breast Cancer Research Centre (London, UK).

*DNA labelling and array hybridisation.* No whole genome DNA amplification was performed. DNA labelling, array hybridisations and image acquisition were performed as follows [56, 57]: reference (normal DNA extracted from blood lymphocytes pooled from 24 females) and tumour DNA samples (300 ng aliquots) were labelled with Cy3- or Cy5-conjugated dCTP respectively (Amersham Biosciences, Buckinghamshire, UK) using random primed BioPrime DNA labelling (Invitrogen Life Technologies) according to the manufacturer's protocol, modified to incorporate 1.0 mM Cy dye, 0.6 mM dCTP and 1.2 mM dATP, dGTP and dTTP. After labelling at 37 °C for 16 h, non-incorporated reaction constituents were removed by MinElute Reaction Cleanup (Qiagen Ltd, Crawley, UK).

## 2.2 Material and Methods

Labelled reference and tumour DNA were co-ethanol precipitated with 100 µg human Cot-1 DNA (Invitrogen Life Technologies) and re-suspended in 45 µl hybridisation buffer (50% deionised formamide, 10% w/v dextran sulphate, 2× SSC, 2% SDS, 20 µg yeast tRNA). Labelled DNA was denatured at 70 °C for 15 min, followed by a 30 min incubation at 37°C to allow blocking of repetitive sequences by human Cot-1 DNA. Denatured DNA samples were applied to the microarray under a coverslip and hybridised at 37 °C for 18 h. After hybridisation, the coverslips were removed by washing slides in 2× SSC/1% SDS for 15 min at 45 °C. Slides were then washed in 50% deionised formamide/2× SSC for 15 min at 45 °C, followed by 2× SSC/1% SDS for 30 min at 45 °C and twice in 0.2× SSC for 15 min at room temperature. After washing, the arrays were dried by centrifugation at 2000 r.p.m. for 2 min. aCGH slides were scanned using an Axon 4000B scanner (Axon Instruments, Burlingame, CA, USA) and images were processed using Genepix Pro 4.0 image analysis software (Axon Instruments) (Fig. 2.4).

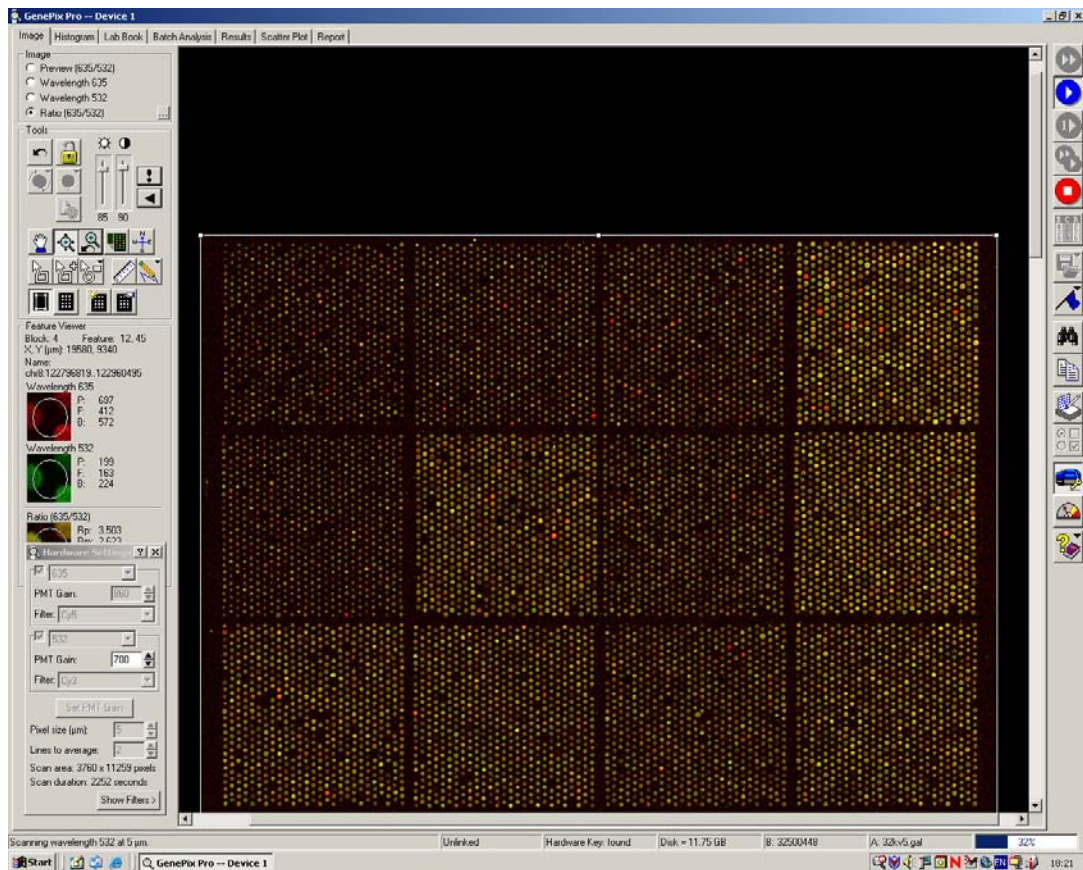


**Figure 2.4:** Screen shot of a chip during scanning using Axon 4000B scanner and GenePix Pro 4.0 image analysis software (Axon Instruments).

*Data analysis.* aCGH data were pre-processed and analysed using an in-house R script (BACE.R) in R version 2.8.0 [58, 59]. After filtering polymorphic BACs, a final dataset of 31544 clones with unambiguous mapping information according to the March 2006 build (hg18) of the human genome (<http://www.ensembl.org>) was smoothed using the circular binary segmentation (cbs) algorithm [56, 60]. A categorical analysis was applied to the BACs after classifying them as representing amplification ( $>0.45$ ), gain ( $>0.08$  and  $\leq 0.45$ ), loss ( $<-0.08$ ), or no-change according to their cbs-smoothed  $\text{Log}_2$  ratio values [56, 57]. Threshold values were chosen to correspond to three standard deviations of the normal ratios obtained from the filtered clones mapping to chromosomes 1-22, assessed in multiple hybridisations between DNA extracted from a pool of male and female blood donors as previously described [54]. Low level gain was defined as a smoothed  $\text{Log}_2$  ratio of between 0.12 and 0.45, corresponding to approximately 3-5

## 2.2 Material and Methods

copies of the locus, whilst gene amplification was defined as having a  $\text{Log}_2$  ratio  $> 0.45$ , corresponding to more than 5 copies.

### 2.2.4 Hierarchical Cluster Analysis

Unsupervised hierarchical cluster analysis was performed using the `hclust` function from Bioconductor R aCGH package, using aCGH smoothed ratios or categorical data from the filtered set of 31544 clones as the distance and Ward's clustering algorithm [61, 62].

### 2.2.5 In Situ Hybridisation

Chromogenic (CISH) and fluorescence *in situ* hybridisation (FISH) were carried out for validation of aCGH results in selected cases. Ready-to-use digoxigenin-labelled SpotLight amplification probes for the epidermal growth factor receptor gene (*EGFR*) and *HER2* (Invitrogen, Paisley, UK) and biotin-labelled in-house made probes for 3q24, 8p11.2 and 12q14 were used. In-house probes were generated according to protocols described by Lambros et al. [63] and tested for their specificity. The BACs used were RP11-597O1 and RP11-725I19 for 3q24, RP11-104D16 for 8p11.2, and RP11-66N19, RP11-277A02 and RP11-549D07 for 12q14. Each BAC and probe were FISH mapped using slides containing normal lymphocyte metaphase spreads (Vysis Inc., Downers Grove, USA) and end sequencing verified using SP6 or T7 primers [63]. Tissue pre-treatment, hybridisations and washes were performed as previously described [63]. Signals were counted in non-overlapping nuclei of 60 morphologically unequivocal neoplastic cells. Amplification was defined as the presence of gene clusters or more than 5 signals in at least 50% of the neoplastic cells [28, 50].

### 2.2.6 Immunohistochemistry

Formalin-fixed, paraffin-embedded sections were cut at 3µm and mounted on silane-coated slides. Immunohistochemistry was performed using antibodies raised against oestrogen receptor (ER, clone ID5, Dako, 1:40), progesterone receptor (PR, clone PgR636, Dako, 1:200), HER2 (Herceptest, Dako), p53 (clone DO7, Dako, 1:200) and 'basal-like' markers (EGFR (clone 31G7, Invitrogen, 1:50), cytokeratin (CK) 5/6 (clone D5/16B4, Chemicon, 1:600), CK14 (clone LL002, Vector Labs, 1:40)). Heat induced antigen retrieval was employed for ER, PR, p53, CK 5/6, CK 14 and HER2 by heating the sections in citrate buffer pH6 either for 2 min in a pressure cooker (ER, PR and p53), for 18 min in a microwave oven (CK 5/6 and CK 14), or for 40 min in the LabVision pre-treatment module (HER2) [64]. Antigen retrieval for EGFR was performed using 0.1% pronase for 10 minutes at 37°C [50]. ER and PR were considered positive if >1% of cells in each distinct component displayed nuclear reactivity. For CKs, membranous or cytoplasmic staining in more than 1% of morphologically unequivocal neoplastic cells was recorded as positive. HER2 was evaluated according to current clinical guidelines [65] and EGFR as previously described [50]. For p53, strong nuclear staining in more than 50% of the neoplastic cells was recorded as positive.

### 2.2.7 p53 Mutation Analysis

Sequencing of known mutation hotspots of *TP53* on exons 5-9 [66] was performed in selected cases (cases 2, 5 and 6 and matched adjacent normal breast tissues). The primers used for *TP53* sequencing have been previously described [66] (Tab. 2.3). 50ng tumour DNA was amplified and sequencing reactions were carried out using the DNA Sequencing Kit BigDye Terminator v 1.1 Cycle Sequencing Ready Reaction Mix (Applied Biosystems, Warrington, UK). Sequences were analysed with Mutation

## 2.2 Material and Methods

Surveyor software (Softgenetics, PA, USA). Mutations were confirmed by repeat PCR using the same DNA samples subjected to aCGH followed by sequencing reactions, PCR of DNA extracted from re-microdissected material of each component followed by sequencing reactions, and by sequencing forward and reverse strands.

Exon		Sequence 5'-3'	PCR product size, bp
<b>5</b>	<b>Fw</b>	CTTGTGCCCTGACTTTCAACTCTGTCTC	270
	<b>Rv</b>	TGGGCAACCAGCCCTGTCGTCTCTCCA	
<b>6</b>	<b>Fw</b>	CCAGGCCTCTGATTCCTCACTGATTGCTC	202
	<b>Rv</b>	GCCACTGACAACCACCCTTAACCCCTC	
<b>7</b>	<b>Fw</b>	GCCTCATCTTGGGCCTGTGTTATCTCC	173
	<b>Rv</b>	GGCCAGTGTGCAGGGTGGCAAGTGGCTC	
<b>8</b>	<b>Fw</b>	GTAGGACCTGATTCCTTACTGCCTCTTGC	239
	<b>Rv</b>	ATAACTGCACCCTTGGTCTCCTCCACCGC	
<b>9</b>	<b>Fw</b>	CACTTTTATCACCTTTCCTTGCCTCTTTCC	144
	<b>Rv</b>	AACTTTCCACTTGATAAGAGGTCCCAAGAC	

**Table 2.3: PCR primers for p53 analysis.**

### 2.2.8 HUMARA Assay

The HUMARA assay was performed in selected cases by DNA methylation-sensitive digestion followed by nested PCR. Aliquots of 200ng of tumour DNA were digested with 10 units of HpaII restriction enzyme (New England Biolabs, Ipswich, MA, USA) at 37° overnight in a 20µl reaction volume. Separate aliquots of DNA were subjected to mock digestion without the enzyme. After incubation the restriction enzyme was inactivated at 65° for 20 minutes according to the manufacturer's recommendations. 5µl of digested or

mock-digested DNA was submitted to a nested PCR reaction [67], where the forward primer of the second set of PCR was 5' FAM labelled. Primer sequences have been previously described by Kuijper et al. [67] (Tab. 2.4). PCR products were run on the Applied Biosystems 3100 Genetic Analyser (Applied Biosystems, Warrington, UK).

Primers	Sequence 5'-3'
<b>Outer1</b>	TGTGGGGCCTCTACGATG
<b>Outer3</b>	CCGTCCAAGACCTACCGA
<b>Inner2</b>	CCGAGGAGCTTCCAGAATC
<b>Inner4*</b>	TACGATGGGCTTGGGGAGAA

**Table 2.4: Primers used for HUMARA assay.** \*: Primer 4 was fluorescently labelled with FAM.

### 2.2.9 Quantitative real-time reverse transcriptase PCR (qRT-PCR)

Reverse transcription of total RNA from case 6 was carried out using Superscript III (Invitrogen, UK). Quantitative real-time reverse transcriptase PCR (qRT-PCR) was performed for ERB-B2 (Applied Biosystems) using TaqMan® chemistry on the ABI Prism 7900HT (Applied Biosystems), using the standard curve method. In addition, two reference genes (TFRC and MRPL19 - Applied Biosystems) were used, having been previously selected as effectively normalising for degradation of RNA [68]. Target gene expression levels were normalised to the geometric mean of the two reference genes.



## 2.3 RESULTS

### 2.3.1 Cases 1-4

In cases 1 to 4, which were carcinomas with heterologous elements, composed of ductal, chondroid and/ or spindle areas, the morphologically distinct components (Figures. 2.5a, 2.5d, 2.5g) harboured strikingly similar immunohistochemical and genomic profiles (Figures. 2.5b, 2.5e, 2.5h; Table 2.5). All components displayed a triple negative phenotype (i.e. ER-, PR- and HER2-negative) and were classified as of basal-like subtype according to a validated immunohistochemical definition [69] (Table 2.5). Our aCGH analysis revealed similar patterns of copy number changes between the components of each of these four cases (Figure 2.5), with <23% of the genomes showing different genetic aberrations. Pearson's correlation, performed using smoothed aCGH ratios from the components of each case, revealed r values >0.75, which indicate a good correlation in the patterns of genetic changes displayed by the distinct components of each case. In case 2, the three components strongly expressed p53 protein (Table 2.5), and harboured an identical, tumour specific 13824 C>T *TP53* mutation (Figures 2.5c, 2.5f, 2.5i; Table 2.6) and the same pattern of X-chromosome inactivation by the HUMARA assay (Table 2.6), confirming their clonality. Analysis of germline DNA extracted from adjacent normal breast tissue from case 2 demonstrated wild-type *TP53*.

## 2.3 Results

Case	Component	Histological Grade <sup>o</sup>	Immunohistochemical Analysis							Molecular Subgroup*
			ER	PR	HER2	CK5/6	CK14	EGFR	p53	
1	chondroid spindle	3	-	-	-	+	+	-	-	Basal-like
		3	-	-	-	+	+	-	-	Basal-like
2	chondroid spindle rhabdoid	3	-	-	-	+	+	+	+	Basal-like
		3	-	-	-	-	-	+	+	Basal-like
		3	-	-	-	-	-	+	+	Basal-like
3	epithelial chondroid	3	-	-	-	+	+	+	+	Basal-like
		3	-	-	-	+	+	+	+	Basal-like
4	chondroid spindle	2	-	-	-	+	+	-	-	Basal-like
		3	-	-	-	+	+	-	-	Basal-like

**Table 2.5: Histological features, immunohistochemical analysis and molecular subgroups of morphologically distinct components of cases 1 to 4.** <sup>o</sup>Nottingham grading system. \*Breast cancer molecular subtypes as defined by Nielsen et al. [69] criteria. ER: oestrogen receptor; CK: cytokeratin; EGFR: epidermal growth factor receptor; PR: progesterone receptor.

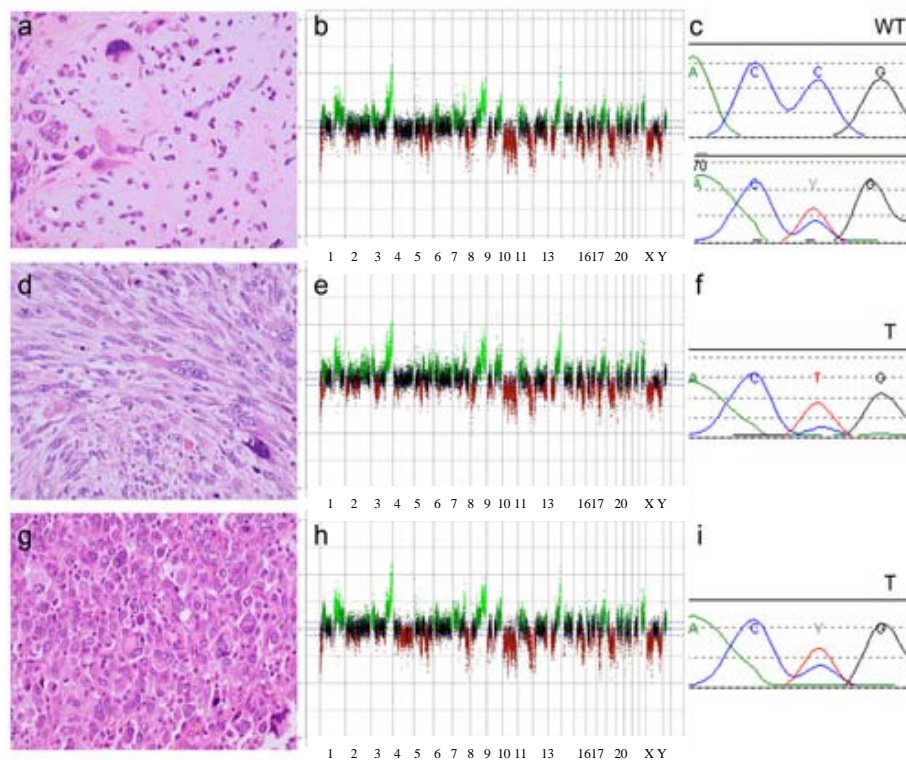


**Figure 2.5: Case 2 – Metaplastic carcinoma with heterologous elements.** The distinct morphological components harbour remarkably similar genomic profiles and identical 13824 C>T TP53 gene mutation. Representative micrographs, genome plots and TP53 mutation analysis of the chondroid (a, b and c), spindle (d, e and f) and rhabdoid (g, h and i) components. In the genome plots, Log<sub>2</sub> ratios are plotted on the Y axis against each clone according to genomic location on the X axis. BACs categorised as displaying genomic gains or amplification are plotted in green and bright green, respectively, and those categorised as regions of genomic losses are depicted in red. Raw: examples of similar alterations.

Case	Component	TP53 Mutation Analysis					HUMARA assay
		Exon 5	Exon 6	Exon 7	Exon 8	Exon 9	
2	chondroid	WT	WT	WT	13824 C>T	WT	Identical pattern
	spindle	WT	WT	WT	13824 C>T	WT	
	rhabdoid	WT	WT	WT	13824 C>T	WT	
	normal adjacent breast	WT	WT	WT	WT	WT	Polyclonal

**Table 2.6: Clonality analysis between the morphologically distinct components of case 2.** NP: not performed; WT: wild type.

### 2.3.2 Cases 5-6

In contrast, in case 5, an adenosquamous carcinoma composed of lobular and squamous components (Figures 2.6a and 2.6c), the genetic differences between the two components were such that only 20% of the genome harboured similar copy number changes. The lobular component, which was of classic variant and low histological grade, displayed a ‘simplex’ profile [70] with the expected copy number changes for a lobular breast carcinoma (i.e. concurrent 1q gain, 16p gain and 16q loss) [42] (Figure 2.6b). The squamous component was characterised by a complex ‘sawtooth’ genetic profile [54], lack of 16q loss and amplification of 7p11 (*EGFR*) (Fig. 2.6d). The divergent copy number status of the *EGFR* gene (i.e. no changes and amplification in the lobular and squamous components respectively) was further validated by chromogenic *in situ* hybridisation (Figures 2.7a and 2.7d, Table 2.9).

Case	Component	Histological Grade <sup>o</sup>	Immunohistochemical Analysis							Molecular Subgroup*
			ER	PR	HER2	CK5/6	CK14	EGFR	p53	
5	squamous Lobular	3	-	-	-	+	+	+	-	Basal-like Luminal
		2	+	+	-	-	-	-	-	
6	Ductal	3	-	-	2+	+	+	+	+	HER2
	squamous	3	-	-	3+	+	+	+	+	HER2
	Spindle	3	-	-	1+	+	-	+	+	Basal-like
	metastasis	3	-	-	1+	-	-	+	+	Basal-like

**Table 2.5: Histological features, immunohistochemical analysis and molecular subgroups of morphologically distinct components of cases 5 and 6.** <sup>o</sup>Nottingham grading system. \*Breast cancer molecular subtypes as defined by Nielsen et al. [69] criteria. ER: oestrogen receptor; CK: cytokeratin; EGFR: epidermal growth factor receptor; PR: progesterone receptor.

## 2.3 Results

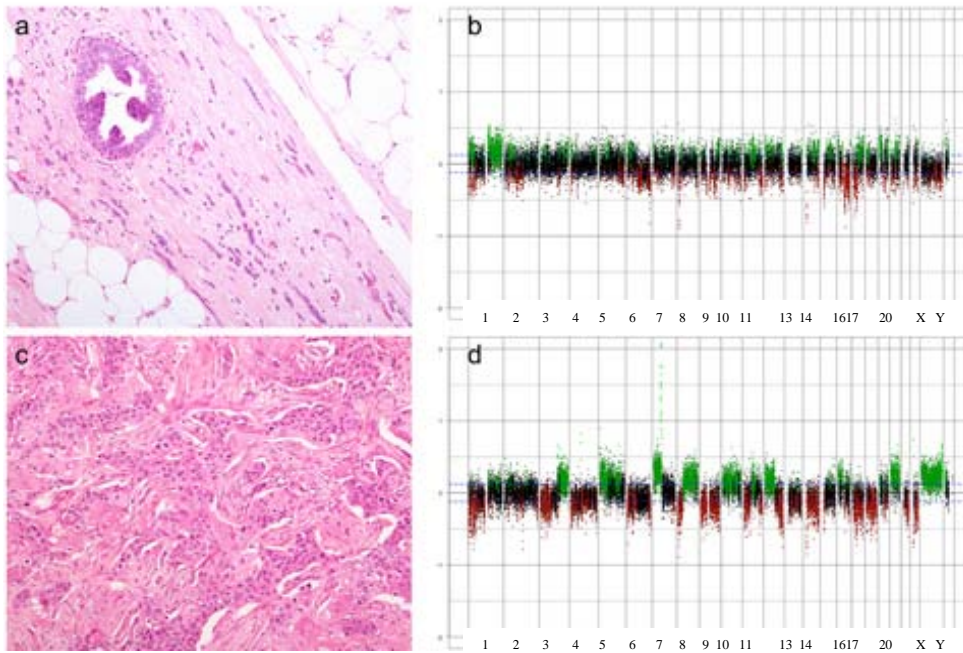


**Figure 2.6: Case 5 – Genetic profiles.** The two morphological distinct components harbour distinct genomic profiles. Representative micrographs and genome plots of the lobular (a and b) and squamous (c and d) components.  $\text{Log}_2$  ratios are plotted on the Y axis against each clone according to genomic location on the X axis. Note that the lobular component displayed a ‘simplex’ genomic profile [70] with the typical pattern of genetic aberrations found in lobular cancers (i.e. concurrent 1q gain, 16p gain and 16q loss), lacked *EGFR* gene amplification (7p11), whereas the squamous component harboured a ‘sawtooth’ profile [71] with *EGFR* gene amplification in the form of large gene clusters (7p11).

Immunophenotypically, each component was also distinct: whilst lobular cells expressed hormone receptors and lacked EGFR expression, squamous cells displayed the opposite pattern (Figures 2.7b-2.7c-2.7e-2.7f; Tab. 2.8). Clonality between the two components could not be established, as both displayed wild-type *TP53* and an identical pattern of X-chromosome inactivation as defined by the HUMARA assay (Table 2.8). The distinct patterns of genetic aberrations in each component and their immunophenotypic differences are suggestive of either a ‘collision tumour’ (i.e. two distinct neoplasms affecting the same anatomical site but being clonally unrelated) or a tumour which originated from a single cell that acquired divergent genetic aberrations at an early stage of tumourigenesis leading to emergence of distinct morphological components.

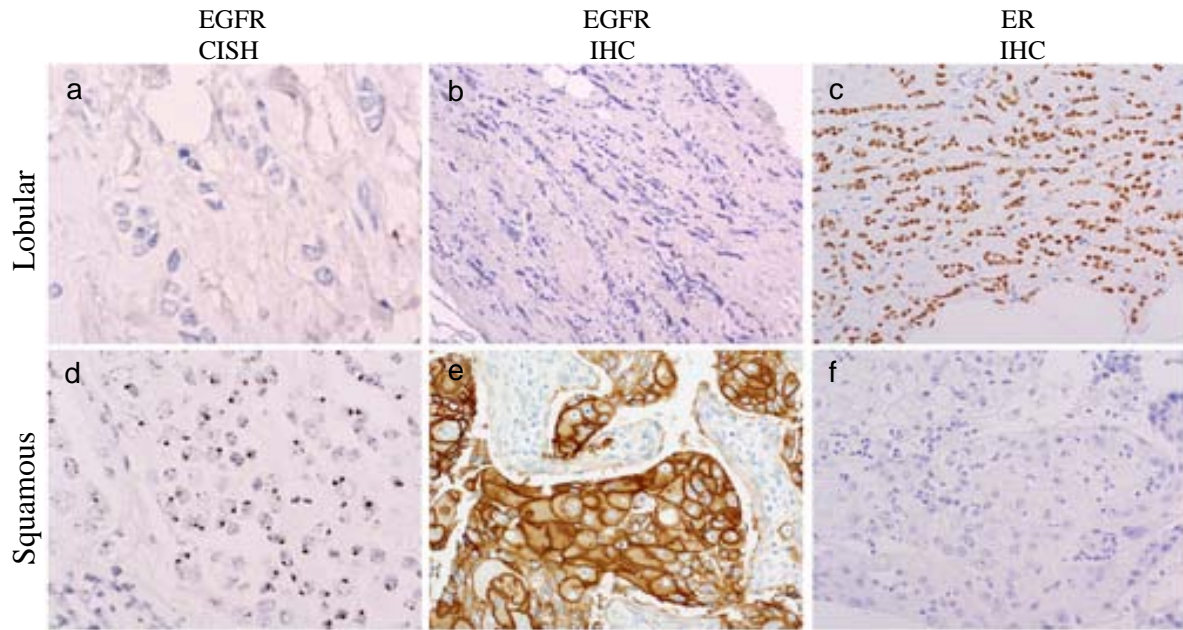


**Figure 2.7: Case 5 - Immunohistochemical profiles.** The two morphological distinct components harbour distinct immunohistochemical profiles. Note that the lobular component lacked *EGFR* gene amplification (a) and overexpression (b), and displayed strong and diffuse ER expression (c), whereas the squamous component harboured *EGFR* gene amplification in the form of large gene clusters (h) and strong EGFR protein expression (e), and was ER negative (f).

Case	Component	TP53 Mutation Analysis					HUMARA assay
		Exon 5	Exon 6	Exon 7	Exon 8	Exon 9	
5	Squamous	WT	WT	WT	WT	WT	Identical pattern
	Lobular	WT	WT	WT	WT	WT	
	normal adjacent breast	WT	WT	WT	WT	WT	
6	Ductal	12512 G>A	NP	WT	WT	WT	Identical pattern
	Squamous	12512 G>A	NP	WT	WT	WT	
	Spindle	12512G>A	NP	WT	WT	WT	
	Metastasis	12512 G>A	NP	WT	WT	WT	

**Table 2.8: Clonality analysis between the morphologically distinct components of case 5 and 6.** NP: not performed; WT: wild type.

## 2.3 Results

Case	Component	EGFR CISH	FISH				HER2 qRT- PCR <sup>o</sup>
			HER2	3q24	8p11.2	12q14	
5	squamous	AMP	NP	NP	NP	NP	NP
	lobular	Not AMP	NP	NP	NP	NP	NP
6	ductal	NP	AMP	Not AMP	AMP	AMP	5.01763929
	squamous	NP	AMP	Not AMP	AMP	AMP	6.21651644
	spindle	NP	AMP	AMP	Not AMP	Not AMP	0.54737271
	metastasis	NP	Heterogeneous*	Not AMP	Not AMP	Not AMP	0.60340944

**Table 2.9: *In situ* hybridisation and quantitative RT-PCR analysis of morphologically distinct components of cases 5 and 6.** \*15% of neoplastic cells displayed more than 5 signals and/ or large gene clusters. <sup>o</sup>Arbitrary expression units. AMP: amplified; CISH: chromogenic *in situ* hybridisation; EGFR: epidermal growth factor receptor; FISH: fluorescence *in situ* hybridisation; Not AMP: not amplified; NP: not performed; qRT-PCR: quantitative reverse transcriptase PCR.

Case 6, a biphasic spindle cell carcinoma, was characterised by ductal and squamous, and spindle cell areas (Figs. 2.8a, 2.8b, 2.8c). The three components lacked hormone receptors and expressed the basal markers EGFR and CK5/6. Although all components harboured an amplification of 17q12 encompassing the *HER2* gene, *HER2* overexpression was limited to the ductal and squamous components at the protein and mRNA levels (Fig. 2.10; Tab. 2.9). Both epithelial components were genetically highly correlated (Pearson *r* value=0.89), shared with the spindle component similar gains, losses and amplification of 9p22.3 and 17q12 (*HER2*) (Figures 2.9a, 2.9b, 2.9c), and harboured an identical 12512 G>A *TP53* mutation (Figure 2.10; Table 2.8) (which was not present in DNA extracted from adjacent normal breast tissue), providing direct evidence of their clonal nature. It should be noted, however, that divergent focal amplifications specific to each component were present, such as 3q24, 5p15, 9p24, 10q21 and 15q23 in the spindle and 8p11.2, 12q14 and 17q23 in the squamous and ductal

## 2. Metaplastic heterogeneity

components. Fluorescence *in situ* hybridisation validated the copy number status of *HER2*, 3q24, 8p11.2 and 12q14 regions in the distinct morphological components of the primary tumour, providing support for the robustness of our aCGH findings (Figure 2.10, Table 2.9) and the association between the morphologically distinct components and the amplifications of different genetic regions. *HER2* amplification was confirmed in the modal population of each component of the primary tumour. Amplification of 3q24 was restricted to the spindle component and amplification of 8p11.2 and 12q14 was present only in the ductal and squamous components (Figure 2.10; Table 2.9). Taken together, our results suggest that the *TP53* mutation and 17q12 amplification are likely to have been early events in the progression of this metaplastic carcinoma, which were followed by the acquisition of secondary genetic events.

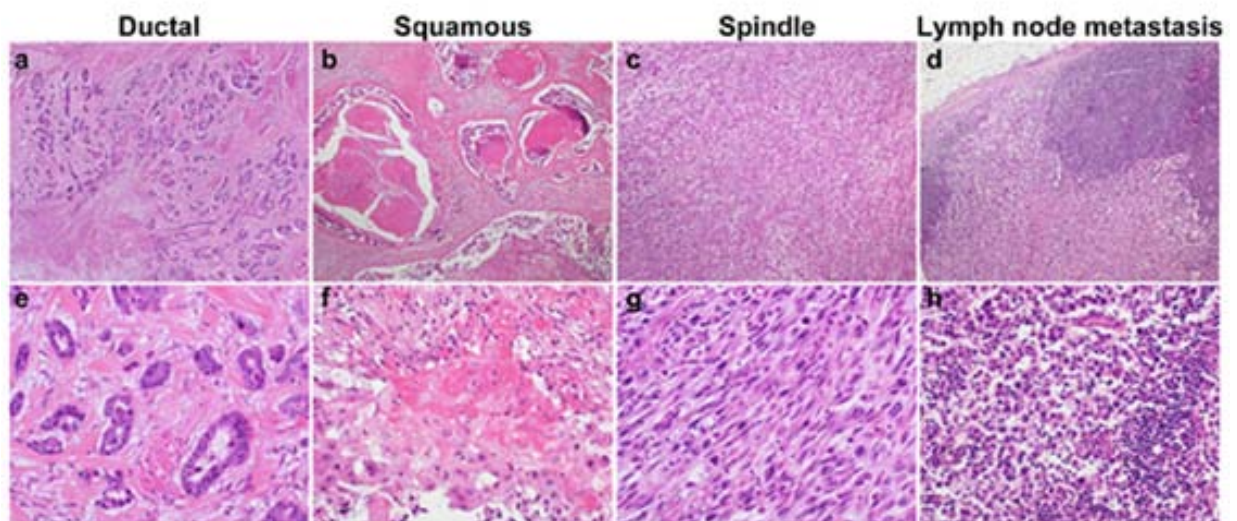


**Figure 2.8: Case 6 – Metaplastic primary biphasic spindle cell carcinoma and axillary lymph node metastasis.** Representative micrographs at low (40X) and high power (200X) magnification of the ductal (a and e), squamous (b and f) and spindle (c and g) components of the primary tumour and lymph node metastasis (d and h).

## 2.3 Results

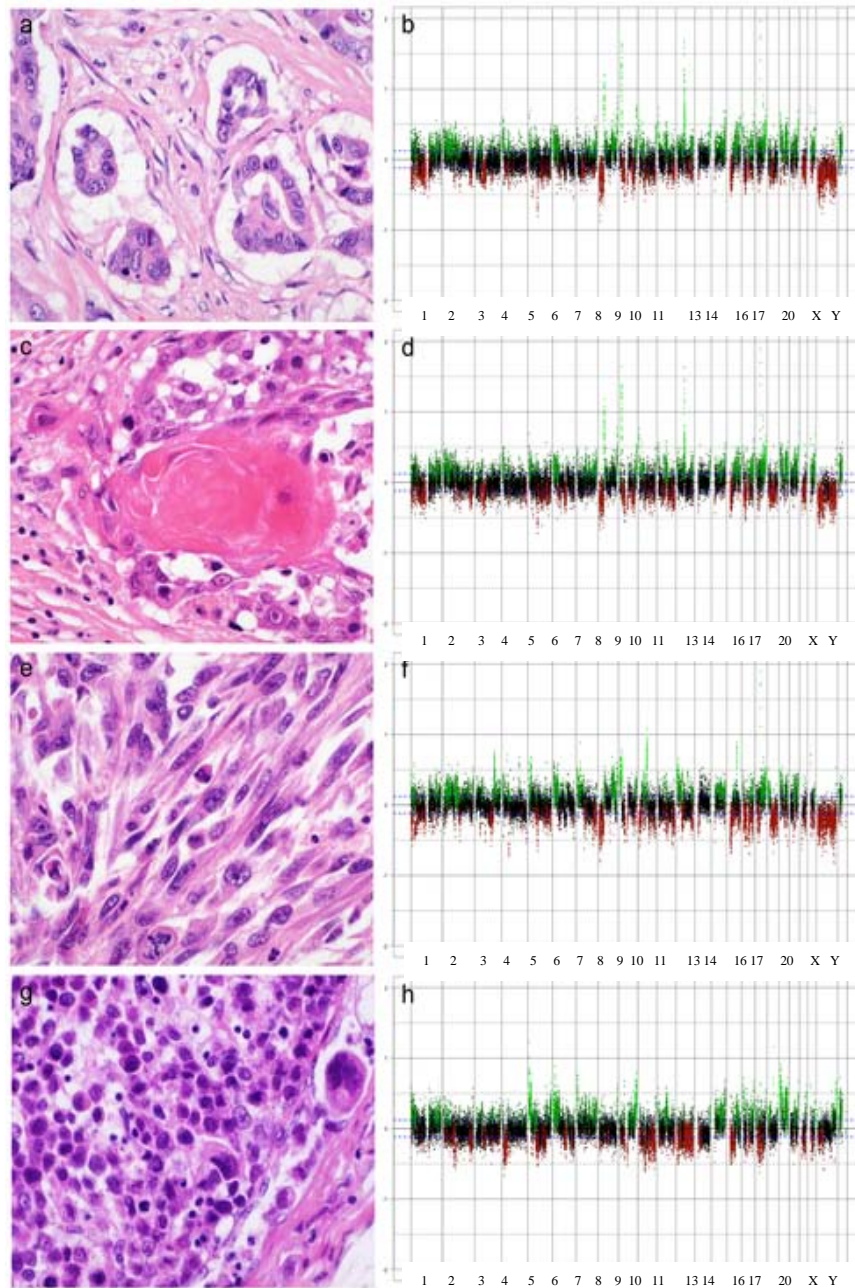


**Figure 2.9: Case 6 – Metaplastic primary biphasic spindle cell carcinoma and matched axillary lymph node metastasis.** The distinct morphological components and metastasis, albeit clonal, harbour divergent focal high-level amplifications. The matched lymph node metastasis has a genomic profile distinct from that of the three components of the primary tumour. Representative micrographs and genome plots of the ductal (a and b), squamous (c and d) and spindle (e and f) components and lymph node metastasis (g and h).  $\log_2$  ratios are plotted on the Y axis against each clone according to genomic location on the X axis. BACs categorised as displaying genomic gains or amplification are plotted in green and bright green, respectively, and those categorised as regions of genomic losses are depicted in red.

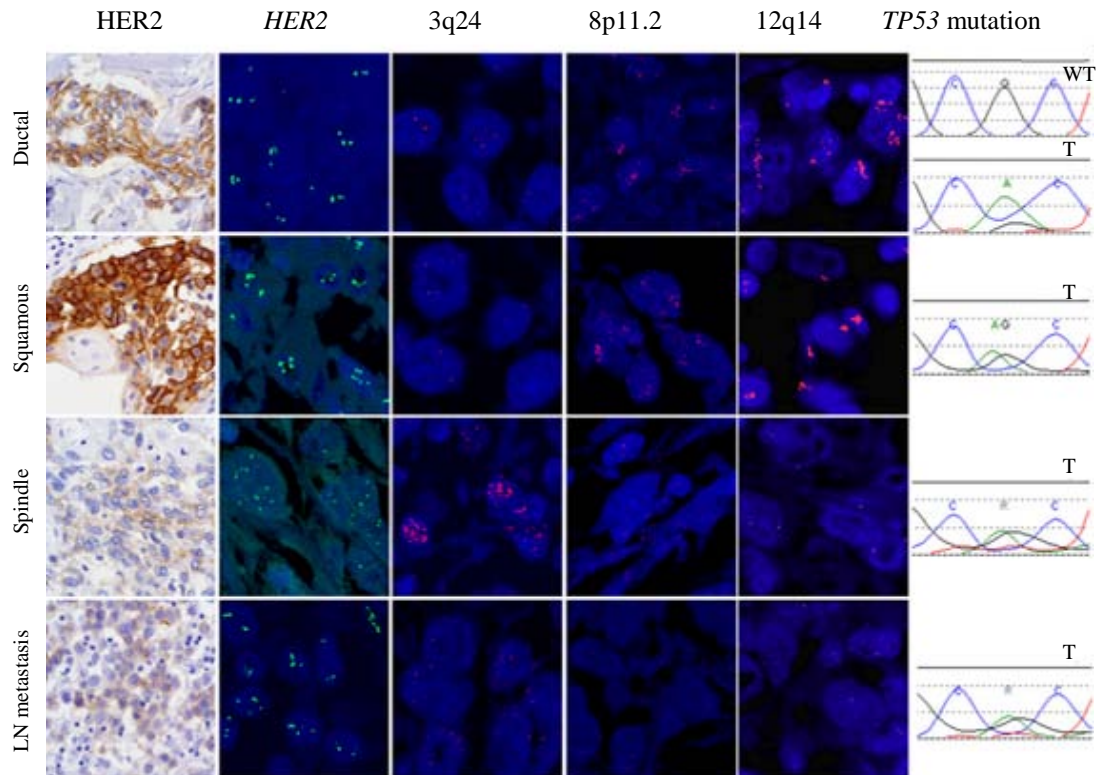


**Figure 2.10: Case 6 – Immunohistochemical, *in situ* hybridisation and sequencing analysis** revealed the presence of *HER2* gene amplification and an identical 12512 G>A *TP53* mutation in all components of the primary tumour (>50% of the neoplastic cells) and in the metastatic deposit (15% of the neoplastic cells). Each component displayed specific patterns of amplification: 3q24 amplification was restricted to the spindle component and amplifications of 8p11.2 and 12q14 were present only in the ductal and squamous components.

Analysis of the axillary lymph node metastasis from this patient, which was poorly differentiated and composed of smaller but highly atypical and discohesive cells (Figures 2.8d and 2.8h); we established its clonal nature with the primary tumour, as it harboured a 12512 G>A *TP53* mutation and inactivation of the same chromosome X (Fig. 2.10; Tab. 2.8). Importantly, the metastatic deposit harboured specific genetic aberrations (Fig. 2.9d), including focal high-level amplifications of 5p15, 6p24, 9q34, 19q13 and Xq28, which were not present in the modal populations of the ductal, squamous and spindle components. aCGH revealed a lower level of 17q12 amplification in the metastatic deposit (Figure 2.9d) when compared to that of components of the primary tumour (Figures 2.9a, 2.9b, 2.9c). Fluorescence *in situ* hybridisation with *HER2* probes

## 2.3 Results

demonstrated that the metastasis was composed of a mosaic of cells with (15%) and without (85%) *HER2* gene amplification (as defined by >5 copies in the nucleus of each neoplastic cell) and lacked *HER2* mRNA and protein expression (Figure 2.10; Table 2.9). Our results could imply that this metastasis might have originated from a malignant clone that did not harbour *HER2* gene amplification and that a non-modal neoplastic population in the lymph node acquired this amplification over time independently, recapitulating the genetic events of the primary tumour. In fact, some studies have suggested that metastases may occur early during carcinogenesis and follow a distinct clonal progression [72, 73]. This is unlikely, however, as the breakpoints of 17q12 amplification in the primary tumour components and metastatic deposit were identical. Alternatively, the modal population of metastatic cells either lost this amplification, as *HER2* was not expressed in any of the metastatic cells, or the metastasis was composed of multiple neoplastic clones from the primary tumour that drained to the same lymph node over time, one of which lacked *HER2* gene amplification.

### 2.3.3 Cluster Analysis

We further evaluated the genetic similarities between the 15 morphologically distinct components of the six studied cases by unsupervised hierarchical clustering with the aCGH data (Figure 2.11). As expected, the distinct components of cases 1 to 4 clustered together, underlining the high similarity at the genomic level and clonal relationship between the components. In contrast, the lobular and squamous components of case 5, which had been found to display different genetic profiles (i.e. ‘simplex’ vs. ‘sawtooth’) including an *EGFR* amplification in the squamous component, clustered separately. Although the primary tumour components of case 6 and the axillary lymph node

## 2. Metaplastic heterogeneity

metastasis clustered in the same branch, the ductal, squamous and spindle components of the primary tumour were more similar to each other than to the metastasis.

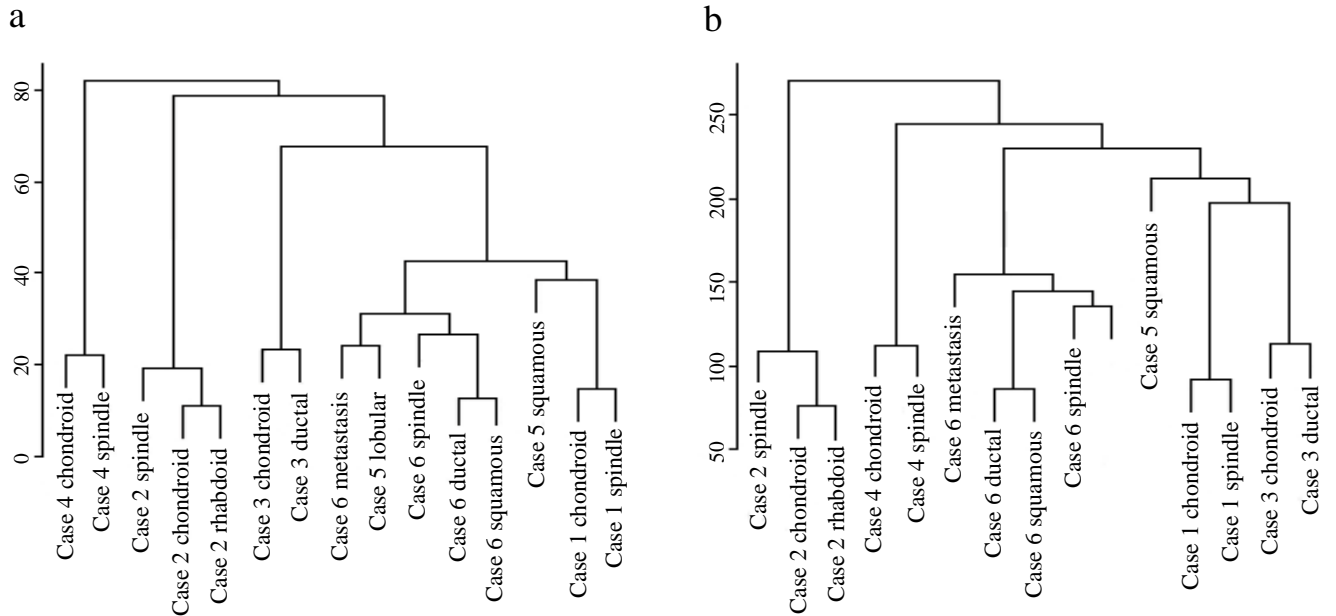


**Figure 2.11: Unsupervised hierarchical cluster analysis.** Hierarchical clustering of 15 morphologically distinct components of six metaplastic breast carcinomas performed using microarray comparative genomic hybridisation cbs smoothed ratios (a) and categorical data (i.e. losses, no change, gain and amplification) (b) derived from the filtered set of 31544 clones.



## 2.4. DISCUSSION AND CONCLUSIONS

Our results indicate that at least some breast cancers are composed of multiple non-modal populations of clonally related cells and provide evidence of clonal evolution in breast cancer.

Intra-tumour phenotypic heterogeneity can be explained by several genetic and non-genetic mechanisms [19, 22, 28, 30, 75-77]. The distinct morphological features of cases 5 and 6 were coincidental with the copy number changes detected by aCGH, suggesting that, in these cases, genetic heterogeneity may have driven the phenotypic diversity. In cases 1 to 4, no significant differences in copy number aberrations were observed in the distinct morphological components. It is plausible that using techniques with a higher resolution, such as massively parallel sequencing, one could detect specific mutations or structural somatic rearrangements that would underpin the histological differences [78]. Alternatively, the phenotypic diversity observed in those cases may be explained by epigenetic changes, interaction with the tumour microenvironment [19, 22, 23] or by the plasticity of cancer stem cells [26-29]. Gene expression studies have recently suggested that a subgroup of sarcomatoid breast cancers may be of 'claudin-low' subtype, which has features of stem cells and epithelial-mesenchymal transition [79].

Moreover, our results suggest that the methods that detect only the genetic aberrations present in the modal population of cancer cells in a given tumour may not be sufficient to identify all of its drivers. Although the prevalence of the phenomena illustrated by cases 5 and 6 needs to be determined in a large collection of tumours, our findings have important implications for a successful implementation of targeted therapies in clinical practice, in particular those that target genes whose activation is primarily mediated by a genetic hit. Furthermore, analysis of a single sample at a given

## 2.4 Discussion and Conclusions

moment (e.g. primary tumour prior to the administration of adjuvant systemic therapy) may not provide a complete assessment of the genomic profile of the tumour and, therefore, may not be sufficient to determine the sensitivity of disseminated cells to a given agent. As demonstrated in one of the cases analysed in this study, acquisition of specific high level amplifications may occasionally only be detectable in the metastatic deposits. In this proof of principle study based on high resolution genome-wide genetic analysis of morphologically distinct components of metaplastic breast carcinomas, we demonstrate that at least some breast cancers are composed of multiple non-modal populations of clonally related cells and provide direct evidence of intra-tumour genetic heterogeneity in breast cancer. In agreement with our results, previous studies using conventional comparative genomic hybridisation or loss of heterozygosity techniques have described the existence of intra-tumour heterogeneity in a significant proportion of breast cancers [74, 80, 81] and the analyses of matched ductal carcinoma *in situ* and invasive carcinoma or matched invasive carcinoma and lymph node metastases [74] have also demonstrated genetic divergence between the matched lesions. In contrast with previous studies, however, we focused on the phenotypic heterogeneity within each tumour to guide the selection of the distinct samples from a given tumour. It should be noted that here we have performed an extensive microdissection of each component to obtain sufficient DNA, avoiding the use of whole genome DNA amplification.

Intra-tumour phenotypic heterogeneity can be explained by several genetic and non-genetic mechanisms [19, 75]. Our results suggest that the intra-tumour morphological diversity of cases 1 to 4 may be caused by genetic aberrations other than changes in copy number of specific genes (i.e. gene mutations or balanced somatic rearrangements), epigenetic changes or interaction with the tumour microenvironment [19, 22, 23]. Alternatively, the intra-tumour phenotypic diversity of these cancers may be attributable

to ‘cancer stem cells’ [26-29]. In fact, gene expression studies have shown that metaplastic sarcomatoid breast cancers may be of ‘claudin-low’ subtype, which has features of stem cells and epithelial-mesenchymal transition [82]. In contrast, the distinct morphological features of cases 5 and 6 were coincidental with the copy number changes detected by aCGH, suggesting that, in these cases, genetic heterogeneity may have driven the phenotypic diversity.

In conclusion, this proof of principle study provides direct evidence that at least some types of breast cancers are composed of multiple non-modal clones harbouring distinct genetic aberrations, which at least in some cases are coincidental with and may underpin the morphological heterogeneity of breast cancers. Given that aCGH is only suited to detect clonal copy number aberrations, the existence of subclones with distinct genetic aberrations within a given tumour and the differences in the genetic aberrations in the primary lesion and metastatic deposit of a metaplastic breast cancer provide evidence that the acquisition of distinct genetic aberrations is associated with and may lead to distinct phenotypes and disease progression. However, we cannot rule out that an even greater genetic heterogeneity, not detectable by aCGH analysis (i.e. structural genetic aberrations and base pair changes) may exist in breast cancers. Moreover, our results suggest that the intra-tumour complexity of breast cancer genomes is greater than previously anticipated and that methods that detect only the genetic aberrations present in the modal population of cancer cells in a given tumour may not be sufficient to identify all of its drivers.

Although the prevalence of the phenomena illustrated by cases 5 and 6 needs to be determined in a large collection of tumours, our findings have important implications for a successful implementation of targeted therapies in clinical practice, in particular those that target genes whose activation is primarily mediated by a genetic hit. Furthermore, analysis of a single sample at a given point in time (e.g. primary tumour prior to the

## 2.4 Discussion and Conclusions

administration of adjuvant systemic therapy) may not provide a complete assessment of the genomic profile of the tumour and, therefore, may not be sufficient to determine the sensitivity of disseminated cells to a given agent. As demonstrated in one of the cases analysed here, acquisition of specific high-level amplifications may occasionally only be detectable in the metastatic deposits.

## REFERENCES

1. Luini, A., et al., *Metaplastic carcinoma of the breast, an unusual disease with worse prognosis: the experience of the European Institute of Oncology and review of the literature*. Breast Cancer Res Treat, 2007. **101**(3): p. 349-53.
2. Tavassoli, F.A. and V. Eusebi, *Tumors of the Mammary Gland*. ATLAS of Tumor Pathology, ed. AFIP. 2009, Washington, DC: American Registry of Pathology.
3. Castella, E., et al., *Fine-needle aspiration biopsy of metaplastic carcinoma of the breast: report of a case with abundant myxoid ground substance*. Diagn Cytopathol, 1996. **14**(4): p. 325-7.
4. Foschini, M.P., R.E. Dina, and V. Eusebi, *Sarcomatoid neoplasms of the breast: proposed definitions for biphasic and monophasic sarcomatoid mammary carcinomas*. Semin Diagn Pathol, 1993. **10**(2): p. 128-36.
5. Dunne, B., et al., *An immunohistochemical study of metaplastic spindle cell carcinoma, phyllodes tumor and fibromatosis of the breast*. Hum Pathol, 2003. **34**(10): p. 1009-15.
6. Oberman, H.A., *Metaplastic carcinoma of the breast. A clinicopathologic study of 29 patients*. Am J Surg Pathol, 1987. **11**(12): p. 918-29.
7. Tavassoli, F.A., *Classification of metaplastic carcinomas of the breast*. Pathol Annu, 1992. **27 Pt 2**: p. 89-119.
8. Smith, D.M., et al., *Metaplastic breast carcinoma*. J Am Osteopath Assoc, 1996. **96**(7): p. 419-21.
9. Huvos, A.G., J.C. Lucas, Jr., and F.W. Foote, Jr., *Metaplastic breast carcinoma. Rare form of mammary cancer*. N Y State J Med, 1973. **73**(9): p. 1078-82.
10. Wargotz, E.S. and H.J. Norris, *Metaplastic carcinomas of the breast. III. Carcinosarcoma*. Cancer, 1989. **64**(7): p. 1490-9.
11. Wargotz, E.S., P.H. Deos, and H.J. Norris, *Metaplastic carcinomas of the breast. II. Spindle cell carcinoma*. Hum Pathol, 1989. **20**(8): p. 732-40.
12. Brenner, R.J., et al., *Metaplastic carcinoma of the breast: report of three cases*. Cancer, 1998. **82**(6): p. 1082-7.
13. Wargotz, E.S. and H.J. Norris, *Metaplastic carcinomas of the breast. I. Matrix-producing carcinoma*. Hum Pathol, 1989. **20**(7): p. 628-35.
14. Rayson, D., et al., *Metaplastic breast cancer: prognosis and response to systemic therapy*. Ann Oncol, 1999. **10**(4): p. 413-9.
15. Kurian, K.M. and A. Al-Nafussi, *Sarcomatoid/metaplastic carcinoma of the breast: a clinicopathological study of 12 cases*. Histopathology, 2002. **40**(1): p. 58-64.
16. Chao, T.C., et al., *Metaplastic carcinomas of the breast*. J Surg Oncol, 1999. **71**(4): p. 220-5.
17. Rosen, P.P. and D. Ernsberger, *Low-grade adenosquamous carcinoma. A variant of metaplastic mammary carcinoma*. Am J Surg Pathol, 1987. **11**(5): p. 351-8.
18. Nowell, P.C., *The clonal evolution of tumor cell populations*. Science, 1976. **194**(4260): p. 23-8.
19. Polyak, K., *Breast cancer: origins and evolution*. J Clin Invest, 2007. **117**(11): p. 3155-63.
20. Edwards, S.L., et al., *Resistance to therapy caused by intragenic deletion in BRCA2*. Nature, 2008. **451**(7182): p. 1111-5.

## References

21. Mullighan, C.G., et al., *Genomic analysis of the clonal origins of relapsed acute lymphoblastic leukemia*. *Science*, 2008. **322**(5906): p. 1377-80.
22. Merlo, L.M., et al., *Cancer as an evolutionary and ecological process*. *Nat Rev Cancer*, 2006. **6**(12): p. 924-35.
23. Nakshatri, H., E.F. Srouf, and S. Badve, *Breast cancer stem cells and intrinsic subtypes: controversies rage on*. *Curr Stem Cell Res Ther*, 2009. **4**(1): p. 50-60.
24. Tomaskovic-Crook, E., E.W. Thompson, and J.P. Thiery, *Epithelial to mesenchymal transition and breast cancer*. *Breast Cancer Res*, 2009. **11**(6): p. 213.
25. Stingl J. *Detection and analysis of mammary gland stem cells*. *J Pathol*, 2009. **271**(2): p. 229-41
26. Al-Hajj, M. and M.F. Clarke, *Self-renewal and solid tumor stem cells*. *Oncogene*, 2004. **23**(43): p. 7274-82.
27. Kakarala, M. and M.S. Wicha, *Implications of the cancer stem-cell hypothesis for breast cancer prevention and therapy*. *J Clin Oncol*, 2008. **26**(17): p. 2813-20.
28. Shackleton, M., et al., *Heterogeneity in cancer: cancer stem cells versus clonal evolution*. *Cell*, 2009. **138**(5): p. 822-9.
29. Al-Hajj, M., et al., *Therapeutic implications of cancer stem cells*. *Curr Opin Genet Dev*, 2004. **14**(1): p. 43-7.
30. Polyak, K. and W.C. Hahn, *Roots and stems: stem cells in cancer*. *Nat Med*, 2006. **12**(3): p. 296-300.
31. Reis-Filho, J.S., et al., *Metaplastic breast carcinomas are basal-like tumours*. *Histopathology*, 2006. **49**(1): p. 10-21.
32. Weigelt, B., et al., *Refinement of breast cancer classification by molecular characterization of histological special types*. *J Pathol*, 2008. **216**(2): p. 141-50.
33. Lien, H.C., et al., *p53 overexpression and mutation in metaplastic carcinoma of the breast: genetic evidence for a monoclonal origin of both the carcinomatous and the heterogeneous sarcomatous components*. *J Pathol*, 2004. **204**(2): p. 131-9.
34. Reis-Filho, J.S., et al., *The molecular genetics of breast cancer: the contribution of comparative genomic hybridization*. *Pathol Res Pract*, 2005. **201**(11): p. 713-25.
35. Tan, D.S. and J.S. Reis-Filho, *Comparative genomic hybridisation arrays: high-throughput tools to determine targeted therapy in breast cancer*. *Pathobiology*, 2008. **75**(2): p. 63-74.
36. Tan, D.S., et al., *Getting it right: designing microarray (and not 'microawry') comparative genomic hybridization studies for cancer research*. *Lab Invest*, 2007. **87**(8): p. 737-54.
37. Lockwood, W.W., et al., *Recent advances in array comparative genomic hybridization technologies and their applications in human genetics*. *Eur J Hum Genet*, 2006. **14**(2): p. 139-48.
38. Pinkel, D. and D.G. Albertson, *Array comparative genomic hybridization and its applications in cancer*. *Nat Genet*, 2005. **37 Suppl**: p. S11-7.
39. Ylstra, B., et al., *BAC to the future! or oligonucleotides: a perspective for micro array comparative genomic hybridization (array CGH)*. *Nucleic Acids Res*, 2006. **34**(2): p. 445-50.
40. Johnson, N.A., et al., *Application of array CGH on archival formalin-fixed paraffin-embedded tissues including small numbers of microdissected cells*. *Lab Invest*, 2006. **86**(9): p. 968-78.

41. Little, S.E., et al., *Array CGH using whole genome amplification of fresh-frozen and formalin-fixed, paraffin-embedded tumor DNA*. Genomics, 2006. **87**(2): p. 298-306.
42. Simpson, P.T., et al., *Molecular evolution of breast cancer*. J Pathol, 2005. **205**(2): p. 248-54.
43. Reis-Filho, J.S., et al., *FGFR1 emerges as a potential therapeutic target for lobular breast carcinomas*. Clin Cancer Res, 2006. **12**(22): p. 6652-62.
44. Elbauomy Elsheikh, S., et al., *FGFR1 amplification in breast carcinomas: a chromogenic in situ hybridisation analysis*. Breast Cancer Res, 2007. **9**(2): p. R23.
45. Cappuzzo, F., et al., *Epidermal growth factor receptor gene and protein and gefitinib sensitivity in non-small-cell lung cancer*. J Natl Cancer Inst, 2005. **97**(9): p. 643-55.
46. Lynch, T.J., et al., *Activating mutations in the epidermal growth factor receptor underlying responsiveness of non-small-cell lung cancer to gefitinib*. N Engl J Med, 2004. **350**(21): p. 2129-39.
47. Paez, J.G., et al., *EGFR mutations in lung cancer: correlation with clinical response to gefitinib therapy*. Science, 2004. **304**(5676): p. 1497-500.
48. Pao, W., et al., *EGF receptor gene mutations are common in lung cancers from "never smokers" and are associated with sensitivity of tumors to gefitinib and erlotinib*. Proc Natl Acad Sci U S A, 2004. **101**(36): p. 13306-11.
49. Pao, W., V.A. Miller, and M.G. Kris, *'Targeting' the epidermal growth factor receptor tyrosine kinase with gefitinib (Iressa) in non-small cell lung cancer (NSCLC)*. Semin Cancer Biol, 2004. **14**(1): p. 33-40.
50. Reis-Filho, J.S., et al., *EGFR amplification and lack of activating mutations in metaplastic breast carcinomas*. J Pathol, 2006. **209**(4): p. 445-53.
51. Weinstein, I.B., *Cancer. Addiction to oncogenes--the Achilles heel of cancer*. Science, 2002. **297**(5578): p. 63-4.
52. Natrajan, R., et al., *Tiling path genomic profiling of grade 3 invasive ductal breast cancers*. Clin Cancer Res, 2009. **15**(8): p. 2711-22.
53. Elston, C.W. and I.O. Ellis, *Pathological prognostic factors in breast cancer. I. The value of histological grade in breast cancer: experience from a large study with long-term follow-up*. Histopathology, 1991. **19**(5): p. 403-10.
54. Marchio, C., et al., *Genomic and immunophenotypical characterization of pure micropapillary carcinomas of the breast*. J Pathol, 2008. **215**(4): p. 398-410.
55. Coe, B.P., et al., *Resolving the resolution of array CGH*. Genomics, 2007. **89**(5): p. 647-53.
56. Natrajan, R., et al., *An integrative genomic and transcriptomic analysis reveals molecular pathways and networks regulated by copy number aberrations in basal-like, HER2 and luminal cancers*. Breast Cancer Res Treat, 2009: p. Epub ahead of print.
57. Marchio, C., et al., *Does chromosome 17 centromere copy number predict polysomy in breast cancer? A fluorescence in situ hybridization and microarray-based CGH analysis*. J Pathol, 2009. **219**(1): p. 16-24.
58. Natrajan, R., et al., *An integrative genomic and transcriptomic analysis reveals molecular pathways and networks regulated by copy number aberrations in basal-like, HER2 and luminal cancers*. Breast Cancer Res Treat, 2009.
59. Mackay, A., et al., *A high-resolution integrated analysis of genetic and expression profiles of breast cancer cell lines*. Breast Cancer Res Treat, 2009. **118**(3): p. 481-98.

## References

60. Mackay, A., et al., *A high-resolution integrated analysis of genetic and expression profiles of breast cancer cell lines*. Breast Cancer Res Treat, 2009: p. Epub ahead of print.
61. Simpson, P.T., et al., *Molecular profiling pleomorphic lobular carcinomas of the breast: evidence for a common molecular genetic pathway with classic lobular carcinomas*. J Pathol, 2008. **215**(3): p. 231-44.
62. Marchio, C., et al., *Mixed micropapillary-ductal carcinomas of the breast: a genomic and immunohistochemical analysis of morphologically distinct components*. J Pathol, 2009. **218**(3): p. 301-15.
63. Lambros, M.B., et al., *Unlocking pathology archives for molecular genetic studies: a reliable method to generate probes for chromogenic and fluorescent in situ hybridization*. Lab Invest, 2006. **86**(4): p. 398-408.
64. Reis-Filho, J.S., et al., *Pleomorphic lobular carcinoma of the breast: role of comprehensive molecular pathology in characterization of an entity*. J Pathol, 2005. **207**(1): p. 1-13.
65. Wolff, A.C., et al., *American Society of Clinical Oncology/College of American Pathologists guideline recommendations for human epidermal growth factor receptor 2 testing in breast cancer*. J Clin Oncol, 2007. **25**(1): p. 118-45.
66. Cooper, M., et al., *Evaluation of oligonucleotide arrays for sequencing of the p53 gene in DNA from formalin-fixed, paraffin-embedded breast cancer specimens*. Clin Chem, 2004. **50**(3): p. 500-8.
67. Kuijper, A., et al., *Analysis of the progression of fibroepithelial tumours of the breast by PCR-based clonality assay*. J Pathol, 2002. **197**(5): p. 575-81.
68. Arriola, E., et al., *Genomic analysis of the HER2/TOP2A amplicon in breast cancer and breast cancer cell lines*. Lab Invest, 2008. **88**(5): p. 491-503.
69. Nielsen, T.O., et al., *Immunohistochemical and clinical characterization of the basal-like subtype of invasive breast carcinoma*. Clin Cancer Res, 2004. **10**(16): p. 5367-74.
70. Hicks, J., et al., *Novel patterns of genome rearrangement and their association with survival in breast cancer*. Genome Res, 2006. **16**(12): p. 1465-79.
71. Simpson, P.T., et al., *Molecular evolution of breast cancer*. J Pathol, 2005. **205**(2): p. 248-54.
72. Schmidt-Kittler, O., et al., *From latent disseminated cells to overt metastasis: genetic analysis of systemic breast cancer progression*. Proc Natl Acad Sci U S A, 2003. **100**(13): p. 7737-42.
73. Torres, L., et al., *Intratumor genomic heterogeneity in breast cancer with clonal divergence between primary carcinomas and lymph node metastases*. Breast Cancer Res Treat, 2007. **102**(2): p. 143-55.
74. Shipitsin, M., et al., *Molecular definition of breast tumor heterogeneity*. Cancer Cell, 2007. **11**(3): p. 259-73.
75. Heim, S., M.A. Teixeira, and N. Pandis, *Are some breast carcinomas polyclonal in origin?* J Pathol, 2001. **194**(4): p. 395-7.
76. Kakarala, M. and M.S. Wicha, *Implications of the cancer stem-cell hypothesis for breast cancer prevention and therapy*. J Clin Oncol, 2008. **26**(17): p. 2813-20.
77. Shah, S.P., et al., *Mutational evolution in a lobular breast tumour profiled at single nucleotide resolution*. Nature, 2009. **461**(7265): p. 809-13.
78. Hennessy, B.T., et al., *Characterization of a naturally occurring breast cancer subset enriched in epithelial-to-mesenchymal transition and stem cell characteristics*. Cancer Res, 2009. **69**(10): p. 4116-24.

79. Benetkiewicz, M., et al., *Chromosome 22 array-CGH profiling of breast cancer delimited minimal common regions of genomic imbalances and revealed frequent intra-tumoral genetic heterogeneity*. *Int J Oncol*, 2006. **29**(4): p. 935-45.
80. Fujii, H., et al., *Genetic divergence in the clonal evolution of breast cancer*. *Cancer Res*, 1996. **56**(7): p. 1493-7.



### **3. ONCOCYTIC BREAST CARCINOMAS**



### 3. ONCOCYTIC BREAST CARCINOMAS

#### 3.1 INTRODUCTION

Pink cells are characterised by wide, eosinophilic granular cytoplasm. The “pink cells carcinoma” could be grouped in four different ways:

1. Apocrine: incidence of 0.3-4%. They are positive for GCDFP-15 and androgen. Negative for Bcl2, oestrogen and progesterone. The aggregation is due to secrete granules.
2. Neuroendocrine: incidence of 2-5%. Characterised by positivity to neuroendocrine markers (in more than 50% of the cells) and to oestrogen, progesterone and GCDFP-15. The characteristic aggregation is due to neurosecrete granules.
3. Acinic: very rare histotype. They are positive for amylase, lisozyme, chimotripsine, EMA and S-100. The aggregates are composed by zymogen.
4. Oncocytic (see below): very few cases described. The tumour has to be composed by more than 70% of oncocytic cells. An oncocytic cells has more than 60% of cytoplasm occupied by mitochondria. The aggregation is due to mitochondria.

##### 3.1.1 Oncocytic Tumours

Pathologists have long been aware of the existence of a distinctive type of tumour composed of cells with abundant granular cytoplasm and with strong affinity for eosin. These peculiar cells were first described in 1898 in the thyroid gland by Askanazy and in the parathyroid gland by Welsh. In the 1930s Hamperl [1] coined for them the term "oncocyte" (from the Greek word Ογκοῦσθαι [onkoustai], to swell) and pointed out that

### 3.1 Introduction

they may give rise to tumours with corresponding morphologic features - i.e. "oncocyctic tumours" - both benign (oncocyctic adenomas) and malignant (oncocyctic carcinomas). This term is used for those cells exhibiting the characteristic phenotype: in histology sections a finely granular eosinophilic cytoplasm and ultrastructurally an increase in the number of mitochondria.

Oncocyctic tumours represent a distinctive set of lesions with typical granular cytoplasmatic eosinophilia of the neoplastic cells. These cells are called oncocytes because of the "swollen" appearance they have as a result of this striking accumulation of mitochondria in more than 60% of cytoplasm [2]. With exception of thyroid and kidney, neoplasms composed of oncocyctic cells are generally rare. The tumours – benign and malignant – consisting of oncocyctic cells are commonly used to be designated as oncocytomas. The proportion of neoplastic cells exhibiting oncocyctic features required to diagnose a tumour as oncocyctic seems to vary according to the site of origin. For example while it is accepted that thyroid neoplasms with 75% of cells having oncocyctic features can be confidently classified as "oncocyctic"[3, 4], stricter criteria are required for a renal tumour to be diagnosed as oncocyctic [5].

#### **3.1.2 Mitochondria-rich and oncocyctic tumours**

The accumulation of huge numbers of abnormal mitochondria as seen by electron microscopy and immunohistochemistry is the hallmark of oncocyctic cells regardless of the organ of origin (thyroid, parathyroid, kidney, salivary glands) and of the benign or malignant nature of the lesions [6-8]. Such accumulation may also reflect a "normal" process; for example, the parathyroid glands normally present a variable percentage of oncocyctic cells, most probably related with cell ageing [9]. Besides the role played by increased proliferation of mitochondria in the cytoplasm without cell division, it is not

known whether a decreased turnover of the mitochondria may also contribute to their accumulation in oncocytic cells [10]. Oncocyte is a descriptive term for a neoplastic or non-neoplastic cell stuffed with mitochondria that give a granular eosinophilic appearance to its large cytoplasm. In the thyroid, other terms are used: Hürthle cell transformation and Hürthle cell tumours [11]. Finally, there are, in some organs, tumours composed by oncocytes that carry specific designations (e.g. Warthin's tumour of the salivary glands). The prominence of oncocytic cells in endocrine organs, salivary glands, kidney and other parenchymatous organs (and in their respective tumours), is in contrast to the rarity of oncocytic cells in the mucosa and respective tumours of the digestive and respiratory tract. The great majority of oncocytic tumours are epithelial derived tumours, but there are also on record examples of oncocytomas occurring in non-epithelial settings. Hürthle cells can be observed in all sorts of thyroiditis (and are prominent in Hashimoto's thyroiditis of adult and elderly patients), nodular goitre, adenoma, follicular carcinoma, papillary carcinoma (PTC) and poorly differentiated carcinoma of the thyroid. With the exception of undifferentiated carcinoma, every type of benign or malignant thyroid tumour has its oncocytic counterpart.

Warthin's tumour is the second most common salivary gland tumour, arising almost always in the parotid gland (accounts for about 15% of all epithelial tumours of the parotid gland), occasionally causing pain or facial nerve paralysis. Warthin's tumours are constituted by cystic spaces, lined by a double layer of oncocytic cells of questionable neoplastic nature that rest on a lymphoid stroma[12].

#### **3.1.3 Oncocytic in Breast**

Only rare example of breast oncocytic carcinomas have been reported in literature [13, 14]. The incidence is probably underestimated because classified as "apocrine".

### 3.1 Introduction

Hystologically, these tumours are characterized by solid nests and glandular structures composed of round/ polygonal cells, well defined cellular borders, with finely granular, eosinophilic and abundant granular cytoplasm, centrally located monomorphic nuclei and prominent nucleoli, few mitosis [15] (Fig. 3.1).

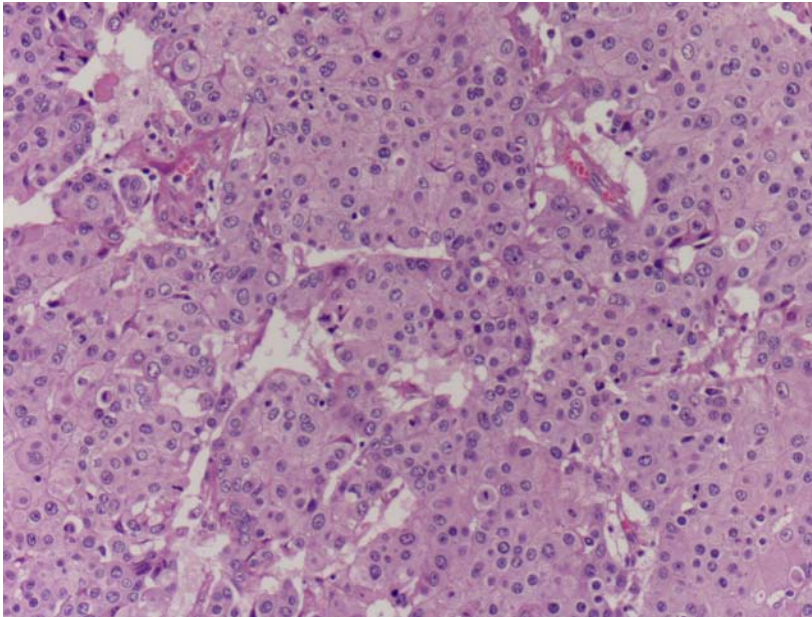


**Figure 3.1:** Haematoxylin and Eosin of an Oncocytic breast carcinoma

Immunohistochemistry, obtained by the 1998 study, was positive for EMA, ER and negative for SMA and progesterone.

The positivity for an anti-mitochondrial antibody was strong, granular and spread, in more than 70% of the cells. Moreover, the positivity was considered strong (3+) when present in more than 60% of cytoplasm [14].

We have to consider the presence of another type of cell rich in mitochondria, the “mitochondrial-rich cells”, described in 1960 as cells of different shape, with cytoplasm enriched in mitochondria grouped preferentially at base or luminal pole of the cell [16].

#### 3.1.4 Mitochondria

Mitochondria were discovered in 1857 by Kolliker in muscle tissue (*μίτος* or *mitos*, thread + *χονδρίον* or *khondrion*, granule). They were aerobic microorganisms (much like *Rickettsia*) that more than a billion years ago colonized primordial eukaryotic cells without the ability to use oxygen. They have since adapted to a permanent symbiotic relationship.

Mitochondria are semi-autonomous organelles that perform essential functions in cellular metabolism and the regulation of cell death. Consistent with their importance in metabolism, they generally occupy a major fraction of the total cell volume. In fact, mitochondria occupy a substantial portion of the cytoplasmic volume of eukaryotic cells, and they have been essential for the evolution of complex animals.

As previously said, mitochondria arose from an endosymbiotic relationship between a glycolytic proto-eucaryotic cell and an oxidative bacterium. These organelles possess a double-membrane structure and contain their own genome along with their own transcription, translation, and protein assembly machinery.

Two distinct genetic systems encode mitochondrial proteins: mitochondrial DNA (mtDNA) and nuclear DNA (nDNA); the vast majority are coded by nDNA and imported to the mitochondrion.

The enzymes of the respiratory chain are embedded in the inner mitochondrial membrane, and they are essential to the process of oxidative phosphorylation, which generates most of the animal cell's ATP.

However, as a consequence of proto-mitochondrial genes integrating into the nuclear genome throughout evolution, most mitochondrial proteins are encoded by nuclear DNA (nDNA) and imported into mitochondria. Although the replication of mitochondrial DNA (mtDNA) is not synchronized with nDNA replication, the overall number of mitochondria

### 3.1 Introduction

per cell remains fairly constant for specific cell types during proliferation, suggesting that the generation of mitochondria is largely influenced by extra-mitochondrial signal transduction events.

#### 3.1.5 Genetics

The human mtDNA (first sequenced in 1981) is a 16,569-bp, double-stranded, circular molecule containing 37 genes. Of these, 24 are needed for mtDNA translation (2 ribosomal RNAs [rRNAs] and 22 transfer RNAs [tRNAs]), and 13 encode subunits of the respiratory chain (out of the 87 proteins required for oxidative phosphorylation): seven subunits of complex I (ND1, 2, 3, 4, 4L, 5, and 6), one subunit of complex III (cytochrome *b*), three subunits of cytochrome *c* oxidase (COX I, II, and III), and two subunits of ATP synthase (A6 and A8). The mtDNA uses an alternative genetic code as opposed to nDNA.

Mitochondrial genetics differs from mendelian genetics in several aspects:

**Maternal inheritance.** Most of mitochondria (and most of mtDNAs) in the zygote derive from the ovum. Therefore, a mother carrying a mtDNA mutation passes it on to all her children, but only her daughters will transmit it to their progeny.

**Heteroplasmy.** Somatic human cells contain two copies of nuclear DNA but they contain many more copies of mtDNA (from 1000 to 100 000, depending on the cell type). These are all identical in a healthy individual at birth (*homoplasmy*). Patients with mtDNA mutations often have a mixture of mutated and wild-type mtDNA (*heteroplasmy*): the percentage of mutated mtDNA can vary widely among different patients, from organ to organ, between cells, and even at the organellar level: a single mitochondrion can harbour both normal and mutant mtDNAs.

**Threshold effect.** A minimal number of mutant mtDNAs must be present before oxidative dysfunction occurs and clinical signs become apparent. Cells are able to tolerate high percentage levels of mutated mtDNA (typically 70–90%) before they developed a biochemical defect. The threshold for disease is lower in tissues that are highly dependent on oxidative metabolism (brain, heart, skeletal muscle, retina, renal tubules, and endocrine glands).

**Mitotic segregation.** The random redistribution of organelles at the time of cell division can change the proportion of mutant mtDNAs received by daughter cells, leading to changes in the level of mutated mtDNA species in replicating tissues.

**Relaxed replication.** mtDNA replication is independent of nDNA replication (“relaxed”): unlike nDNA which replicates only once during each cell cycle, mtDNA is continuously recycled, even in non-dividing tissues (e.g. skeletal muscle, brain). In a heteroplasmic cell, it is possible that mutated and wild-type mtDNA replicate at subtly different rates: this mechanism could lead to changes in the proportion of mutated mtDNA that have been described in patients with mtDNA disease, providing an explanation for the late onset and progression of some mtDNA disorders.

It is of interest to note that other than the aforementioned 13 respiratory chain components, no other genes for structural proteins are found in human mtDNA. The mitochondrial genome is distinct from the nuclear genome in that it follows a strict maternal inheritance pattern. Within a cell, mtDNA replication is semi-autonomous and is not synchronized with the S phase of the cell cycle. However, the two genetic systems (nuclear and mitochondrial) appear to be closely coordinated by yet unknown mechanisms. Although the mitochondrion contains the necessary machinery to express its genome, many of its protein components are encoded by nuclear DNA. It is known that mtDNA is far more vulnerable to mutations than nuclear DNA due to its lack of histone

### 3.1 Introduction

protection, limited repair capacity, and close proximity to the electron transport chain, which constantly generates superoxide radicals. Considering mtDNA lacks introns, most mutations occur in the coding sequences and are thus, likely to be of biological consequence. Because each cell contains many mitochondria with multiple copies of mtDNA, it is possible that wild-type and mutant mtDNA can co-exist in a state called heteroplasmy. Over time, the proportion of the mutant mtDNA within the cell can vary and may drift toward predominantly mutant or wild type to achieve homoplasmy. Thus, the biological impact of a given mutation may vary. This effect contributes to the various phenotypes observed amongst family members carrying the same pathogenic mtDNA mutation.

#### 3.1.6 Mitochondria dysfunctions

Mitochondrial diseases can be caused by nDNA and mtDNA defects; some of them (e.g. myopathies with "ragged red fibres") show accumulation of mitochondria similar to that seen in oncocytic tumours.

There are six known essential alterations in cell physiology that collectively might dictate malignant transformation: self-sufficiency in growth signals, insensitivity to growth-inhibitory (antigrowth) signals, limitless replicative potential, sustained angiogenesis, tissue invasion and metastasis, and evasion of programmed cell death (apoptosis) [17]. In addition, there is a growing body of evidence suggesting that one of the early recognized peculiarities of tumour cells (i.e. their dependence on glycolysis for ATP generation) might be added to this list. In 1926, Otto Warburg found that cancer cells produce most of their ATP through glycolysis, even under aerobic conditions [18], and there was a correlation between glycolytic ATP production and aggressiveness of the tumour cells [19]. Warburg assumed that such 'aerobic glycolysis' was a universal

property of malignant cells and suggested that cancer is caused by impaired mitochondrial metabolism. He hypothesized that these cells could be eliminated through the inhibition of mitochondrial oxidative phosphorylation, which would reduce the activity of these organelles below a threshold level critical for cell survival, whereas mitochondria in normal cells would still be able to produce enough ATP. Independent of whether mitochondrial respiration is low or not, cancer cells do exhibit high rates of glycolysis aerobic or anaerobic. Mitochondria also produce reactive oxygen species (ROS), which are involved in the regulation of many physiological processes, but which might also be harmful to the cell if produced excessively. These functions are of crucial importance for tumour cell physiology, growth and survival.

#### **3.1.7 Alterations of energy-supplying pathways in tumours**

One of the main characteristics of cancer cells is their fast proliferation. As such, rapidly growing tumours easily become hypoxic owing to the inability of the local vasculature to supply an adequate amount of oxygen. Similar hypoxic conditions are usually lethal to non-malignant cells. However, tumour cells can successfully escape hypoxia-mediated death as a result of lowered expression or mutation of p53 [20]. Owing to the inability of mitochondria to provide enough ATP for cell survival under hypoxic conditions, tumour cells must upregulate the glycolytic pathway. This occurs by induction of hypoxia-inducible factor 1 (HIF-1) [21]. HIF-1 stimulates key steps of glycolysis, but regulates genes that control angiogenesis, cell survival and invasion. However, it should be mentioned that, in addition to hypoxia, other factors (e.g. hormones and growth factors) might cause stabilization of HIF-1 expression [22]. Stimulation of glycolysis can also occur by activation of phosphoinositide 3-kinase (PI3K) and its downstream target, Akt. Activation of Akt triggers increases in cell size, enhanced glycolytic activity and

### 3.1 Introduction

metabolism, and cell survival [23], and is commonly observed in cancer cells [24]. When mitochondrial respiration in tumour cells is downregulated, accumulation of Krebs cycle substrates might serve as a signal for stimulation of glycolysis [25]. Defects in mitochondrial respiration cause enhanced levels of NADH, which can subsequently inactivate PTEN (phosphatase and tensin homologue) through a redox modification mechanism [26]. In addition to upregulating the glycolytic pathway, HIF-1 can initiate apoptosis by stabilization of p53 and/or induction of certain pro-apoptotic proteins. Therefore, during hypoxia, a complicated balance emerges between factors that stimulate or suppress apoptosis.

#### **3.1.8 ROS impairment**

Cancer cells are generally more active than normal cells in metabolic ROS generation and are constantly under oxidative stress. It is conceivable that certain mtDNA mutations may be caused by endogenous ROS in cancer cells. Alterations in mitochondrial functions could in turn cause further increases of ROS production, leading to more mutations and additional oxidative stress. Certain mtDNA mutations in cancer cells are likely to cause malfunctions of the respiratory chain and increase free radical generation. This biochemical change provides an unique opportunity to selectively kill this population of cancer cells by using agents that inhibit free radical elimination and cause further ROS accumulation, leading to lethal damage in the cancer cells [27]. Taken together, it is evident that mtDNA mutations are clinically relevant and have potential therapeutic implications.

The hypoxic environment of proliferating tumour tissue facilitates ROS production. Therefore, under hypoxic conditions and, in particular, after normalization of oxygen supply, production of ROS in tumour cells can be enhanced to an extent that might induce

damage to vital cellular components, including mitochondrial DNA (mtDNA). This might trigger a vicious cycle (i.e. hypoxia, ROS production, mtDNA mutations, malfunction of the mitochondrial respiratory chain, further stimulation of ROS production etc.), thus impairing mitochondrial function and causing a shift to glycolytic ATP production.

#### **3.1.9 Upregulation of glycolysis in tumour**

The seemingly most obvious reason for a glycolytic shift in cancer cells is that molecular oxygen becomes unavailable in fast-proliferating cells, and thus the mitochondria cannot function properly in ATP production. Nevertheless, even after restoration of oxygen supply, tumour cells tend to utilize glucose and to keep mitochondrial activity suppressed. Apparently, ATP production is not the only reason why tumour cells favour this energetically unprofitable pathway. Furthermore, mounting evidence demonstrates that the amount of glucose entering cancer cells exceeds their bioenergetic demands. The high rate of glycolysis in most tumours not only compensates for mitochondrial dysfunction but also is required to support tumour cell proliferation. High intracellular glucose concentrations enable the cell to redirect the accumulated glycolytic end-product, pyruvate, toward lipid synthesis, which is necessary for membrane assembly. In addition, a shift to the glycolytic pathway with production of lactate creates an acidic environment that gives the cancer cells a competitive advantage for invasion, because the acidic environment is toxic for non-malignant cell populations [28]. Another important consequence of the glycolytic shift in tumour cells is their acquired resistance to apoptotic cell death.

## 3.1 Introduction

### 3.1.10 Genetic and biochemical alterations in oncocytic tumours

The best studied oncocytic tumours in terms of mtDNA are those of the thyroid. A large deletion encompassing 4,977 bp of mtDNA, known as the mtDNA common deletion (CD), is almost always detected and was proposed as a hallmark of oncocytic thyroid tumours [10, 29]. This deletion removes seven OXPHOS genes (ATPase6, ATPase8, COIII, ND3, ND4L, ND4 and ND5) and five tRNAs (glycine, arginine, histidine, serine and leucine), thus resulting in severe impairment of the OXPHOS system. The severe impairment of the OXPHOS system (as a consequence of the mtDNA CD) would engage and activate nuclear genes that control mitochondrial number, resulting in an increase in the mitochondrial mass [30]. The analysis of the prevalence of mtDNA mutations has shown that missense somatic mutations in complex I genes were more frequently detected in malignant tumours than in adenomas [10]. A significant association was also observed between D-loop somatic mutations and the occurrence of somatic mutations in other mtDNA genes [10]. The absence of complex I, together with an increase in the remaining complexes and citrate synthase, led to the conclusion that the mitochondrial proliferation might be a compensatory mechanism for a decreased OXPHOS activity [31]. The defective ATP production observed in some studies [32, 33] may explain the characteristic mitochondrial proliferation of oncocytic cells.

Gasparre et al. [34] demonstrated that the oncocytic phenotype in thyroid carcinoma is associated with disruptive mutations in complex I subunits genes. They found a larger prevalence of nonsense and frameshift mutations caused by insertions or deletions in coding regions of mtDNA. Moreover, they found in one case of mitochondria-rich breast carcinoma, out of five analysed, a disruptive mutation. These mutations may arise as a second hit in tumour development and that the oncocytic phenotype in thyroid tumours may be strictly correlated with these mutations.

## 3.2 MATERIAL AND METHODS

### 3.2.1 Case selection

Group 1: 28 cases of surely oncocytic breast carcinomas were selected from Professor Eusebi consultations (8 cases) and from Bellaria Hospital files (20 cases) to identify the morphological and immunohistochemical characteristic of these tumours.

Group 2: 84 consecutive breast carcinomas (years 1997-1998) were retrieved from the files of Bellaria Hospital (Bologna, Italy) and analyzed for checking the frequency of oncocytic tumours and for comparing these non-selected cases with the previous group.

Group 3: A series of 18 putative oncocytic carcinomas of the breast was retrieved from the files of Bellaria Hospital, Bologna, Italy. A control group of 36 grade and ER-matched invasive ductal carcinomas no-special-type (IDC-NSTs) were retrieved from the files of The Breakthrough Breast Cancer Research Centre (Institute of Cancer Research, London - UK).

All cases were revised by two pathologists (GT and VE) and graded according to Elston & Ellis. Immunohistochemistry was assessed using the Ventana system. Representative sections from mt-rich BCs and IDC-NSTs were microdissected and DNA was extracted and subjected to aCGH using a 32K tiling path bacterial artificial chromosome array platform. aCGH results were subjected to unsupervised hierarchical clustering analysis and profiles were compared using a previously validated multi-Fisher's exact test with p values adjusted for multiple comparison by the false discovery rate.

## 3.2 Material and Methods

### 3.2.2 Immunohistochemistry

To perform a semiquantitative analysis of cytoplasmic content of mitochondria, anti-mitochondria antibody (Ab-2, clone MTC02, LabVision Neomarker) has been optimized using as control a Warthin's tumour. Optimal dilution was chosen using as reference the negativity of reaction in lymphocytes. Reaction was performed according to manufacturer's protocol (Ultravision LP Detection System HRP Polymer – LabVision, Fremont, CA, U.S.A.).

Cytoplasmic positivity was scored as follows (Fig.3.2):

3+ ( $\geq 60\%$ ) → Strong Positivity (Oncocytic Cells)

2+ ( $< 60\%$  /  $>30\%$ ) → Moderate Positivity (Mitochondrial Rich Cells)

Neg/1+ → Weak positivity or absent positivity

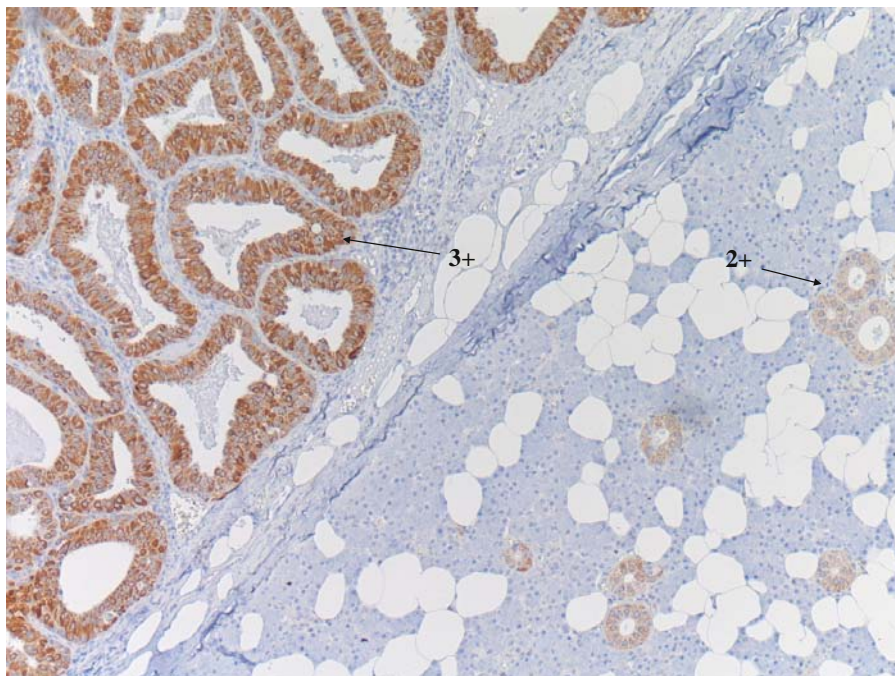


**Figure 3.2:** Staining of a Warthin's tumour using Ab anti-mitochondria. 3+: strong positivity, corresponding to oncocytic cells. 2+: moderate positivity, corresponding to mitochondrial rich cells.

### 3. Oncocytic Breast Carcinoma

Tumours were reclassified according to intensity of positivity and to percentage of positive neoplastic cells (Figures 3.3, 3.4, 3.5).

- Oncocytic Carcinoma (OC): 3+  $\geq$  70% of the cells

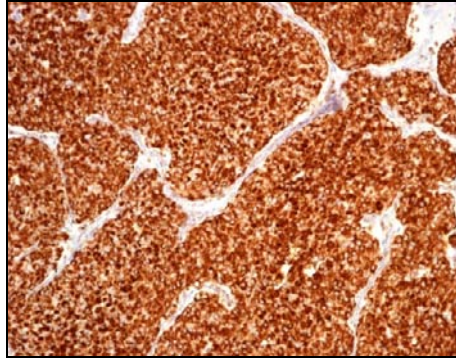


**Figure 3.3**

- Mitochondria-rich carcinoma (mt-rich): 2+  $>$ 50% or 3+  $<$ 70% and  $>$ 30%

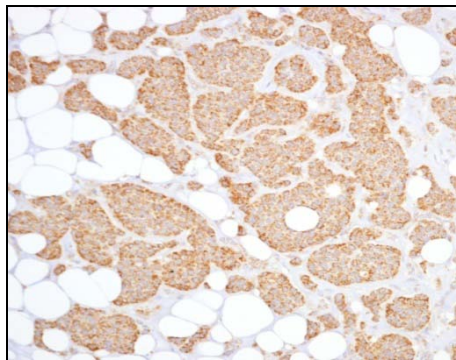


**Figure 3.4**

- Carcinoma not enriched in mitochondria (non mt-rich): 1+/Neg or 2+  $\leq$ 50% or 3+  $\leq$ 30%

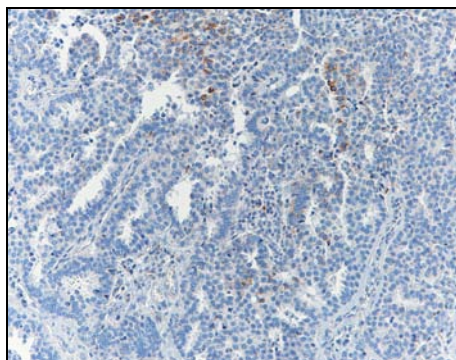


**Figure 3.5**

### 3.2 Material and Methods

Immunohistochemistry was assessed using the Ventana system (Ventana-Benchmark, Tucson, Arizona, U.S.A.) for all the antibodies analysed (Tab. 3.1) but not for anti-mitochondria. Positivity for ER and PR has been evaluated according to St.Gallen criteria 2005 (>10%) and 2009 (>1%).

<b>ANTIBODIES</b>	<b>Clone – Ventana Prediluted</b>	<b>Antigen Retrieval/ Detection System</b>
<b>ER</b>	<b>SP1</b>	<b>CC1<sup>^</sup>#</b>
<b>PR</b>	<b>1E2</b>	<b>CC1<sup>^</sup>#</b>
<b>AR</b>	<b>AR441</b>	<b>CC1<sup>^</sup>#</b>
<b>NEU</b>	<b>CB11</b>	<b>CC1<sup>^</sup>*</b>
<b>GCDFP-15</b>	<b>23A3</b>	<b>CC1<sup>^</sup>*</b>
<b>Chromogranin</b>	<b>LK2H10</b>	<b>CC1<sup>^</sup>*</b>
<b>EMA</b>	<b>E29</b>	<b>CC1<sup>^</sup>*</b>
<b>CK7</b>	<b>OV-TL 12/30</b>	<b>Protease enzymatic digestion*</b>
<b>CK14</b>	<b>LL002</b>	<b>CC1<sup>^</sup>*</b>
<b>CD68</b>	<b>PGM1</b>	<b>CC1<sup>^</sup>*</b>

**Table 3.1: Antibodies used for tumours characterization.** ER: Oestrogen Receptor; PR: Progesterone Receptor; AR: Androgen Receptor; HER2/Neu: Human Epidermal Growth Factor Receptor 2; GCDFP-15: Gross Cystic Disease Fluid Protein; EMA: Epithelial Membrane Antigen; CK: Cytokeratin; CD: Differentiation Cluster. <sup>^</sup> Ventana-Benchmark, Tucson, Arizona, U.S.A. <sup>#</sup>Detected by “Universal alkaline phosphatase red detection system” (Ventana-Benchmark); <sup>\*</sup>Detected by “Ultraview universal DAB detection system (Ventana-Benchmark)

#### 3.2.3 Electron Microscopy

For electron microscopy, small blocks were microdissected from paraffin-embedded samples in 6 cases where mitochondria-positive cells were numerous. These small blocks were dewaxed by overnight immersion in xylol and rehydrated to phosphate buffer, through a graded series of alcohol dilutions. Biopsies were then refixed in buffered glutaraldehyde, postfixed in OsO<sub>4</sub>, dehydrated in alcohol, and embedded in Epon 812 (Fort Washington, Pa). Thick sections stained with toluidine blue were used to select areas to examine. Thin sections were stained with uranyl acetate and Reynold's lead citrate, and observed in a Philips CM 10 TEM (Philips, Eindhoven, Netherlands).

#### 3.2.4 Follow-up

72 out of 81 cases of invasive breast carcinoma belonging to group 2 (years 1997-1998, from 6 to 144 months of FU, mean 96,69) were evaluated for follow-up analysis: 5 were lost to follow-up and 4 excluded because recurrences.

Overall free survival was calculated by GraphPad Prism<sup>®</sup> tool. Kaplan-Maier curves were compared using Wilcoxon and Mantel-Cox test.

#### 3.2.5 Microdissection and DNA extraction

All cases were microdissected to ensure >90% of purity of cancer cells. Microdissection was performed with a sterile needle under a stereomicroscope (Olympus SZ61, Japan) from five consecutive 8µm-thick sections stained with nuclear fast red.

DNA was extracted in 200 µl digestion buffer [100 mM NaCl, 10 mM Tris-HCl (pH 8.0), 25 mM EDTA (pH 8.0), 0.5% SDS, 0.5 mg/ml Proteinase K (Invitrogen Life Technologies)] and was purified by phenol/ chloroform extraction in Phase Lock Gel

## 3.2 Material and Methods

Lighttubes (Eppendorf, Hamburg, Germany). The purified DNA samples were ethanol-precipitated and the DNA resuspended in TE buffer (pH 7.5).

DNA concentration was measured with PicoGreen<sup>®</sup> assay as manufacturer's instructions (Invitrogen, Paisley, UK). DNA quality was assessed using four primer sets in a multiplex PCR [35].

### **3.2.6 Microarray comparative genomic hybridisation analysis (aCGH)**

The 32K BAC re-array collection (CHORI) tiling path aCGH platform used for this study and DNA labelling and array hybridisation were previously described (see “Genetic Heterogeneity in Metaplastic Breast Carcinoma” chapter).

*Data analysis.* Cases with >10% of clones missing and clones where data were not available in  $\geq 10\%$  of cases were excluded. Log<sub>2</sub> ratios were normalised for spatial and intensity dependent biases using a two-dimensional loess regression followed by a BAC-dependent bias correction as previously described. This left a final data set of 30 820 clones with unambiguous mapping information according to the March 2006 build (hg18) of the human genome (<http://www.ensembl.org>). Data were smoothed using a local polynomial adaptive weights smoothing (aws) procedure for regression problems with additive errors. A categorical analysis was applied to the BACs after classifying them as representing gain, loss, or no-change according to their smoothed Log<sub>2</sub> ratio values. A categorical analysis was applied to each clone on the array after classification as gain, loss, or no-change according to their smoothed log<sub>2</sub> ratio values. Smoothed log<sub>2</sub> ratio values less than  $-0.12$  were categorized as losses; those between  $0.12$  and  $0.40$  as gains (corresponding to approximately 3-5 copies of the locus); and those in between as unchanged. Amplifications were defined as smoothed log<sub>2</sub> ratio values greater than  $0.40$  (corresponding to more than 5 copies). Data processing and analysis were carried out in R

2.0.1 (<http://www.r-project.org/>) and BioConductor 1.5 (<http://www.bioconductor.org/>), making extensive use of modified versions of the packages aCGH, marray, and aws in particular. Copy number changes were categorized as gains, losses or amplifications according to the aforementioned thresholds for each clone before using Fisher's exact test (with adjustment for multiple testing).

Data were smoothed using the circular binary segmentation (cbs) algorithm [36, 37]. A categorical analysis was applied to the BACs after classifying them as representing gain, loss or no-change according to their smoothed Log<sub>2</sub> ratio values [38, 39]. Threshold values were chosen to correspond to three standard deviations of the normal ratios obtained from the filtered clones mapping to chromosomes 1-22, assessed in multiple hybridisations between DNA extracted from a pool of male and female blood donors as previously described [40] (Log<sub>2</sub> ratio of  $\pm 0.12$ ). Low level gain was defined as a smoothed Log<sub>2</sub> ratio of between 0.12 and 0.40, corresponding to approximately 3–5 copies of the locus, whilst gene amplification was defined as having a Log<sub>2</sub> ratio  $> 0.40$ , corresponding to more than 5 copies.

#### **3.2.7 Mitochondrial DNA sequencing**

Mitochondrial DNA was sequenced using mitoALL™ Resequencing Amplicon, RSS000056015\_01, for resequencing the entire mitochondrial genome with 46 RSAs mitoSEQr™ Resequencing Amplicons for mtDNA [Applied Biosystems]. The mitoSEQr system is designed for detecting sequence variants in human mtDNA. Pre-designed PCR primers tailed with M13 sequences generate either 9 resequencing amplicons (RSAs) for the mtDNA control region or 46 RSAs for the entire mitochondrial genome, as indicated. The PCR primers are provided ready to use and anneal at the same temperature.

### 3.2 Material and Methods

Alteration of mtDNA in mt-rich BCs mtDNA was analyzed in 12 mt-rich BCs: in 6 cases at least 2000 bp were sequenced (>15% of 16,569-bp genome) (Fig. 3.6); results checked with mitomap ([www.mitomap.org](http://www.mitomap.org)) and **PolyPhen** (*Polymorphism Phenotyping*) (<http://genetics.bwh.harvard.edu/pph/>) MitoRes v1.4 <http://genetics.bwh.harvard.edu/pph/>.

**PolyPhen** (=Polymorphism Phenotyping) is an automatic tool for prediction of possible impact of an amino acid substitution on the structure and function of a human protein. This prediction is based on straightforward empirical rules which are applied to the sequence, phylogenetic and structural information characterizing the substitution.

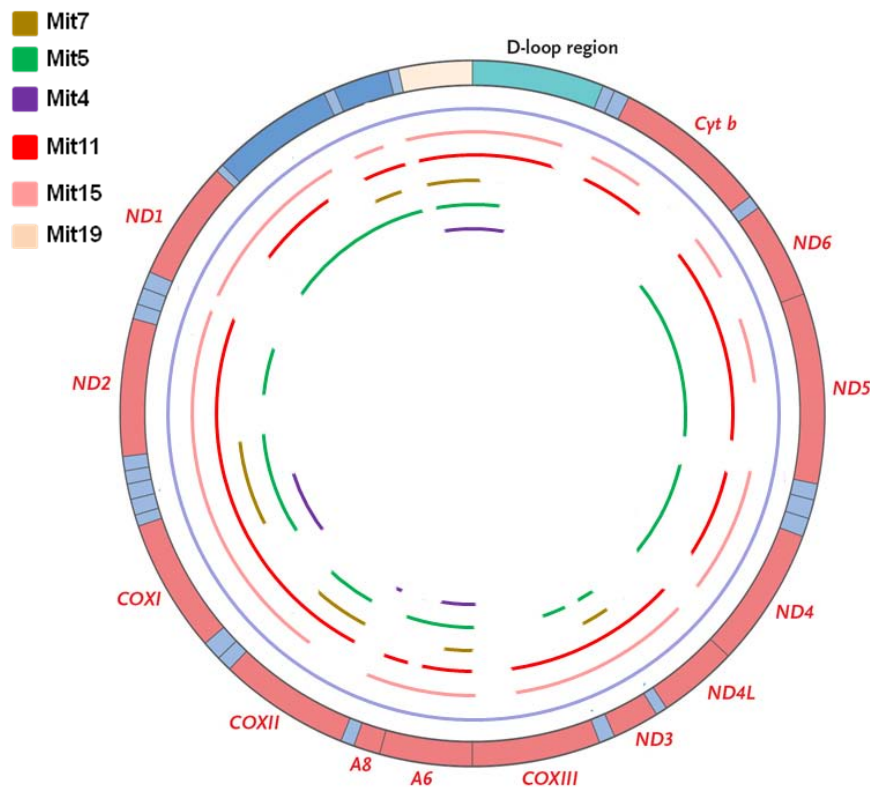


Figure 3.6: Scheme of mt-DNA covered by sequencing in 6 cases analysed

### 3.2.8 Nuclear genes codifying for mitochondrial protein

71 (out of about 800) nuclear genes for mitochondrial functions (chosen because implicated in mitochondrial syndrome or for their functions [41, 42]) were analysed using Fisher's exact test for comparing mt-rich/OC carcinomas (n=17) with IDC-NSTs samples (n=34) (Tab. 3.2).

ABCB7	MNF1	SCO2
ANT1	MFN2	SDHA
ANT2	MIL1	SDHB
ATPAF2	MRPS15	SDHC
BAD	MTIF2	SDHD
BCLB	NDUFA2	SOD1
BCS1L	NDUFB9	SOD2
C10orf2	NDUFS1	SPG7
CHCHD3	NDUFS2	SSBP1
COX10	NDUFS4	SURF1
COX15	NDUFS7	TAZ
CYB5B	NDUFS8	TFBP1
DDX28	NDUFV1	TFBP2
DGUOK	NDUFV2	TIMM44
DNC	OPA1	TIMM8A
DRP1	PDHA1	TK2
ETHE1	PDP1	TOP1MT
FH	PDP2	TYMP
FXN	POLG1	UNG
GFM1	POLG2	UQCRB
GOT2	POLRMT	VDAC1
GRIM19	PTRF	VDAC2
IMMT	RMRP	VDAC3
LRPPRC	SCO1	

**Table 3.2: Analysed nuclear genes codifying for mitochondrial protein**



### **3.3. RESULTS**

#### **3.3.1 Group 1 (selected OC).**

All the 28 patients were female, aged from 26 to 87 years (mean 65,3 y). The cases counted 25 IDC NOS, 2 CDI “special types” and 1 ILC. 57% (16/28) were grade III, 36% (10/28) grade II and 7% (2/28) grade I (Tab. 3.3). All the cases were studied by IHC (Tab. 3.4). According to positivity to anti-mitochondria antibody, 17 cases have been reclassified as “oncocytic”, 10 as “mitochondria rich” and one (Mit17) as “negative” and presented an apocrine differentiation.

### 3.3 Results

CASE	AGE	DIAGNOSIS	GRADE	STAGE	MIT.	ER%	PR%	Neu	APO	CHR	AR	CK7	CK14	EMA	CD68
Mit1	87	IDC	G3	pT2, NO, M1	2+ (80%)	65	60	-	-	-	-	-	-	+	-
Mit2	70	IDC	G2	pT1a, NO, M0	2+ (70%)	90	90	-	-	-	-	+	-	+	-
Mit3*	78	IDC	G3	pT2, N1a	2+ (70%)	90	40	2+	-	-	+	-	-	+	-
Mit4*	68	IDC	G3	pT2, N1a	3+ (90%)	-	-	3+	+	-	+	+	-	+	-
Mit5*	83	IDC	G2	pT1c, NO	2+ (90%)	80	20	2+	-	-	-	-	-	+	-
Mit6*	51	IDC	G3	pT2, N2a	2+ (70%)	20	-	2+	-	-	-	+	-	+	-
Mit7*	45	IDC	G3	pT1c, NO	3+ (90%)	80	50	1+	-	-	+	-	-	+	-
Mit8*	58	IDC	G2	pT1c, N1a	3+ (90%)	90	50	3+	-	-	-	-	-	+	-
Mit9*	66	IDC	G3	pT1c, Ns0	3+ (90%)	-	-	2+	-	-	-	+	-	+	-
Mit10*	49	IDC	G3	pT1c, N1a	2+ (70%)	80	70	2+	-	-	-	+	-	Foc	-
Mit11*	50	IDC	G3	pT1c, Ns1a	2+ (70%)	-	-	3+	Foc	-	+	+	-	+	-
Mit12*	79	IDC	G3	pT3, N0	3+ (90%)	10	-	3+	+	-	+	+	-	+	-
Mit13*	26	IDC	G3	pT2, N2	3+ (80%)	15	-	3+	Foc	-	-	+	-	+	-
Mit14*	71	ILC	G3	pT3, N3	2+ (80%)	80	-	-	-	-	-	+	-	+	-
Mit15*	76	IDC	G3	pT2, N0	3+ (80%)	90	-	3+	-	-	-	-	-	-	-
Mit16*	61	IDC	G2	pT1b, Ns0	3+ (90%)	95	95	-	Foc	-	+	+	-	+	-
Mit17*	72	IDC	G2	pT1c, NO	-	95	30	-	+	-	+	Foc	-	+	-
Mit18*	76	IDC	G2	pT2, N0	3+ (90%)	85	45	1+	Foc	-	-	+	-	+	-
Mit19*	76	IDC	G3	pT2, N3	3+ (90%)	95	45	2+	-	+	+	+	-	+	-
Mit20*	65	IDC	G3	pT1c, Ns0	2+ (70%)	-	-	-	-	-	-	+	Foc	+	-
Mit21	52	IDC "simil Hashimoto"	G2	pT1b, N1	3+ (90%)	90	40	-	-	-	+	-	-	+	-
Mit22	41	IDC	G2	pT2, N0	3+ (90%)	95	90	-	-	-	+	+	-	+	-
Mit23	58	IDC BTRPTC	G1	pT1b	3+ (90%)	50	-	-	-	-	-	+	-	Foc	-
Mit24	76	IDC	G2	pT2, N0	2+ (60%)	95	15	-	-	-	-	Foc	-	-	-
Mit25	85	IDC	G2	n.d.	3+ (90%)	95	95	-	-	-	-	+	-	+	-
Mit26	70	IDC	G1	pT2	3+ (80%)	90	70	-	-	+	-	-	-	+	-
Mit27	55	IDC	G3	pT4	3+ (70%)	90	80	-	-	-	-	+	-	+	-
Mit28	66	IDC	G3	pT2, N1	3+ (80%)	90	-	3+	-	-	-	-	-	+	-

**Table 3.3: Results of anatomico-clinical results of group 1 carcinomas.** IDC: Invasive Ductal Carcinoma; ILC: Invasive Lobular Carcinoma; BTRPTC: Breast Tumour Resembling Papillary Thyroid Carcinoma (tall cell variant); Foc: Focal, <20%; \*: cases analyzed by aCGH. In red: oncocytic carcinomas. N.a.: not available; Neu: HER2/Neu score according to guidelines of ASCO CAP 2007 [43].

AB	Positive Cases	%
APO (focal)	3/28 (4/28)	10,7 (14,3)
Chromogranin	2/28	7,1
ER (>10%) (>1%)	22/28 (23/28)	78,6 (82,1)
PR (>10%) (>1%)	17/28 (17/28)	60,7 (60,7)
HER2/Neu	7/28	25
AR	10/28	35,7
EMA (focal)	24/28 (2/28)	85,7 (7,1)
CK7 (focal)	17/28 (2/28)	60,7 (7,1)
CK14 (focal)	0/28 (1/28)	/ (3,6)
CD68	0/28	/

**Table 3.4: Pannell of immunohistochemistry results of 28 cases belonging to group 1.**

### 3.3.2 Group 2 (consecutive cases 1997-1998)

81 consecutive breast carcinomas (years 1997-1998), 78 women and 3 men, aged from 32 to 96 years (mean 66.1 y). Series included 58 IDC, 11 ILC, 2 mixed (ductal/lobular) and 10 “special types”: grade III were 31/81 (38.3%), grade II were 42/81 (51.8%) and grade I 8/81 (9.9%).

### 3.3 Results

All cases were analyzed by anti-mitochondria antibody, Out of these 81 cases, 47 (58%) were reclassified as “not enriched in mitochondria”, 18 (22.2%) as “mt-rich” and 16 (19.8%) as “OC” (Tab. 3.5).

Frequency of oncocytic carcinoma was so estimated as 19.8%.

	SEX	AGE (y)	FU (m)	DG	G	STAGE	IHC MIT	RECLASS
1	F	66	26 A	IDC Mix. Muc.	G2	pT2, N0,	2+ (80%)	Mt-Rich
2	F	47	144 A	ILC	G2	pT2, N1a	neg	Not Mt-Rich
3	F	51	144 A	IDC Pure Muc.	G1	pT2	1+ (90%)	Not Mt-Rich
4	F	85	56 D	IDC	G3	pT3, N1a	1+ (70%)	Not Mt-Rich
5	F	60	26 D	IDC	G3	pT2, N0,	3+ (80%)	OC
6	F	76	143 A	IDC	G2	pT2, N0	neg	Not Mt-Rich
7	F	77	143 A	IDC	G1	pT1c, N0,	2+ (70%)	Mt-Rich
8	F	66	119 A	IDC	G3	pT1b, N0	neg	Not Mt-Rich
9	F	66	142 A	IDC	G2	pT2, N1,	1+ (60%)	Not Mt-Rich
10	F	74	29 D	IDC	G3	pT1c, N0	3+ (70%)	OC
11	F	77	26 D	IDC	G2	pT1b	2+ (60%)	Mt-Rich
12	F	83	12 Dx	IDC	G1	pT1c, N0	neg	Not Mt-Rich
13	F	56	82 D	IDC Apo.	G3	Rec	2+ (80%)	Mt-Rich
14	F	65	52 D	ILC	G2	pT1c, N3a	2+ (60%)	Mt-Rich
15	F	84	101 Dx	IDC	G2	pT1c, N0,	1+ (70%)	Not Mt-Rich
16	F	32	140 A	IDC	G3	pT1c, N1,	1+ (30%)	Not Mt-Rich
17	F	69	140 A	ILC	G2	pT1c, N0	neg	Not Mt-Rich
18	F	58	139 A	IDC	G3	pT2, N0	3+ (70%)	OC
19	F	68	n.d.	IDC	G3	pT2, N1	3+ (80%)	OC
20	F	76	34 D	IDC Pure Muc.	G1	pT2	1+ (30%)	Not Mt-Rich
21	F	67	139 A	IDC Pure Muc.	G1	pT2, N0	neg	Not Mt-Rich
22	F	45	65 D	IDC	G3	pT2, N3a,	1+ (25%)	Not Mt-Rich
23	F	57	138 A	ILC	G2	pT2, N2a	2+ (60%)	Mt-Rich

### 3. Oncocytic Breast Carcinomas

	SEX	AGE (y)	FU (m)	DG	G	STAGE	IHC MIT	RECLASS
24	F	55	122 D	ILC	G2	pT4, N3a	1+ (50%)	Not Mt-Rich
25	F	79	25 Dx	IDC Pure Muc.	G1	pT1c	3+ (70%)	OC
26	M	68	137 A	IDC	G2	pT4, N0	3+ (80%)	OC
27	F	76	136 A	IDC	G2	pT1a, N1	neg	Not Mt-Rich
28	F	86	41 D	ILC+IDC	G2	pT4, N0	1+ (10%)	Not Mt-Rich
29	F	84	29 D	IDC Apo.	G3	pT4, N3a, M1	3+ (70%)	OC
30	F	58	136 A	IDC	G3	pT2, N1,	1+ (80%)	Not Mt-Rich
31	F	96	6 Dx	IDC	G2	pT2	1+ (10%)	Not Mt-Rich
32	F	52	70 Dx	IDC	G2	pT4, N0	1+ (70%)	Not Mt-Rich
33	M	76	96 Dx	IDC	G1	pT1b, N1, M1	1+ (40%)	Not Mt-Rich
34	F	75	134 A	IDC	G2	pT1c, N0	1+ (20%)	Not Mt-Rich
35	F	77	134 A	ILC	G3	Rec	1+ (15%)	Not Mt-Rich
36	F	49	134 A	IDC	G2	pT2, N0	1+ (20%)	Not Mt-Rich
37	F	65	134 A	IDC	G2	pT1c, N2	neg	Not Mt-Rich
38	F	57	15 D	IDC	G3	pT2, N1, M1	3+ (70%)	OC
39	F	70	55 A	IDC	G3	pT2, N2,	2+ (70%)	Mt-Rich
40	F	64	15 D	ILC pleomorphic	G3	Rec	2+ (50%)	Mt-Rich
41	F	40	133 A	IDC	G3	pT3, N1,	2+ (60%)	Mt-Rich
42	F	54	50 D	IDC	G3	pT2, N2	1+ (10%)	Not Mt-Rich
43	F	63	133 A	IDC	G3	pT1c, N1,	1+ (60%)	Not Mt-Rich
44	F	67	116 Dx	IDC	G2	pT1c, N0	1+ (25%)	Not Mt-Rich
45	M	66	29 D	IDC	G2	pT4, N1	1+ (50%)	Not Mt-Rich
46	F	67	88 D	IDC	G2	pT2, N1	3+ (90%)	OC
47	F	68	131 A	IDC	G3	pT2, N0	3+ (90%)	OC
48	F	49	130 A	IDC	G3	pT2, N0	3+ (70%)	OC
49	F	81	69 D	IDC	G1	pT1a, N0	1+ (10%)	Not Mt-Rich
50	F	68	129 A	IDC	G3	pT1c, N0	2+ (60%)	Mt-Rich

### 3.3 Results

	SEX	AGE (y)	FU (m)	DG	G	STAGE	IHC MIT	RECLASS
51	F	58	128 A	ILC	G2	pT2, N2	1+ (30%)	Not Mt-rich
52	F	52	128 A	IDC	G3	pT1c, N0	2+ (80%)	Mt-Rich
53	F	60	127 A	IDC	G3	pT4, N2	neg	Not Mt-Rich
54	F	60	127 A	IDC	G2	pT2, N1,	1+ (10%)	Not Mt-Rich
55	F	74	77 D	IDC	G2	pT4, N0	3+ (70%)	OC
56	F	63	127 A	IDC	G2	pT1c, N2	2+ (60%)	Mt-Rich
57	F	71	100 D	IDC	G2	pT4, N1	1+ (50%)	Not Mt-Rich
58	F	70	127 A	ILC	G2	pT1c, N0	1+ (30%)	Not Mt-Rich
59	F	74	10 D	ILC	G2	pT2, N3a	2+ (60%)	Mt-Rich
60	F	85	n.d.	IDC Mix Muc	G2	pT3	3+ (90%)	OC
61	F	50	21 A	IDC.	G2	pT2, N1,	2+ (60%)	Mt-Rich
62	F	50	38 D	AMC	G3	pT2, N1	1+ (40%)	Not Mt-Rich
63	F	94	126 A	IDC	G2	pT4	3+ (90%)	OC
64	F	66	n.d.	IDC	G3	pT1c, N2	2+ (60%)	Mt-Rich
65	F	75	126 A	ILC	G2	pT2, N0,	1+ (30%)	Not Mt-Rich
66	F	64	38 D	IDC	G3	pT4, N3a	2+ (60%)	Mt-Rich
67	F	59	37 D	IDC	G3	Rec	3+ (80%)	OC
68	F	40	125 A	IDC	G2	pT2, N1b	1+ (30%)	Not Mt-Rich
69	F	81	124 A	IDC+ILC	G2	pT1c, N1	neg	Not Mt-Rich
70	F	80	35 D	IDC	G2	pT1c, N0	neg	Not Mt-Rich
71	F	84	51 Dx	IDC	G2	pT2	1+ (50%)	Not Mt-Rich
72	F	60	7 D	IDC	G3	Rec, M1	2+ (60%)	Mt-Rich
73	F	50	43 A	IDC	G3	pT1c, N1,	1+ (30%)	Not Mt-Rich
74	F	65	64 D	IDC	G3	pT1a, N0,	1+ (60%)	Not Mt-Rich
75	F	69	122 A	IDC	G2	pT1b, N0	2+ (50%)	Mt-Rich
76	F	70	122 A	IDC	G3	pT2, N3a,	3+ (90%)	OC
77	F	49	122 A	ILC	G2	pT1c, N1	1+ (30%)	Not Mt-Rich
78	F	73	113 Dx	IPC	G2	pT4, N0	1+ (20%)	Not Mt-Rich
79	F	68	121 A	IDC	G2	pT1b, N0,	neg	Not Mt-Rich

	SEX	AGE (y)	FU (m)	DG	G	STAGE	IHC MIT	RECLASS
<b>80</b>	F	56	n.d.	IDC	G2	pT1c, N0	1+ (10%)	Not Mt-Rich
<b>81</b>	F	69	132 A	IDC	G2	pT1c, N1,	1+ (10%)	Not Mt-Rich

**Table 3.5: Reclassification of invasive breast carcinomas from 1997 to 1998 (Group 2).** Has been reported the values of positivity for tumours reclassification. IDC: Invasive Ductal Carcinoma; ILC: Invasive Lobular Carcinoma; AMC: Atypical Medullary Carcinoma; IPC: Invasive Papillary Carcinoma; Reclass: reclassification; Mix Muc Mixed Mucinous; FU: Follow-up; A: alive; D: death of breast carcinoma; Dx: death for other causes; n.a.: not available.

### 3.3.3 Oncocytic carcinomas

To determinate the anatomo-clinical and immunohistochemical characteristic of oncocytic carcinoma we put together the cases reclassified as OC from the group 1 and group 2. In this way we obtained a total of 33 oncocytic carcinomas (17 from group 1 and 16 from group 2).

Of these 33 samples, 32 were female (96.97%) and one case was a male (3.03%), age ranged from 26 and 94 years (mean 65.8 y). All 33 cases were IDC: 28/33 (84.8%) were NOS and 5 (15.2%) “special-types” (Tab. 3.6).

### 3.3 Results

Case	Age	FU	Diagnosis	G	Stage	Mit	APO	CHR	ER%	PR%	Neu	AR	EMA	CK14	CK7	CD68
5	60	26 D	IDC	G3	pT2, N0	3+ (80%)	-	-	10	5	-	-	+	-	+	-
10	74	29 D	IDC	G3	pT1c, N0	3+ (70%)	+	-	90	60	2+	-	+	-	+	-
18	58	139 V	IDC	G3	pT2, N0	3+ (70%)	-	-	90	5	-	-	+	-	+	-
25	79	25 Dx	IDC pure Muc	G1	pT1c	3+ (70%)	-	+	85	85	-	-	+	-	+	-
26	M68	137 V	IDC	G2	pT4, N0	3+ (80%)	-	-	70	20	-	-	Foc	-	+	-
29	84	29 D	IDC Apo.	G3	pT4, N3a	3+ (70%)	+	-	2	2	-	+	+	-	+	-
38	57	15 D	IDC	G3	pT2, N1	3+ (70%)	Foc	-	-	-	3+	-	+	-	+	-
46	67	88 D	IDC	G2	pT2, N1	3+ (90%)	+	-	90	90	-	-	+	-	+	-
47	68	131 V	IDC	G3	pT2, N0	3+ (90%)	-	-	-	-	3+	-	+	-	+	-
48	49	130 V	IDC	G3	pT2, N0	3+ (70%)	Foc	-	70	20	-	-	+	-	+	-
55	74	77 D	IDC	G2	pT4, N0	3+ (70%)	-	-	90	85	-	-	+	-	+	-
63	94	126 V	IDC	G2	pT4	3+ (90%)	-	-	-	-	-	-	+	-	+	-
76	70	122 V	IDC	G3	pT2, N3a	3+ (90%)	-	-	50	20	-	-	+	-	Foc	-
19	68	Nd	IDC	G3	pT2, N1	3+ (80%)	-	-	-	-	-	-	+	+	+	-
60	85	Nd	IDC Mix Muc	G2	pT3	3+ (90%)	-	-	90	70	-	-	+	-	Foc	-
67	59	Nd	IDC	G3	Rec	3+ (80%)	Foc	-	80	5	-	-	+	-	+	-
Mit4	68	Nd	IDC	G3	pT2, N1a	90 (3+)	+	-	-	-	3+	+	+	-	+	-
Mit7	45	Nd	IDC	G3	pT1c, N0	90 (3+)	-	-	80	50	1+	+	+	-	-	-
Mit8	58	Nd	IDC	G2	pT1c, N1a	90 (3+)	-	-	90	50	3+	-	+	-	-	-
Mit9	66	Nd	IDC	G3	pT1c, Ns0	90 (3+)	-	-	-	-	2+	-	+	-	+	-
Mit12	79	Nd	IDC	G3	pT3, N0	95 (3+)	+	-	10	-	3+	+	+	-	+	-
Mit13	26	Nd	IDC	G3	pT2, N2	90 (3+)	+	-	15	10	3+	-	+	-	+	-
Mit15	77	Nd	IDC	G3	pT2, N0	80 (3+)	-	-	85	10	3+	-	-	-	-	-
Mit16	61	Nd	IDC	G2	pT1b, Ns0	90 (3+)	-	-	95	95	-	+	+	-	+	-
Mit18	76	Nd	IDC	G2	pT2, N0	90 (3+)	-	-	85	45	1+	-	+	-	+	-
Mit19	76	Nd	IDC	G3	pT2, N3	90 (3+)	-	+	95	45	2+	+	+	-	+	-
Mit21	52	Nd	IDC like Hashimoto	G2	pT, N1	90 (3+)	-	-	90	40	-	+	+	-	-	-
Mit22	41	Nd	IDC	G2	pT2, N0	90 (3+)	-	-	95	90	-	+	+	-	+	-

### 3. Oncocytic Breast Carcinomas

Case	Age	FU	Diagnose	G	Stage	Mit	APO	CHR	ER%	PR%	Neu	AR	EMA	CK14	CK7	CD68
Mit23	58	Nd	IDC BTRPTC	G1	pT1b	90 (3+)	-	-	50	-	-	-	+ (FOC)	-	+	-
Mit25	85	Nd	IDC	G2	nd	90 (3+)	-	-	95	95	-	-	+	-	+	-
Mit26	70	Nd	IDC	G1	pT2	80 (3+)	-	+	90	70	-	-	+	-	-	-
Mit27	55	Nd	IDC	G3	pT4	70 (3+)	- (FOC)	-	80	80	-	-	+	-	+	-
Mit28	66	Nd	IDC	G3	pT2, N1	80 (3+)	-	-	90	5	3+	-	+	-	-	-

**Table 3.6: Anatomico-clinical and immunohistochemical characteristic of 33 OC.** IDC: Invasive Ductal Carcinoma; BTRPTC: Breast Tumour Resembling Papillary Thyroid Carcinoma (tall cell variant); Mix Muc: Mixed Mucinous; Rec: recurrent; Foc: Focal, <20%; A: alive; D: death for pathology; Dx: death for other cause; N.a.: not available; Neu: HER2 score according to ASCO CAP 2007 guidelines [43]

### 3.3 Results

#### 3.3.4 Anatomico-clinical features

The cases were especially of grade II and III, with dimension ranged from 2 cm e 5 cm (pT2), with or without lymphnodal metastases (Tab. 3.7).

Grade	Cases(%)
I	3/33 (9%)
II	11 /33 (33%)
III	19/33 (58%)
T	
1	7/30 (23%)
2	16/30 (53%)
3	2/30 (7%)
4	5/30 (17%)
N	
0	14/25 (56%)
1	7/25 (28%)
2	1/25 (4%)
3	3/25 (12%)

**Table 3.7: Grade, pT and N of oncocytic carcinomas**

Morphologically appeared with solid nests, cellular shape from round to polygonal, eosinophilic cytoplasm. Nuclei were especially pleomorphic and sometimes could be associated a lymphoid stroma (Tab. 3.8; Figs. 3.7-3.10).

Features	Description	Number of cases (%)
Patterns of Growth	<b><i>Solid Nests</i></b>	<b>23 (70%)</b>
	Glandular	2 (6%)
	Cribriform	15 (24%)
	Plexiform	2 (6%)
	Papillary	1 (3%)
Margins	Infiltrative	16 (48%)
	Pushing	17 (52%)
Cellular Shape	<b><i>Round to Polygonal</i></b>	<b>32 (97%)</b>
	Columnar to Cuboidal	1 (3%)
Cytoplasm	<b><i>Eosinophilic</i></b>	<b>30 (91%)</b>
	Clear	3 (9%)
Nuclei	Monomorphic	8 (24%)
	Pleomorphic	25 (76%)
Nucleoli	Prominent	23 (70%)
	Inconspicuous	10 (30%)
Lymphoid Stroma	Present	19 (57%)
	Absent	14 (43%)

Table 3.8: Main morphological characteristics of oncocytic carcinomas

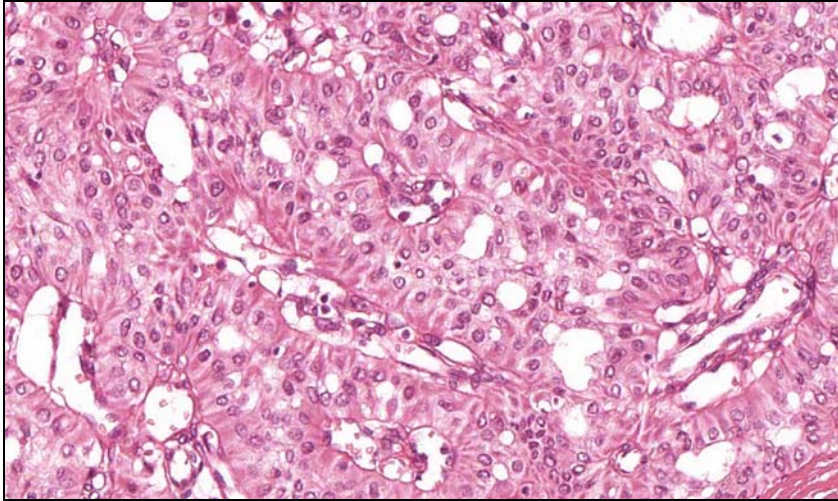


**Figure 3.7: H&E of a GI oncocytic carcinoma**

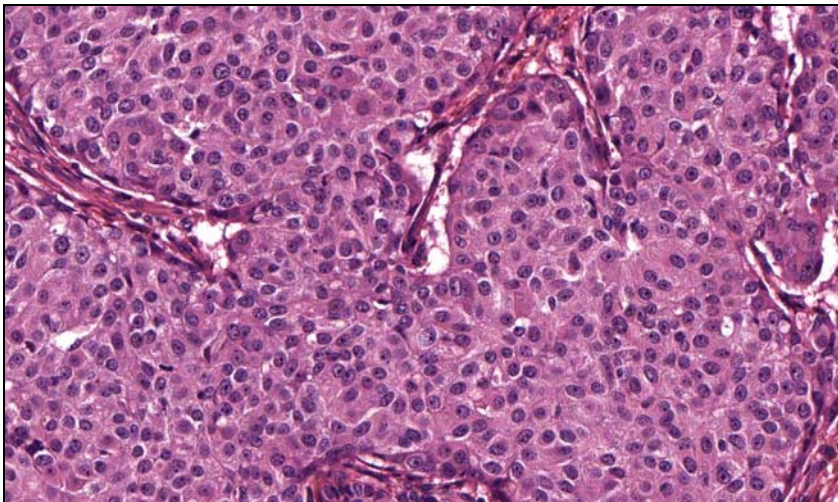


**Figure 3.8: H&E of a GII oncocytic carcinoma**

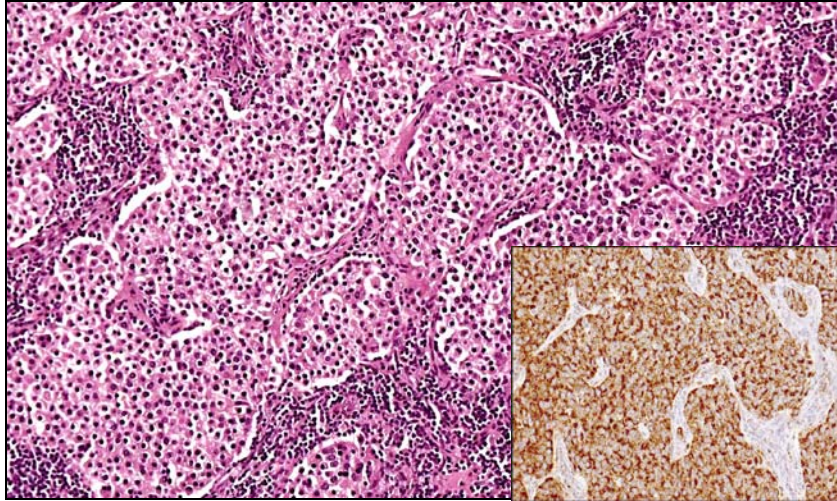


**Figure 3.9: E/E of a GII oncocytic carcinoma lymphnodal.** Inside square: IHC with anti-mitochondria antibody

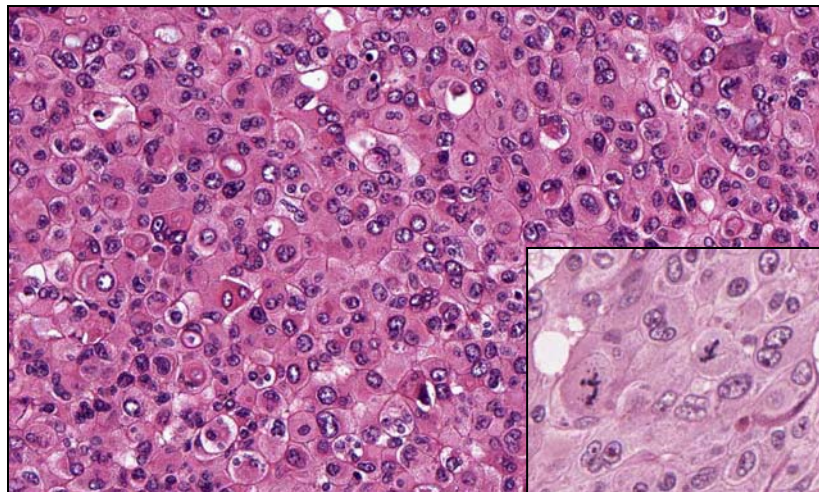


**Figure 3.10: E H&E of a GIII oncocytic carcinoma.**  
Inside square: mitosis detail.

### 3.3 Results

#### 3.3.5 Immunohistochemical features

At immunohistochemical level, most of the cases showed a positivity for ER, EMA and CK7. Sometimes could be associated an endocrine or apocrine differentiation (Tab. 3.9).

Ab	Cases +	%
APO (focal)	6/33 (6/33)	18,1 (18,1)
Chromogranin	3/33	9,1
ER (>10%) (>1%)	24/33 (27/33)	72,7 (81,8)
PR (>10%) (>1%)	18/33 (25/33)	54,5 (75,6)
HER2/Neu (3+)	8/33	24,2
AR	8/33	24,2
EMA (focal)	30/33 (2/33)	90,9 (6,1)
CK14	1/33	3
CK7 (focal)	25/33 (2/33)	75,8 (6,1)
CD68	0/33	/

**Table 3.9: Immunohistochemical pattern of oncocytic carcinomas.**

### 3.3.6 Electron Microscopy

At electron microscopy, the six OC samples showed similar ultrastructural features. Numerous mitochondria were present scattered throughout the cytoplasm, from round to ovoid, sometimes swollen with flattened cristae. No secretory granules, vesicles or lysosome have been observed (Fig. 3.11).

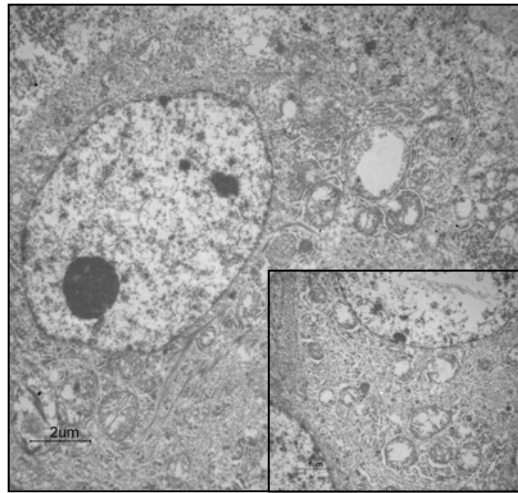


**Figure 3.11: Electronic Microscopy of an OC.** The mitochondria are swollen with flattened cristae. Inside square: particular of mitochondria.

### 3.3.7 Follow-up

No statistically significant differences in prognosis were observed in survival analysis (Wilcoxon and Mantel-Cox test,  $p < 0.05$ ), even if oncocytic carcinomas seemed to show a tendency towards a worst prognosis in comparison to IDC not enriched in mitochondria. This pattern was observed considering OC associated, or not, with mitochondria-rich carcinomas (Fig. 3.12) and reached a statistical significance ( $p < 0.05$ ) comparing OC/mt-rich (grade II) with not-mtRich (grade II) (Fig. 3.14A) and mt-rich (grade II) with not-mtRich (grade II) (Fig. 3.16A). No differences were reported comparing grades III (Figs. 3.12-3.16) or different pT (pT2, pT4) (Figs. 3.12-3.16).

### 3.3 Results

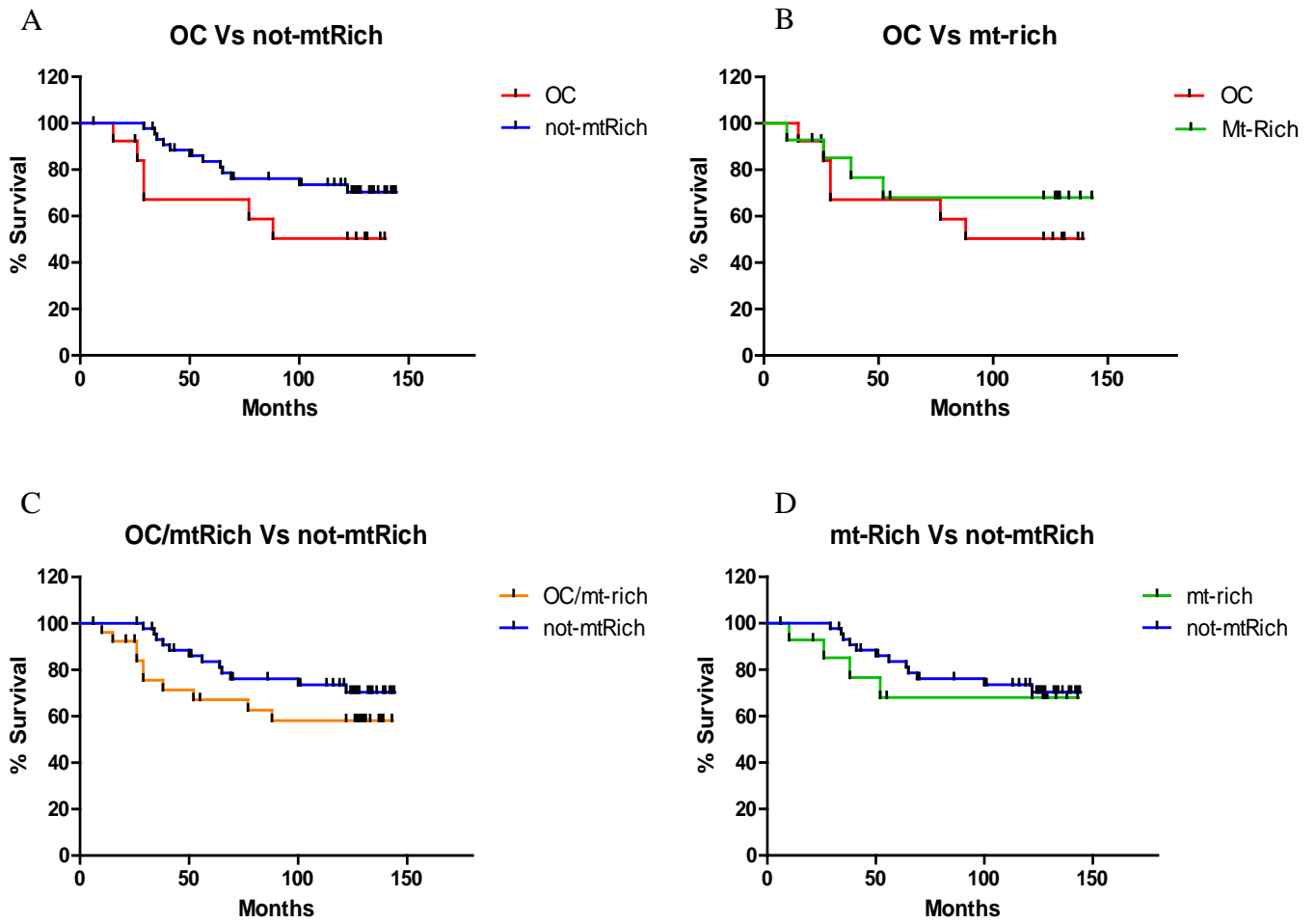


**Figure 3.12: Kaplan-Meier. Analysis of overall survival for OC, mt-rich and not-mtRich. N.S. Wilcoxon and Mantel-Cox tests.**

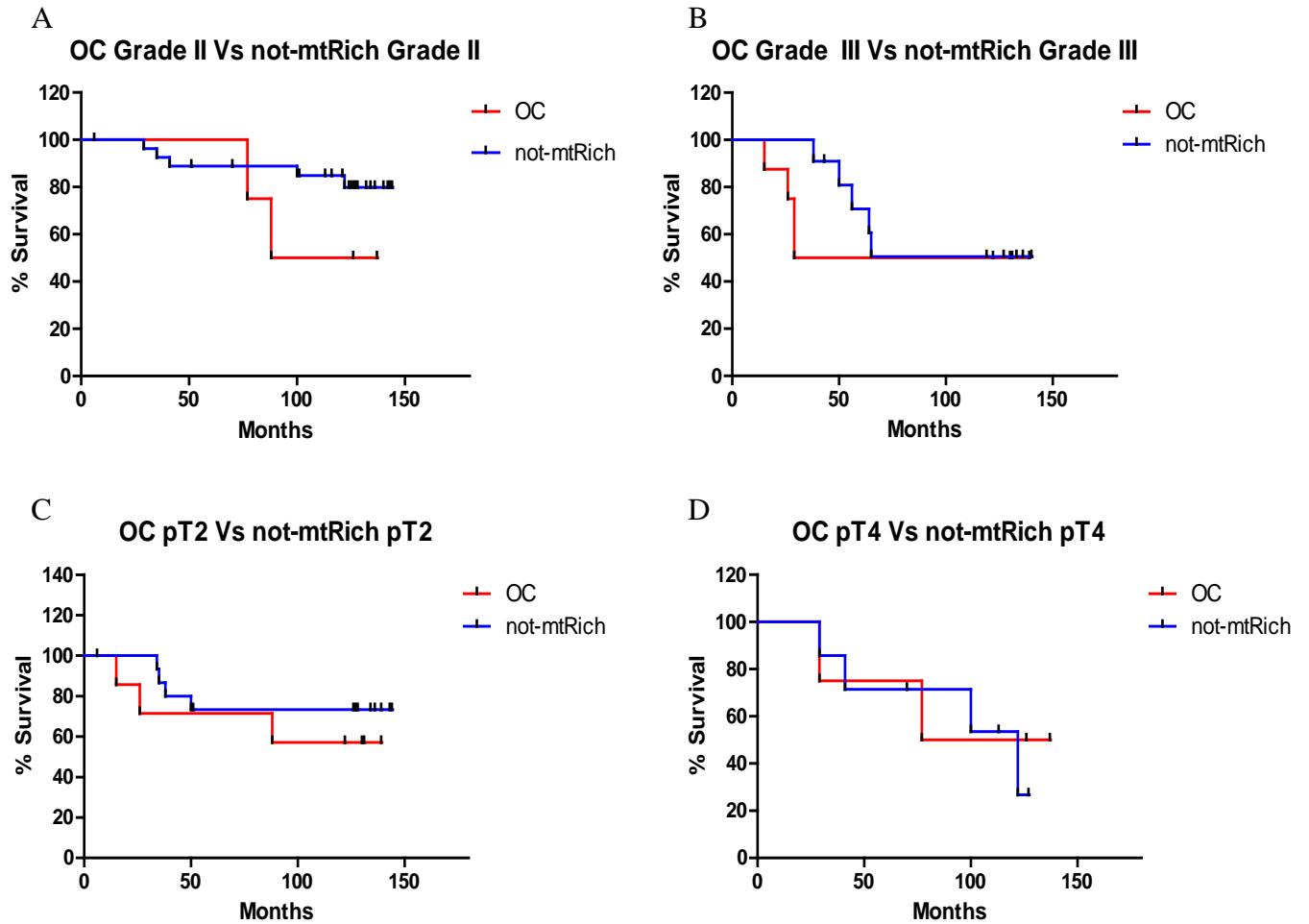
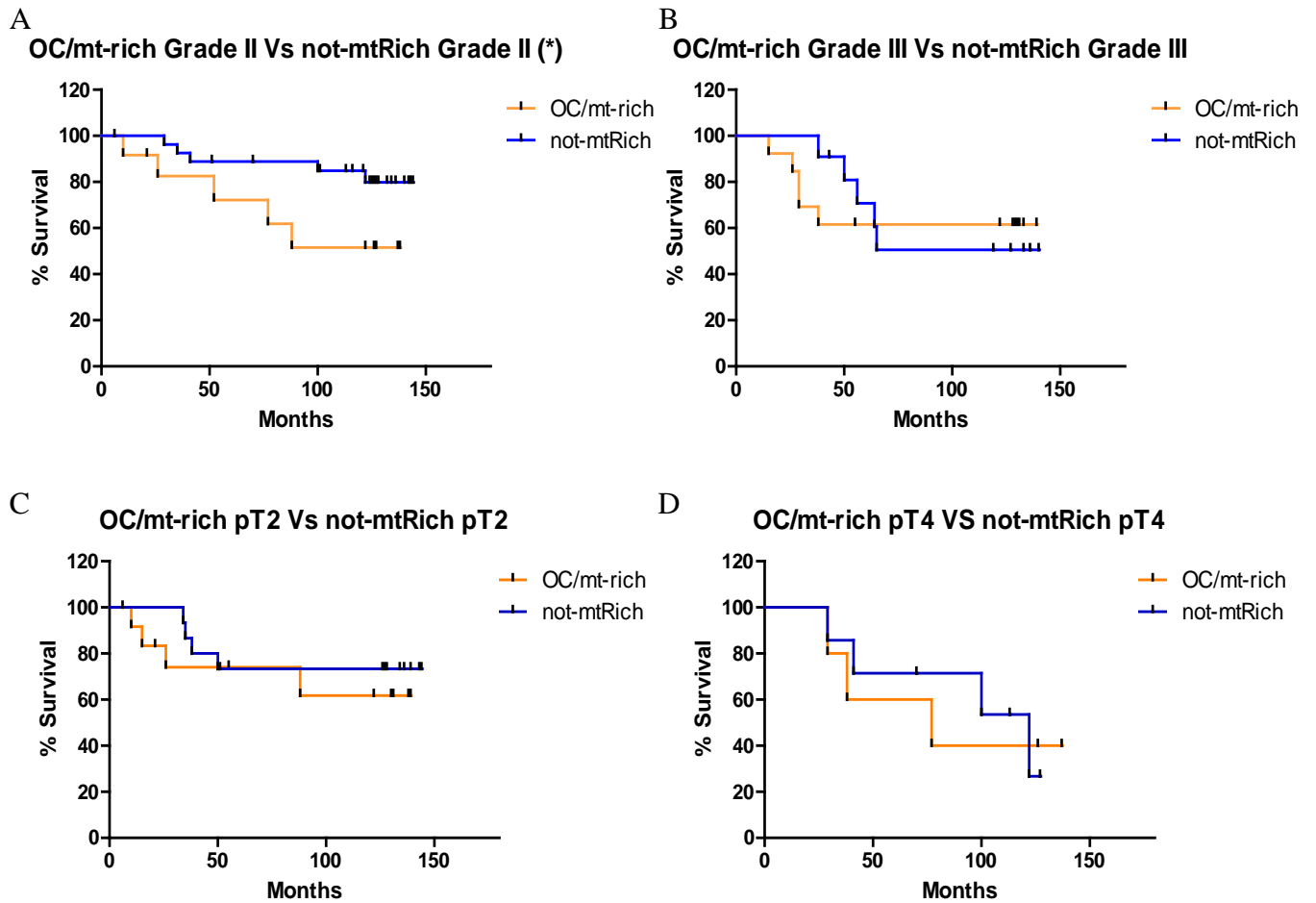


Figure 3.13: Kaplan-Meier. Analysis of overall survival in OC in comparison to not-mtRich. N.S. Wilcoxon and Mantel-Cox Test.

### 3.3 Results



**Figure 3.14: Kaplan-Meier. Analysis of overall survival of OC/mt-rich in comparison to not-mtRich. N.S. Wilcoxon and Mantel-Cox Test. \*: statistically different at Wilcoxon Test ( $p < 0.05$ ).**

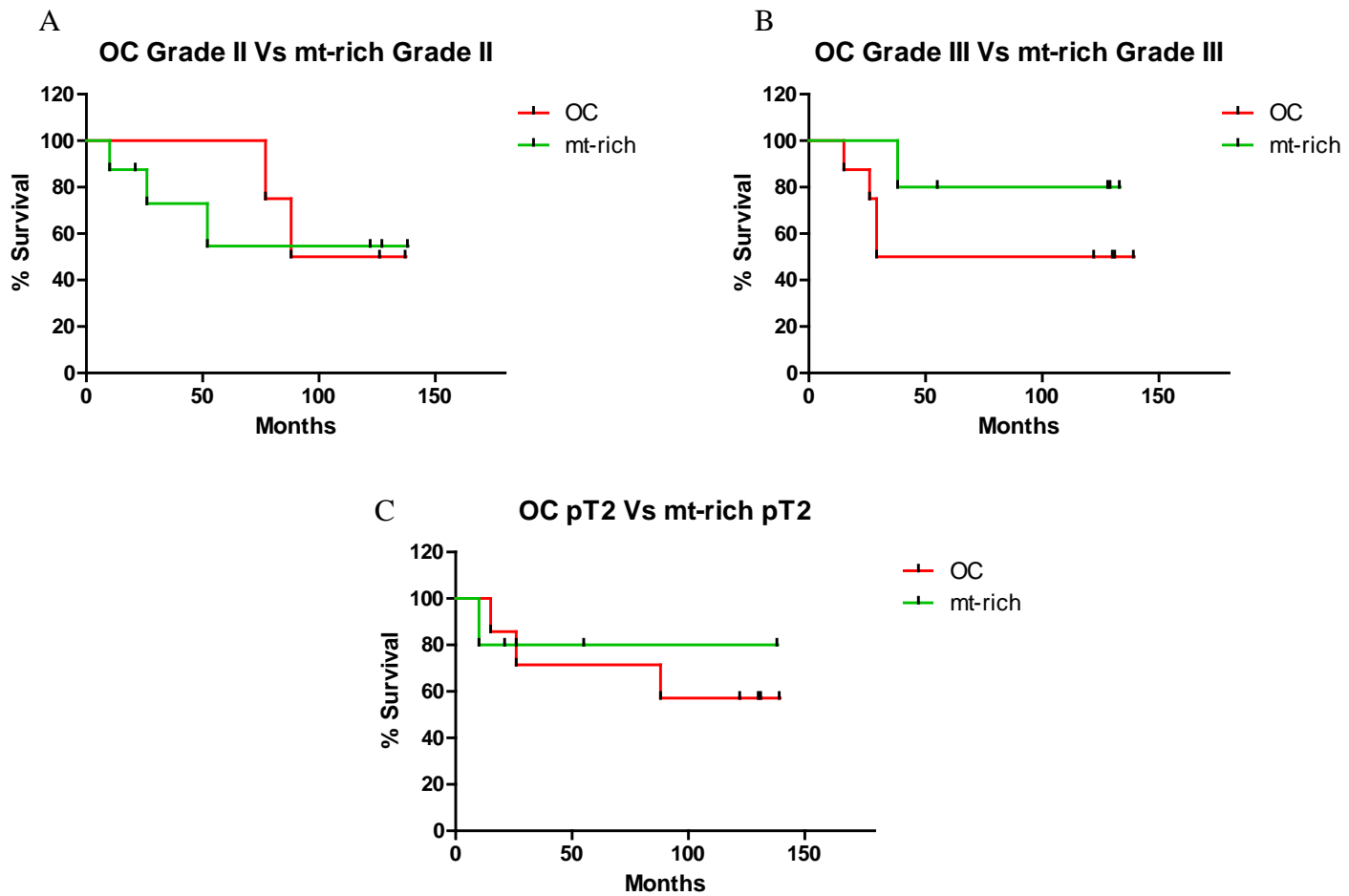
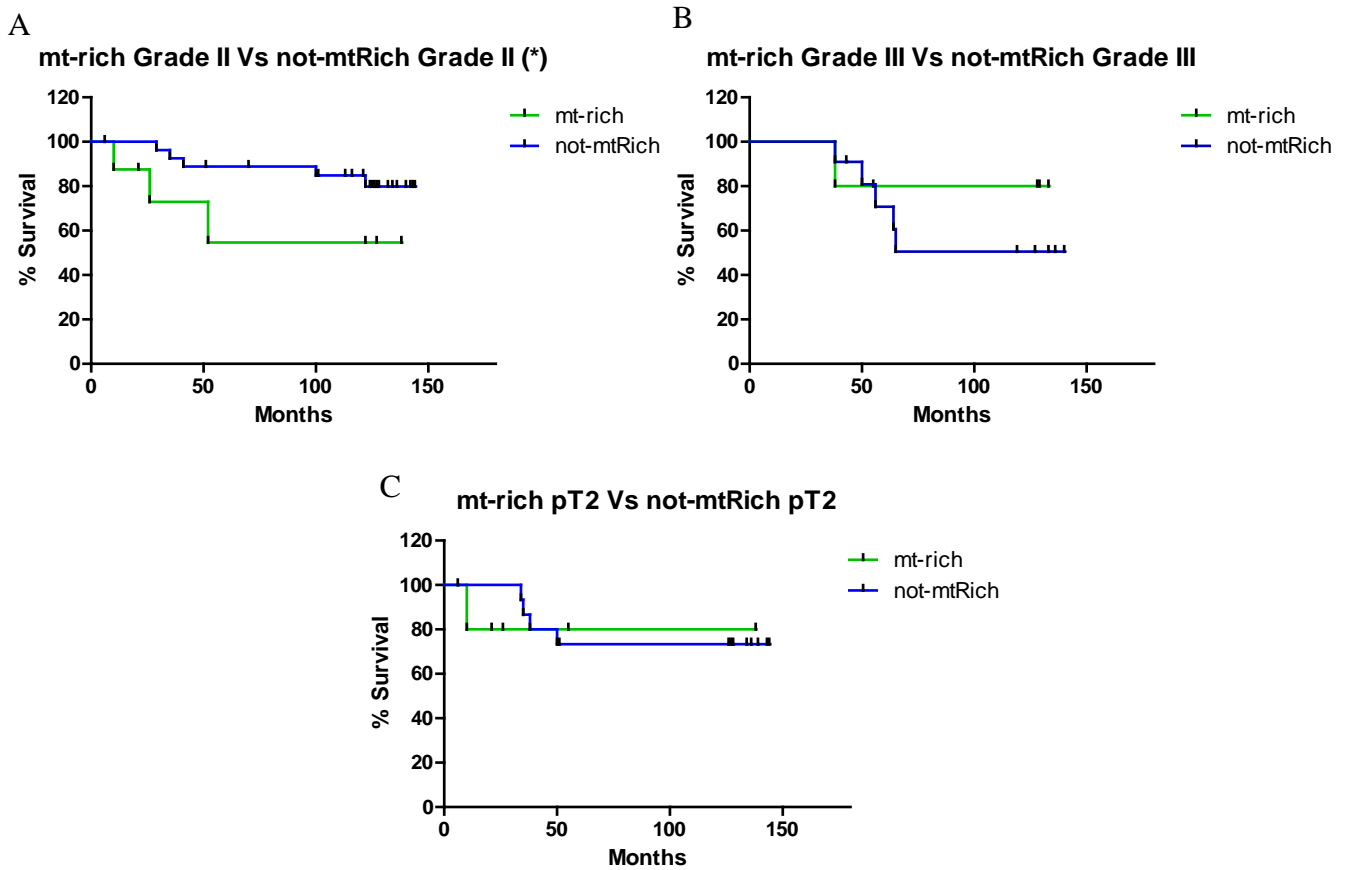


Figure 3.15: Kaplan-Meier. Analysis of overall survival of OC in comparison to mtRich. N.S. Wilcoxon and Mantel-Cox Test.

### 3.3 Results



**Figure 3.16: Kaplan-Meier. Analysis of overall survival of mt-rich in comparison to not-mtRich. N.S. Wilcoxon and Mantel-Cox Tests. \*: statistically different at Wilcoxon Test ( $p < 0.05$ ).**

### 3.3.8 Molecular Analysis (aCGH)

Out of 18 cases belonging to group 1 and analyzed by aCGH BAC, 7 cases were classified as “mt-rich”, 10 as “OC” and 1 as “not mt-rich” (Tab. 4.1).

Unsupervised cluster analysis revealed that OC and mt-rich carcinomas were different at molecular level if compared to IDC NAS. It is possible to observe two different group (Fig. 3.17): one with a prevalence of IDC NAS and another one with abundance of OC/mt-rich carcinomas. 13 out of 18 selected samples grouped in the same cluster (considering data smoothed or thresholded), while 5 fell out: 1 control (mit17, negative at IHC, with an apocrine differentiation); 3 mt-rich (mit5, mit6, mit20); 1 OC (mit4).

### 3.3 Results

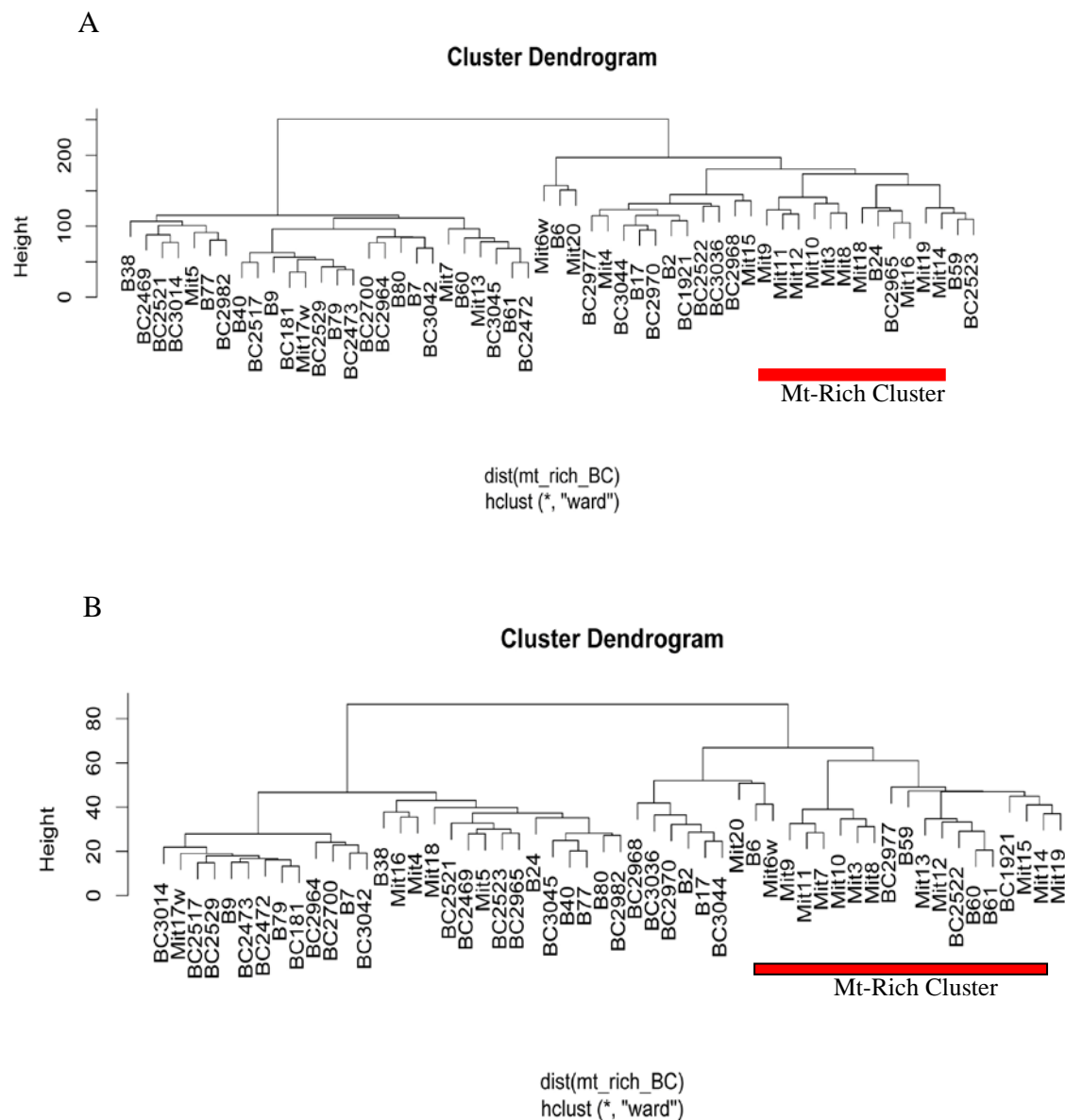


**Figure 3.17: Hierarchical clustering analysis based on the adaptive weight smoothed data (A) or thresholded data (B, gains, losses and amplifications).** Although cluster “red” is significantly enriched for mt-rich breast cancers (cluster A vs other clusters, Fisher’s exact test p values <0.005 and 0.001 for A and B, respectively), these tumours are still heterogeneous at the genetic level.

Data were smoothed using the circular binary segmentation (cbs) algorithm. A categorical analysis was applied to the BACs after classifying them as representing gain, loss or no-change according to their smoothed Log<sub>2</sub> ratio values (Fig. 3.18).

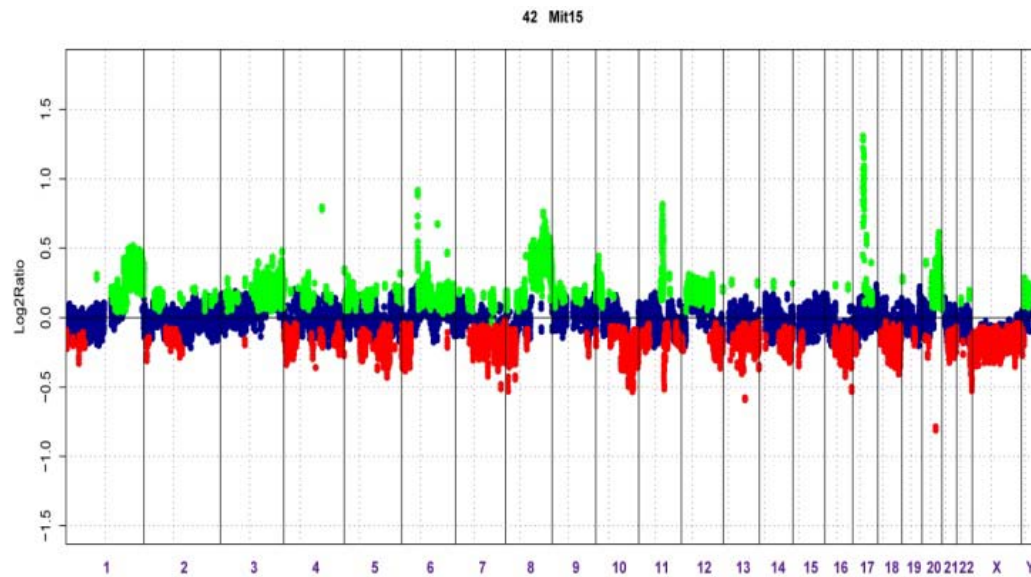


**Figure 3.18: Genome plot of mt-rich BCs.** Log<sub>2</sub> ratios are plotted on the Y axis against each clone according to genomic location on the X axis. Log<sub>2</sub> ratios of each BAC clone are plotted on the Y axis according to its genomic location on X axis. BACs in green represent copy number gains and in red, copy number losses.

IDCs were significantly different from mt-rich/OC at genomic level in several chromosomal regions: gains on chromosomes 3q29, 5q35.2, 6p21.2, 7q22.1, 8p11.1, 9q34.11, 11q13.1, 12q13.13, 16p13.3, 17q21.2, 19q13.2 and 20q11.21, and losses on 2p11.2, 3p12.2, 4p12, 5q21.3, 6p22.1, 7q31.31-q31.32, 10q23.1, 11p14.1, 12q24.11, 14q13.3-q21.1, 15q15.1-q15.3, 18q21.32, 21q21.3 e Xq13.1 were more frequent in mt-rich BC. Moreover high amplification level on chromosome 5q23.2, 6q24.2, 7q34, 8q23.1-q23.2, 9q34.3 and 17q25.3 were associated with these tumours.

Profiles of IDC NAS and selected mt-rich/ oncocytic (Fig. 3.19) carcinomas were compared using a previously validated multi-Fisher's exact test with p values adjusted for multiple comparison by the false discovery rate.

### 3.3 Results

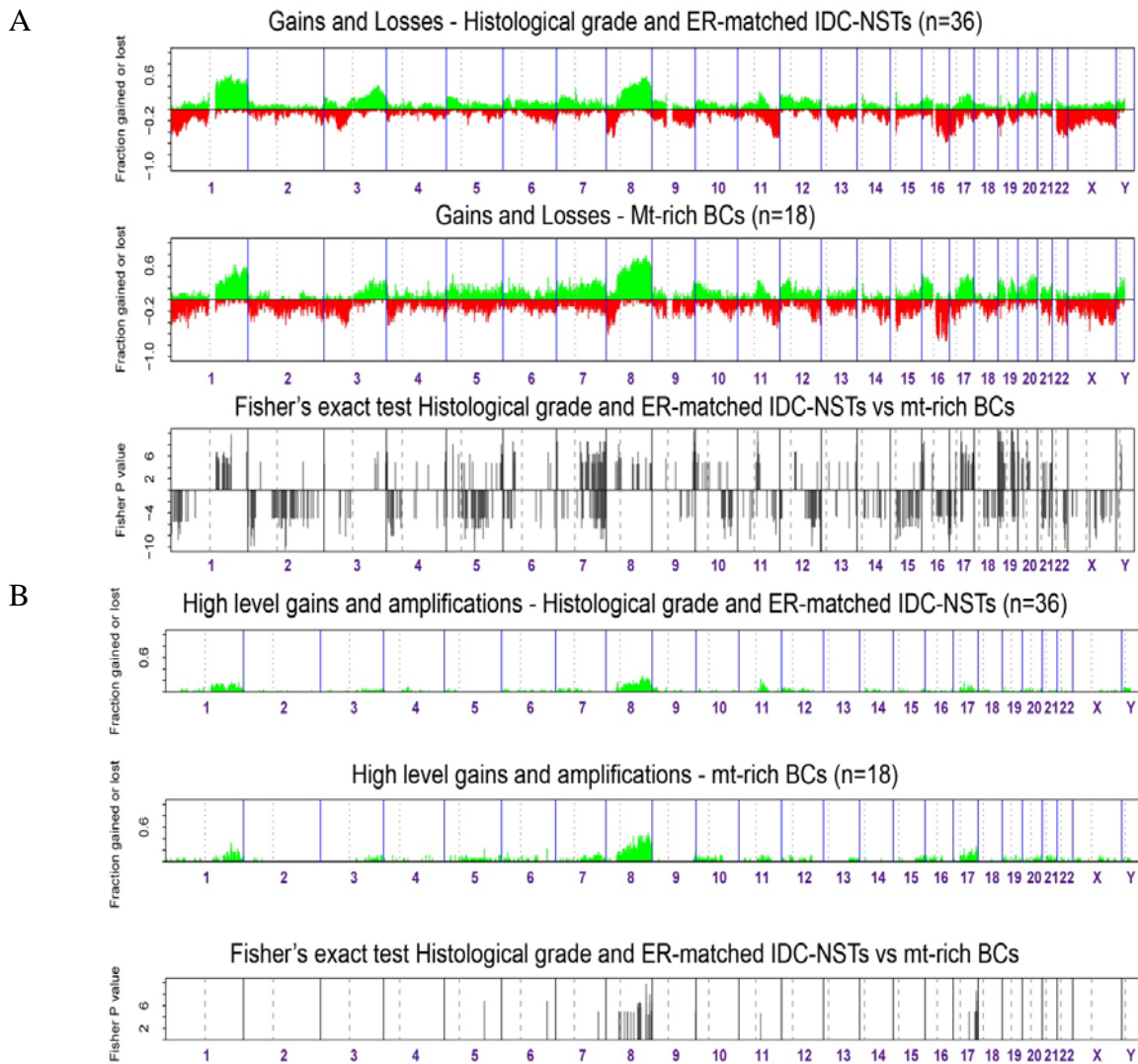


**Figure 3.19: Frequency plots of amplifications in grade and ER-matched IDC-NSTs and mt-rich BCs.** A) Frequency of gains and losses in each group. The proportion of tumours in which each clone is gained (green bars) or lost (red bars) is plotted (Y axis) for each BAC clone according to genomic location (X axis). Vertical dotted lines represent chromosome centromeres. B) Frequency of amplifications in each group. The proportion of tumours in which each clone is gained at high level or amplified (green bars) is plotted (Y axis) for each BAC clone according to genomic location (X axis). Vertical dotted lines represent chromosome centromeres. The bottom plots in A and B illustrate the results of the Fisher's exact tests carried out on the segmented values for each clone, and those with a permutation corrected p value of less than 0.05 are plotted (inverse log p value Y axis) according to genomic location (X axis). P values associated with loss of a region are indicated as negative values.

### **3.3.9 Nuclear genes codifying for mitochondrial proteins**

26 out of 71 genes analysed (37%) were statistically different ( $p < 0.05$ ) between the 17 mitochondrial-rich/OC tumours and IDC. Of these 26 cases, 16 presented gains and 10 showed losses (Tab. 3.10; Figs. 3.20 – 3.21).

Analysing only the 10 OC, 23 out of 71 genes (32%) were altered in comparison to IDC-NSTs, 16 presented gains and 7 losses. TK2, DDX28, GOT2, SSBP1, CHCHD3, TFBP2 resulted no more statistically significant comparing only OC with IDC. Moreover TAZ, MFN2, VDAC3 became statistically significant.

### 3.3 Results

Gene	Location	Function	Altered in Mt Disorders	Gain	Loss	p	Tumour
<b>TK2 (Thymidine kinase 2)</b>	16q21	mtDNA stability	√ (Mt DNA depletion syndrome)		√	0.05	Mt-rich
<b>SSBP1 (Single-stranded DNA-binding protein)</b>	7q34	mtDNA replication		√		0.05	Mt-Rich
<b>TOP1MT (mitochondrial DNA topoisomerase 1)</b>	8q24.3	mtDNA replication and mtRNA transcription		√		0.05*	Mt-Rich/OC
<b>DDX28 (DEAD Asp-Glu-Ala-Asp box)</b>	16q22.1	mtRNA processing			√	0.01	Mt-Rich
<b>POLMRT (mitochondrial DNA-directed RNA polymerase)</b>	19p13.3	mtRNA transcription		√		0.05	Mt-Rich/OC
<b>TFBP2 (Transcription factor B2)</b>	1q44	mtRNA transcription		√		0.05	Mt-Rich
<b>MTIF2 (Translation initiation factor IF-2)</b>	2p16.1	mtRNA translation			√	0.05	Mt-Rich/OC
<b>PTRF (release factor for polymerase I and RNA transcript)</b>	17q21.31	mtRNA transcription		√		0.01	Mt-Rich/OC
<b>PDP2 (Pyruvate dehydrogenase/phosphatase regulatory subunit 2)</b>	16q22.1	mt metabolism			√	0.05	Mt-Rich/OC
<b>PDP1 (Pyruvate dehydrogenase/phosphatase)</b>	8q22.1	mt metabolism		√		0.01	Mt-Rich/OC
<b>GOT2 (Aspartate aminotransferase 2)</b>	16q21	mt metabolism			√	0.05	Mt-Rich
<b>SPG7 (Spastic paraplegia protein 7)</b>	16q24.3	mt metabolism	√ (Hereditary spastic paraplegia)		√	0.05*	Mt-Rich/OC
<b>ETHE1</b>	19q13.31	mt metabolism		√		0.01	Mt-Rich/OC
<b>TAZ (tafazzin)</b>	Xq28	mt metabolism	√ (Barth syndrome)	√		0.05	OC
<b>SURF1 (Surfeit locus protein 1)</b>	9q34.2	OXPHOS structure	√ (Leigh syndrome)	√		0.01	Mt-Rich/OC
<b>NDFUS7 (Complex I subunit)</b>	19p13.3	OXPHOS structure	√ (Leigh syndrome)	√		0.05*	Mt-Rich/OC
<b>NDFUS8 (Complex I subunit)</b>	11q13.2	OXPHOS structure	√ (Leigh syndrome)	√		0.01	Mt-Rich/OC
<b>NDUFA2 (Complex I accessory subunit)</b>	5q12.1	OXPHOS structure			√	0.05*	Mt-Rich/OC

### 3. Oncocytic Breast Carcinomas

Gene	Location	Function	Altered in Mt Disorders	Gain	Loss	p	Tumour
<b>NDUFA13 (Complex I accessory subunit, a.k.a. GRIM19)</b>	19p13.11	OXPPOS structure	√ (PTC and sporadic oncocytic thyroid ca.)	√		0.05*	Mt-Rich/OC
<b>CHCHD3 (coil-helix domain-containing protein 3)</b>	7q32.3-q33	mt fusion		√		0.01	Mt-Rich/OC
<b>MNF2 (Transmembrane GTPase, Mitofusin 2)</b>	1p36.22	mt fusion		√		0.05	OC
<b>IMMT (inner membrane mitochondrial protein, a.k.a. mitofilin)</b>	2p11.2	mt fusion			√	0.01	Mt-Rich/OC
<b>DRP1 (dynamin related protein 1)</b>	12q24.31	mt fission			√	0.01	Mt-Rich/OC
<b>MIL1 (Bcl-2-like protein a.k.a. Bcl-rambo)</b>	22q11.21	apoptosis		√		0.05	Mt-Rich/OC
<b>BAD (Bcl2-antagonist of cell death)</b>	11q13.1	apoptosis		√		0.01	Mt-Rich/OC
<b>VDAC3 (voltage dependent anion channel 3)</b>	8p11.21	apoptosis		√		0.05	OC
<b>TIMM44 (translocase inner membrane subunit 44)</b>	19p13.2	carrier (protein import in mt matrix)		√		0.05*	Mt-Rich/OC
<b>DNC (Deoxynucleotide carrier)</b>	17q25.1	carrier (dNTP uptake in mt matrix)		√		0.05	Mt-Rich/OC
<b>TIMM8A (translocase inner membrane subunit 8A, a.k.a. DDP1)</b>	Xq22.1	carrier (chaperone-like protein)	√ (X-linked deafness dystonia syndrome)		√	0.05^	Mt-Rich/OC

**Table 3.10: Genes compared between Mt-rich/OC and IDC-NSTs.** \*: p<0.01 in mt-rich/OC but p<0.05 in OC. ^: p<0.05 in mt-rich but p<0.01 in OC.

### 3.3 Results

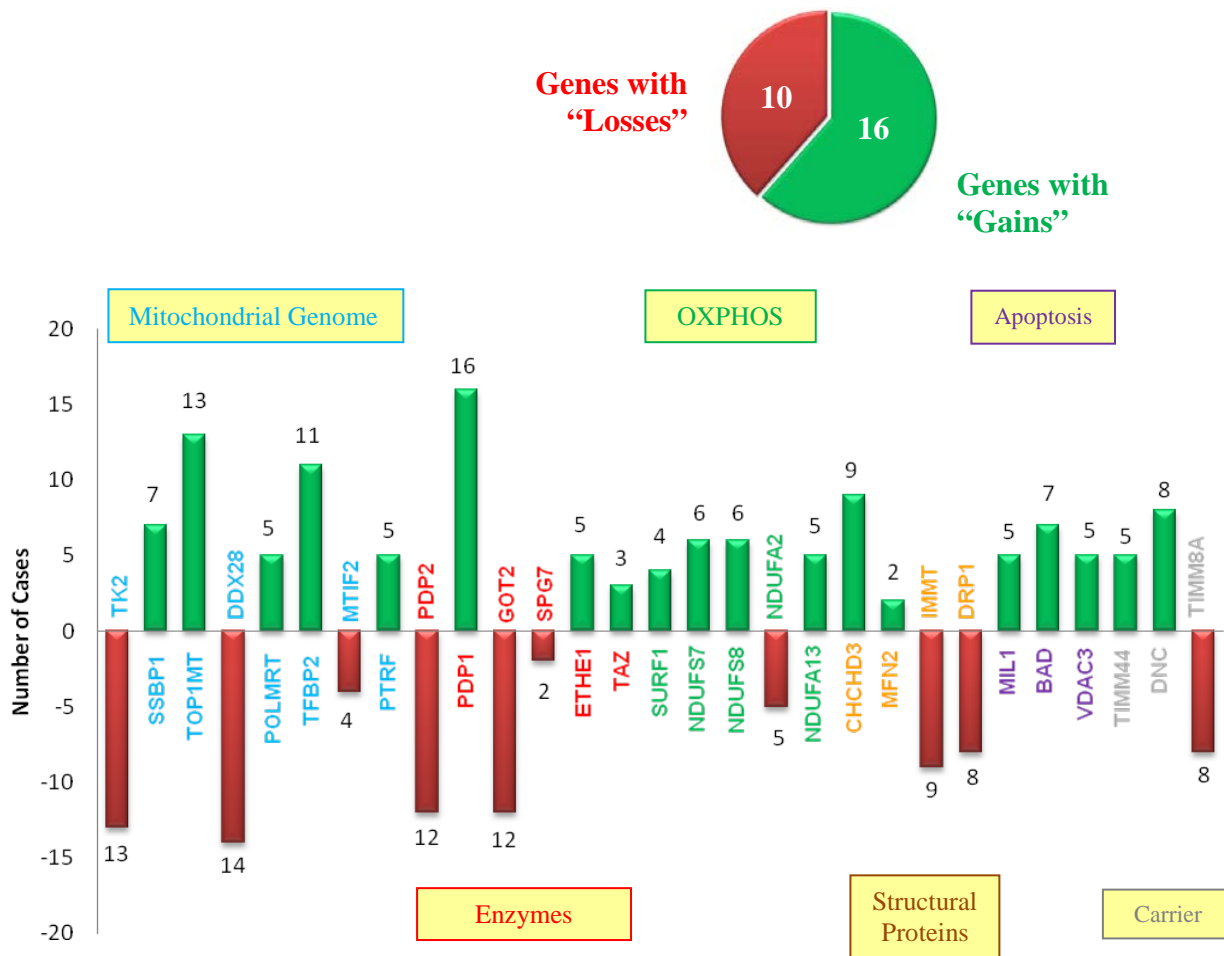


Figure 3.20: Number of altered cases each analysed genes.

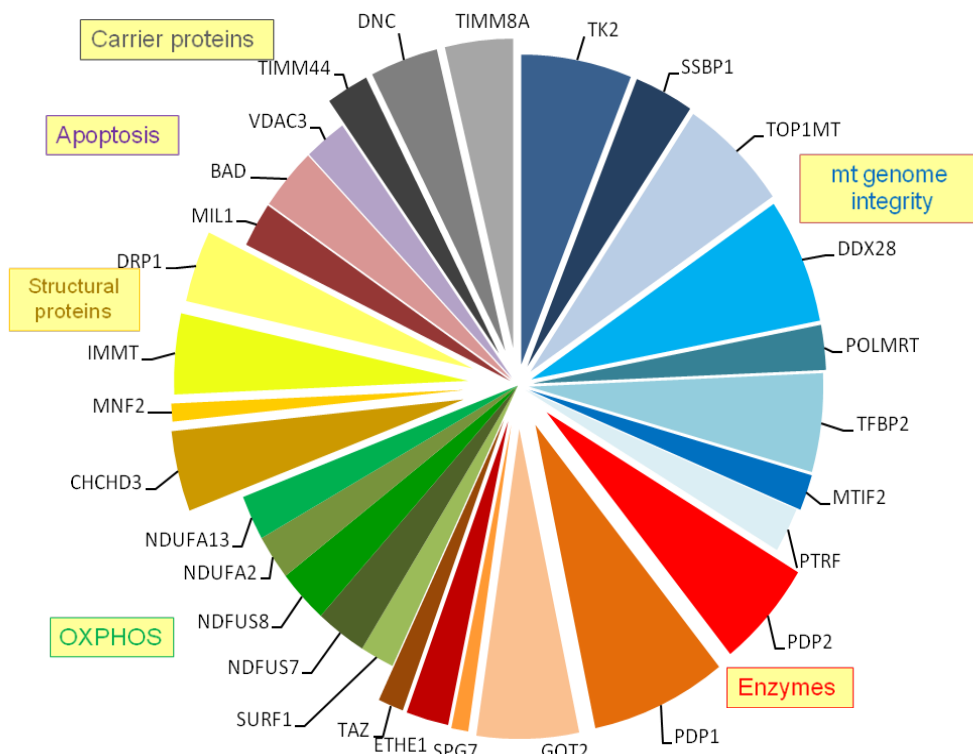


Figure 3.21: Proportion of altered cases each analysed gene. The genes are grouped according their function.

### 3.3.10 Mitochondrial DNA sequencing

3 cases, out of the 6 with more than 60% of mtDNA sequenced, presented an alteration of mtDNA (Tab 3.11). One mutation has been hypothesized to be benign, one silent, one could be generate damages and only one has been just reported in literature in oncocytic carcinoma of thyroid [34, 44].

Sample	Nucleotidic Change	Gene	Aminoacid Change	Effect (PolyPhen or Mitomap)
Mit11	T10237C het	ND3	60 Thr>Ile	Possibly damaging (PSIC 2,372)
Mit15	3571insC	ND1	-	Complex I damages^
Mit19	C12964 homo	ND5	210 Leu>Ile	Benign
Mit19	T729C homo	12S	-	-

**Table 3.11: Mt-DNA Alterations mt-DNA observed in OC samples.** T: Thymine; C: Cytosine; het: heterozygosis; homo: homozygosis; ins: insertion; Thr: Threonine; Ile: Isoleucine; Leu: Leucine. Effect of mutation has been hypothesized by a prediction tool (PolyPhen). ^[34, 44]

### 3.3 Results

In table 3.12 molecular results are summarized: number of altered genes codifying for mitochondrial protein (with gain or losses); OC/ mt-rich cluster group according to “smoothed” or “thresholded” analysis; alterations of mitochondrial DNA.

	Mt ICH	Tumour	Smoot.	Thres.	Gains	Losses	mtDNA alt.
<b>Mit3</b>	2+ (70%)	Mt-Rich	IN	IN	13	6	-
<b>Mit4</b>	3+ (90%)	OC	OUT	OUT	5	4	NO
<b>Mit5</b>	2+ (90%)	Mt-Rich	OUT	OUT	3	5	NO
<b>Mit6</b>	2+ (70%)	Mt-Rich	OUT	OUT	10	5	-
<b>Mit7</b>	3+ (90%)	OC	IN	OUT	11	2	NO
<b>Mit8</b>	3+ (90%)	OC	IN	IN	16	5	-
<b>Mit9</b>	3+ (90%)	OC	IN	IN	17	1	-
<b>Mit10</b>	2+ (70%)	Mt-Rich	IN	IN	9	9	-
<b>Mit11</b>	2+ (70%)	Mt-Rich	IN	IN	11	2	T60I
<b>Mit12</b>	3+ (90%)	OC	IN	IN	11	5	-
<b>Mit13</b>	3+ (80%)	OC	IN	OUT	4	6	-
<b>Mit14</b>	2+ (80%)	Mt-Rich	IN	IN	5	7	-
<b>Mit15</b>	3+ (80%)	OC	IN	IN	3	8	3571insC
<b>Mit16</b>	3+ (90%)	OC	OUT	IN	6	2	-
<b>Mit17</b>	Neg	Ctrl	OUT	OUT	2	0	-
<b>Mit18</b>	3+ (90%)	OC	OUT	IN	7	9	-
<b>Mit19</b>	3+ (90%)	OC	IN	IN	4	5	L210I
<b>Mit20</b>	2+ (70%)	Mt-Rich	OUT	OUT	5	7	-

**Table 3.12: Molecular features of 18 samples analysed by aCGH.** Mt-IHC: positivity for anti-mitochondria antibody; Ctrl: control; Smoot.: smoothed; Thres.: thresholded; IN: included in cluster; OUT: out of cluster; Gains/Losses: number of nuclear genes, codifying for mitochondrial protein, with gains or losses; mt-DNA alt: mtDNA alterations.

### 3.4 DISCUSSION AND CONCLUSIONS

Oncocytic tumours have been described in several organs, even if with different frequencies. The percentage of neoplastic cells need for classifying a tumour as oncocytic is different according to organ. For example, in thyroid the proportion is 75% [3, 4], while in kidney the tumour should be entirely composed by ossifilic cells [5]. Even if this tumours could arise in any organs, endocrine system and some parenchymatous organs seem to be particularly prone to develop this type of carcinoma. Thyroid is the main site of onset, then kidney, salivary and parotid glands, while gastrointestinal and respiratory tract and skin are rarely affected [45]. With regard to breast, till now only 4 cases have been reported in literature [13, 14].

In this study we have analysed 33 cases of oncocytic invasive breast carcinoma of the breast, selected according to morphological (cells with wide and eosinophilic cytoplasm) and immunohistochemical criteria (at least 70% of neoplastic cells strongly positive for anti-mitochondria antibody). For performing a semiquantitative analysis of mitochondria inside neoplastic cells, we have optimized a safe and consistent immunohistochemistry reaction.

Oncocytic carcinomas have reported a frequency of 19.8%. Moreover we have observed another group of “mitochondria-rich” breast tumours: these carcinoma could be morphologically not distinguishable from oncocytic carcinoma and are differentiated only according to immunohistochemistry.

The 4 cases reported in literature were all well or moderately differentiated (GI or GII) and, in one case, was an in situ carcinoma. In this study we have considered infiltrating type and we have observed a prevalence of GIII carcinoma, characterized by solid nest growth pattern and infiltrative margins. We found cytological characteristic reported

### 3.4 Discussion

previously in literature (monomorphic nuclei, prominent nucleoli and rare mitosis) only in well differentiated form (GI and some GII). Moreover our cases could show other features as nuclei with faint to strong pleomorphism, cells with at least two nuclei and inconspicuous nucleoli. Cytoplasm was characteristically wide and eosinophilic.

Immunohistochemically, most part of the cases showed a luminal profile, with CK7 and EMA expression and positivity for hormonal receptor, especially oestrogenic. In one case we observed a case with basal features, CK14 positive and NEU and hormonal receptors negative. Interestingly, could coexist apocrine, neuroendocrine and/or mucoid differentiation.

Interestingly, CK7 resulted negative or focal in 8 cases and this could be a diagnostic trouble, in the event of metastatic localization of these carcinomas.

The evidence that mitochondrial accumulation is a slow phenomenon and that cellular culture of oncocyctic tumours tend to loss this phenotype after “n” replication, has lead to hypothesize that oncocyctic neoplasia are benign or with low grade of malignancy [11]. This is true for oncocytoma of kidney, parathyroid, pituitary gland, and for fibrolamellar epatoma, but in other site the prognosis of oncocyctic carcinoma is overlapping to those of non oncocyctic part, as in gastroenteric tract, or could be worst, as in thyroid, salivary glands and meningioma.

With regard to prognosis, we have not found statistically significant differences between oncocyctic and non-oncocyctic carcinomas. However, we have observed a tendency to worst prognosis of OC, and this trend is statistically significant comparing OC/mt-rich grade II with not enriched in mitochondria grade II.

Mitochondria are cytoplasmatic organelles involved in several processes of cellular homeostasis, as ATP production by respiratory chain and apoptosis by releasing cytocrome c in intermembrane space [46]. In 1956, Otto Warburg demonstrated as human

tumours presented an increase in glycolysis rate with reduction of OXPHOS chain activity even in presence of oxygen, suggesting that defects in this mechanism could be at the base of many type of neoplasia [18]. This dependence of tumoural cells on glycolysis for ATP production, is considered a typical aspect of malignant transformation, together with 6 principle alteration of cellular physiology described by Hanahan e Weinberg (independence on promoting and inhibiting growth factors, limitless replication, induction of angiogenesis, invasive and metastatic skill and apoptosis evasion) [17]. In last year's, the discover of mitochondrial DNA mutation and of nuclear genes codifying for mitochondrial protein in many sporadic or familiar tumour with or without oncocytic features, has supplied genetic bases of mitochondrial dysfunction observed in tumourigenesis. From a molecular point of view, the most studied oncocytic tumours are the thyroid one, in which has been observed a wide deletion in mt-DNA, called "common deletion". This alteration concerns 7 genes involved in respiratory chain and it is a characteristic defects of oncocytic neoplasia of thyroid [46].

In our study, molecular results obtained by aCGH show that OC and mt-rich harbour characteristic chromosomic aberration in comparison to IDC NOS. Unsupervised hierarchical analysis revealed that OC and mt-rich tend to form a distinct cluster as opposed to IDC NOS. Although mitochondria have own DNA, producing 13 out of 87 protein arranging enzymatic complex involved in oxidative phosphorylation, most part of the protein are codified by nuclear genes. Analyzing these genes, we have observed that, out of 71 genes under study, 26 showed differences (gains and losses) statistically significant between OC/mt-rich and IDC NOS groups. Most part of these genetic alterations involves enzyme or proteins are associated with mitochondrial genome (for example operate in replication, transcription, traduction or stability).

### 3.4 Discussion

With regard to sequencing of mitochondrial genome, we have not observed significant alterations, even if we know that the number is not sufficient to hypothesize some theory.

These molecular results, other than confirming that OC/mt-rich carcinomas represent a particular and independent entity in breast carcinoma overview, suggest that mitochondria aggregation is not only a simple morphologic correlation with oncocytic phenotype but could play a functional role.

In conclusion:

- Oncocytic breast carcinoma is a morphologic entity with distinctive ultrastructural and histological features.
- Immunohistochemically, it is characterized by a luminal profile and could be associated with an apocrine, neuroendocrine and/or mucoid differentiation.
- In our study it has a frequency of 19.8% out of invasive breast carcinomas.
- It is not characterized by specific grade or stage
- It has not distinctive clinical features and we have not observed significant differences in comparison invasive breast carcinoma with regard to prognosis.
- At molecular level, OC/mt-rich carcinoma clusterizes independently from IDC NOS and show a specific constellation of genetic aberration.

## REFERENCES

1. Hamperl, H., *Beiträge zur normalen und pathologischen Histologie menschlicher Speicheldrüsen*. Z Mikrosk Anat Forsch, 1931. **27**: p. 1-55.
2. Ghadially, F.N., *Diagnostic electron microscopy of tumors*, 2nd ed. 2nd ed. 1985, London: Butterworth & Company.
3. Bronner, M.P. and V.A. LiVolsi, *Oxyphilic (Askanazy/Hürtle cell) tumors of the thyroid: Microscopic features predict biologic behavior*. Surg Pathol, 1988. **1**: p. 137-150.
4. Tallini, G., M.L. Carcangiu, and J. Rosai, *Oncocytic neoplasms of the thyroid gland*. Acta Pathol Jpn, 1992. **42**: p. 305-315.
5. Murphy, W.M., D.J. Grignon, and E.J. Perlman, *Tumors of the kidney, bladder and related urinary structure*. AFIP Atlas of Tumor Pathology. 2004, Washington. DC: American Register of Pathology.
6. Maximo, V. and M. Sobrinho-Simoes, *Hurthle cell tumours of the thyroid. A review with emphasis on mitochondrial abnormalities with clinical relevance*. Virchows Arch, 2000. **437**(2): p. 107-15.
7. Ebner, D., et al., *Functional and molecular analysis of mitochondria in thyroid oncocytoma*. Virchows Arch B Cell Pathol Incl Mol Pathol, 1991. **60**(2): p. 139-44.
8. Ortmann, M., et al., *Renal oncocytoma. I. Cytochrome c oxidase in normal and neoplastic renal tissue as detected by immunohistochemistry--a valuable aid to distinguish oncocytomas from renal cell carcinomas*. Virchows Arch B Cell Pathol Incl Mol Pathol, 1988. **56**(3): p. 165-73.
9. Muller-Hocker, J., et al., *Defects of the respiratory chain in oxyphil and chief cells of the normal parathyroid and in hyperfunction*. Hum Pathol, 1996. **27**(6): p. 532-41.
10. Maximo, V., et al., *Mitochondrial DNA somatic mutations (point mutations and large deletions) and mitochondrial DNA variants in human thyroid pathology: a study with emphasis on Hurthle cell tumors*. Am J Pathol, 2002. **160**(5): p. 1857-65.
11. Sobrinho-Simoes, M., et al., *Hurthle (oncocytic) cell tumors of thyroid: etiopathogenesis, diagnosis and clinical significance*. Int J Surg Pathol, 2005. **13**(1): p. 29-35.
12. Honda, K., et al., *Clonal analysis of the epithelial component of Warthin's tumor*. Hum Pathol, 2000. **31**(11): p. 1377-80.
13. Costa, M.J. and S.G. Silverberg, *Oncocytic carcinoma of the male breast*. Arch Pathol Lab Med, 1989. **113**(12): p. 1396-9.
14. Damiani, S., et al., *Oncocytic carcinoma (malignant oncocytoma) of the breast*. Am J Surg Pathol, 1998. **22**(2): p. 221-30.
15. Tavassoli, F.A. and P. Devilee, *WHO. Pathology and Genetics of Tumours of the Breast and Female Genital Organs*. 3<sup>rd</sup> ed. 2003, Lyon: IARC Press.
16. Tremblay, G. and A.G. Pearse, *Histochemistry of oxidative enzyme systems in the human thyroid, with special reference to Askanazy cells*. J Pathol Bacteriol, 1960. **80**: p. 353-8.
17. Hanahan, D. and R.A. Weinberg, *The hallmarks of cancer*. Cell, 2000. **100**(1): p. 57-70.
18. Warburg, O., F. Wind, and E. Negelein, *The metabolism of tumors in the body*. J Gen Physiol, 1927. **8**: p. 519-530.

## References

19. Simonnet, H., et al., *Low mitochondrial respiratory chain content correlates with tumor aggressiveness in renal cell carcinoma*. *Carcinogenesis*, 2002. **23**(5): p. 759-68.
20. Moll, U.M. and L.M. Schramm, *p53--an acrobat in tumorigenesis*. *Crit Rev Oral Biol Med*, 1998. **9**(1): p. 23-37.
21. Wang, G.L. and G.L. Semenza, *General involvement of hypoxia-inducible factor 1 in transcriptional response to hypoxia*. *Proc Natl Acad Sci U S A*, 1993. **90**(9): p. 4304-8.
22. Hagg, M. and S. Wennstrom, *Activation of hypoxia-induced transcription in normoxia*. *Exp Cell Res*, 2005. **306**(1): p. 180-91.
23. Plas, D.R. and C.B. Thompson, *Akt-dependent transformation: there is more to growth than just surviving*. *Oncogene*, 2005. **24**(50): p. 7435-42.
24. Elstrom, R.L., et al., *Akt stimulates aerobic glycolysis in cancer cells*. *Cancer Res*, 2004. **64**(11): p. 3892-9.
25. Gottlieb, E. and I.P. Tomlinson, *Mitochondrial tumour suppressors: a genetic and biochemical update*. *Nat Rev Cancer*, 2005. **5**(11): p. 857-66.
26. Pelicano, H., et al., *Mitochondrial respiration defects in cancer cells cause activation of Akt survival pathway through a redox-mediated mechanism*. *J Cell Biol*, 2006. **175**(6): p. 913-23.
27. Huang, P., et al., *Superoxide dismutase as a target for the selective killing of cancer cells*. *Nature*, 2000. **407**(6802): p. 390-5.
28. Gillies, R.J. and R.A. Gatenby, *Adaptive landscapes and emergent phenotypes: why do cancers have high glycolysis?* *J Bioenerg Biomembr*, 2007. **39**(3): p. 251-7.
29. Maximo, V. and M. Sobrinho-Simoes, *Mitochondrial DNA 'common' deletion in Hurthle cell lesions of the thyroid*. *J Pathol*, 2000. **192**(4): p. 561-2.
30. Heddi, A., et al., *Coordinate expression of nuclear and mitochondrial genes involved in energy production in carcinoma and oncocytoma*. *Biochim Biophys Acta*, 1996. **1316**(3): p. 203-9.
31. Simonnet, H., et al., *Mitochondrial complex I is deficient in renal oncocytomas*. *Carcinogenesis*, 2003. **24**(9): p. 1461-6.
32. Mayr, J.A., et al., *Loss of complex I due to mitochondrial DNA mutations in renal oncocytoma*. *Clin Cancer Res*, 2008. **14**(8): p. 2270-5.
33. Savagner, F., et al., *Mitochondrial activity in XTC.UC1 cells derived from thyroid oncocytoma*. *Thyroid*, 2001. **11**(4): p. 327-33.
34. Gasparre, G., et al., *Disruptive mitochondrial DNA mutations in complex I subunits are markers of oncocyctic phenotype in thyroid tumors*. *Proc Natl Acad Sci U S A*, 2007. **104**(21): p. 9001-6.
35. van Beers, E.H., et al., *A multiplex PCR predictor for aCGH success of FFPE samples*. *Br J Cancer*, 2006. **94**(2): p. 333-7.
36. Natrajan, R., et al., *An integrative genomic and transcriptomic analysis reveals molecular pathways and networks regulated by copy number aberrations in basal-like, HER2 and luminal cancers*. *Breast Cancer Res Treat*, 2009.
37. Mackay, A., et al., *A high-resolution integrated analysis of genetic and expression profiles of breast cancer cell lines*. *Breast Cancer Res Treat*, 2009. **118**(3): p. 481-98.
38. Marchio, C., et al., *Mixed micropapillary-ductal carcinomas of the breast: a genomic and immunohistochemical analysis of morphologically distinct components*. *J Pathol*, 2009. **218**(3): p. 301-15.

39. Reis-Filho, J.S., et al., *ESR1 gene amplification in breast cancer: a common phenomenon?* Nat Genet, 2008. **40**(7): p. 809-10; author reply 810-2.
40. Marchio, C., et al., *Genomic and immunophenotypical characterization of pure micropapillary carcinomas of the breast.* J Pathol, 2008. **215**(4): p. 398-410.
41. *MITOMAP: A Human Mitochondrial Genome Database.* <http://www.mitomap.org>. 2009.
42. Zeviani, M. and V. Carelli, *Mitochondrial disorders.* Curr Opin Neurol, 2007. **20**(5): p. 564-71.
43. Wolff, A.C., et al., *American Society of Clinical Oncology/College of American Pathologists guideline recommendations for human epidermal growth factor receptor 2 testing in breast cancer.* Arch Pathol Lab Med, 2007. **131**(1): p. 18-43.
44. Bonora, E., et al., *Defective oxidative phosphorylation in thyroid oncocytic carcinoma is associated with pathogenic mitochondrial DNA mutations affecting complexes I and III.* Cancer Res, 2006. **66**(12): p. 6087-96.
45. Lima, J., et al., *Mitochondria and Oncocytomas*, in *Mitochondria and Cancer*, Springer, Editor. 2009.
46. Maximo, V., et al., *Mitochondria and cancer.* Virchows Arch, 2009. **454**(5): p. 481-95.